Taming light propagation through strongly scattering media

Master Thesis of Evangelos Marakis

Graduation Committee: Tzortzakis Stelios
Zotos Xenophon
Chalepakis George

UNIS

University of Crete – Physics Department
2013-2014

This page has been left intentionally blank

Author: Evangelos Marakis

Graduation Committee: Stelios Tzortzakis
Xenophon Zotos
Chalepakis Georgios

This page has been left intentionally blank

Abstract

In 2007 a new branch of physics was born, harnessing scattering via wavefront shaping. One of the major bio-imaging obstacles is scattering of light. Techniques to overcome scattering in the mesoscopic regime have been utilized getting advance of light interference. Still there is lack of control in the available scattering media; in most of cases it's a simple TiO_2 sample of random thickness and complexity.
In this work we propose an artificial scattering media, build with Laser micromachining techniques. On such structures we have absolute control of complexity, geometry and size. These media are not only are the missing tool in scattering physics but also can be build such way to imitate the scattering properties of biological tissue. Therefore we investigate the possibility to build media with the same properties of a biological tissue and induce the wavefront techniques to harness scattering.

Περίληψη

Το 2007 ένας νέος κλάδος της φυσικής δημιουργήθηκε, η δυνατότητα να «δαμαστεί» η σκέδαση μέσω της τεχνικής διαμόρφωσης μετώπου κύματος (Wavefront shaping). Ένα από τα μεγαλύτερα εμπόδια στην τεχνικές επισκόπησης βιολογικών ιστών είναι η σκέδαση φωτός. Τεχνικές για να προσπεραστεί η σκέδασή στο μεσοσκοπικό όριο (διατήρηση της συμφωνία φωτός πάρα την σκέδαση) έχουν πραγματοποιηθεί εκμεταλλευομένη την συμβολή φωτός. Σήμερα υπάρχει ακόμα ένα κενό στον έλεγχο των διαθέσιμων σκεδάζουν υλικών. Στις περισσότερες περιπτώσεις χρησιμοποιείτε δείγμα $Ti0_2$ με τυχαίο πάχος και πολυπλοκότητα.

Σε αυτήν την δουλειά προτείνουμε ένα σκεδάζουν υλικό, που δημιουργήθηκε με τεχνικές εγράφης υπερβραχέων παλμών laser (laser micromachining). Σε αυτές τις δομές έχουμε απολυτό έλεγχο της πολυπλοκότητας, γεωμετρίας και μεγέθους. Τέτοιου τύπου μέσα είναι ένα εργαλείο που λείπει από τις φυσικής σκέδασης αλλά επίσης μπορεί να δημιουργηθούν έτσι ώστε να έχουν τα χαρακτηριστικά σκέδασης ενός βιολογικού ιστού. Επομένως διερευνούμε την πιθανότητα να φτιάξουμε υλικά με τις ιδίες ιδιότητες ενός βιολογικού ιστού και να αποκτήσουμε έλεγχο του διερχομένου μετώπου κύματος με τεχνικές wavefront shaping.

Acknowledgments

For this work there is a number of people I would like to thank!

First I am really thankful to Mr. Xenophon Zotos , Mr Chalepakis Georrge who accepted to be in my graduation committee

Then I will start with Mr. Stelios Tzortzakis, my direct supervisor for his welcoming attitude and patience to discuss ideas. It was an honor to work with him and I really value his support to any movement.

Secondly Mr. Giannis Zacharakis, for accepting the collaboration, his friendly stance and thank him for his valuable help for my PhD position.

Diego Di Battista, for everything! His time, trust and straight forward attitude. It was excellent to work with him.

Michalis Loulakis for his therapy sessions and always having an answer to experimental problems.

Andreas Lemonis for his technical support and the fact that everything runned smoothly while he was around.

The rest of the guys in the lab, Alexandriri Christianna, Christina Daskalaki, Eliza Papadopoulou, Vladimir Fedorov, Tasos Koulouklidis, and Mr. Dimitris Papazoglou. For their moral support and unordinary moments!

Table of Contents

1. Introduction

After the emergence of wavefront shaping[1], a number of techniques that suppress or take advantage of scattering phenomena have been developed. An analysis of the existing research has shown that a controlled scattering medium was missing.

Such media are necessary for studying scattering phenomena and can be manipulated to offer specific scattering properties that closely resemble the characteristics/properties of biological tissue. This tool can enhance the dynamic of the field even further.

1.1 Light Propagation through Media

When light propagates through a medium there are two major mechanisms attenuating its propagation: absorption and scattering. During the process of absorption the light is absorbed by the material itself, thereby reducing the light that it is propagating through. The absorbed light will be irradiated again in random directions or if it is fluorescent in longer wavelengths and lost as lattice vibrations.

We speak of scattering, when light is not absorbed by the material and instead is diverted in random directions, depending on the geometry of the scatterer (molecules, micro-structured interfaces etc.) and the light wavefront is scrambled. The general rule is: light will refract whenever it meets two material interfaces with different refractive indexes (even same materials with different densities can have different refractive indexes). In other words, scattering occurs because interfaces that are not smooth, but chaotic, complex or randomly spaced will make light refraction also very complex and this complex refraction pattern is called scattering[2].

This phenomenon is the reason we cannot see through a glossy glass, through milk or what interest us most, why we cannot see red light through our fingers.

1.2 Wavefront Shaping Harnesses Scattering

Until very recently scattering was a barrier when it came to imaging. Most techniques currently used rely on wavelengths that are mostly absorbed (MRI, X-Rays), even ultrasounds techniques are used because of the limited scattering occurring inside a tissue.

Optical techniques that are used to overcome scattering are called optical coherent tomography (OCT), a successful tool which is limited to be limited to only a few μm. Then Vellekoop and Mosk had a scientific breakthrough in 2007[1], when they achieved a tight focus behind a strongly scattering medium with the use of a spatial light modulator (SLM). At that moment the wavefront shaping research field was born, and techniques for pulse[3] and image reconstruction after a scattering medium flourished, either through the use of a SLM or taking advantage of the correlation of light[4,5] (memory effect[6]).

To this day, numerical simulations are made on hypothetical well defined random structures[7], on the other hand experiments are made with samples of TiO_2 pigment or thin

biological tissues, which are notoriously unstable. No one has tried to work with artificial scattering media. As we show in this thesis, there is a way to build controlled strongly scattering structures with laser micromachining.

1.3 Laser Micromachining

With the rise of ultrafast laser technology, a number of labs can create non-linear phenomena. Among those phenomena and applications, laser micromachining of transparent materials is one of the most interesting and variously applicable technology.

As we will cover in full detail in the next chapter, a laser beam of a specific wavelength λ can be focused inside a material (glass or polymer), this material it's transparent to λ. If the intensity of the laser beam is big enough, it can induce permanent refractive index changes on the area of focus.

These changes, more or less, can be initially grouped into-two categories (our discussion is about femtosecond pulses). In the first category a densification of the material on the irradiated area occurs, i.e. a refractive index increase around $\Delta n=10^{-3}$, which is enough for waveguiding. Although there are cases of some glasses (mainly crystals) where a reduction of the refractive index occurs, the physical mechanism behind that is still uncertain, however[8].
The second category, where more energy is deposited inside the material, micro-explosions take place, leaving behind vacuum spheroids, with a refractive index of Δn=30-50% [9,10]. That is the operation regime we are working for this thesis.

By taking advantage of symmetrical vacuum structures, we can build lattices composed of randomly positioned spheroids. These structures work as ~~a~~ strongly scattering media when irradiated, and they are ideal for studying the propagation of light through them. We created structures with varying complexities and geometries that were used for our research purposes.

If the complexity is increased sufficiently, it results in a medium with the scattering properties of biological tissue, just as the literature suggests. After the creation of varying complex structures, we investigate the propagation of coherent radiation through these structures with a laser beam and afterwards we wavefront shaping with a SLM.

References

1. Vellekoop, I. M. & Mosk, A. P. Focusing coherent light through opaque strongly. *Opt. Lett.* **32,** 2309–2311 (2007).

2. Ishimaru, A. *Wave Propagation and Scattering in Random Media*. (Wiley, 1999). at <http://books.google.gr/books?id=wAZnuHdEKL0C>

3. Katz, O., Small, E., Bromberg, Y. & Silberberg, Y. Controlling Ultrashort Pulses in Scattering Media. *Opt. Photonics News* **22,** 45 (2011).

4. Bertolotti, J. *et al.* Non-invasive imaging through opaque scattering layers. *Nature* **491,** 232–234 (2012).

5. Katz, O., Small, E. & Silberberg, Y. Looking around corners and through thin turbid layers in real time with scattered incoherent light. *Nat Phot.* **6,** 549–553 (2012).

6. Freund, I., Rosenbluh, M. & Feng, S. Memory Effects in Propagation of Optical Waves through Disordered Media. *Phys. Rev. Lett.* **61,** 2328–2331 (1988).

7. Choi, W., Mosk, A. P., Park, Q. H. & Choi, W. Transmission eigenchannels in a disordered medium. *Phys. Rev. B* **83,** (2011).

8. Osellame, R. C. G. R. R. *Femtosecond Laser Micromachining Photonic and Microfluidic Devices in Transparent Materials*. (Springer Berlin, 2014).

9. Glezer, E. N. & Mazur, E. utlrafast - laser driven micro-explosion in transparent materials. (1997).

10. Glezer, E. N. *et al.* Three-dimensional optical storage inside transparentmaterials. *Opt. Lett.* **21,** 2023–2025 (1996).

2. Theory

On the following part, the essential physics required are analyzed. We'll cover the theory of scattering and how some basic quantities are formalized.

2.1 Laser Micromachining of Transparent Materials

The field of laser micromachining can apply a number of wavelengths or pulse durations to build structures in micrometer scales. In general thought we usually refer to femtosecond pulses and at wavelengths of 800 nm or 1064 nm which are the most common commercial femtosecond sources.

This technique was firstly demonstrated in 1994, when it was shown that laser ablation can be materialized on silica and silver surfaces. Later in 1996 Hirao's[1] team showed permanent refractive index changes can occur with focused fs irradiation inside fused silica. It was shown that a densification of material occurred inside the irradiated area, causing a refractive index increase of $\Delta n=10^{-3}$, [2]. This value sounds small, but it is enough to directly create a waveguide.

An avalanche of research groups started working on the field, developing new technologies and studying transparent materials and their behavior in fs laser beams. As it has been shown, transparent polymers also indicate refractive index changes up to $\Delta n=10^{-4}$, [3].

The applications of laser micromachining are vast and are not only confined to transparent materials but cell microsurgery, metal processing, nanoscale 3D printing etc. have also boomed with the use of fs laser systems[4] [5]. But in this thesis we will focus on transparent material processing.

Today it is a mature technology that enables us to create optical circuits or more complicated photonic devices (splitters, interferometers, etc.), microfluidic channels, opto-fluidics or a proposal for optical memory[6],[7], [8],[5].

The most apparent advantages are:

- Direct writing with no special preparation.
- Straight application to almost any type of glass, with minor optimizations for each type.
- A true 3D writing technique since the focus can reach any point of the bulk.
- Precision of μm, since any event occurring in the laser focus volume about 0.008μm^3

2.1.1 Physical Mechanism fs Laser-Matter Interaction

Strong intensities produced by commercial femtosecond systems, such as 10 TW/cm^2, can induce non-linear phenomena in media like air filaments, surface ablation etc. In the case of our study non-linear absorption starts, deep in a transparent material. That means energy is deposited in the area where the phenomenon takes place (in the focus of the laser beam).

This accumulated energy will be transferred into the lattice of the bulk in picosecond (ps) scales; this transfer will cause permanent structural changes. The exact mechanisms how these structural changes occur have not been found yet, since there are materials that have

shown a material density decrease during the process, instead of the expected increase. Therefore, we assume the mechanisms differ for each material. But the whole process follows three steps:[5]

1. Generation of free electrons via non-linear laser-matter interaction
2. Energy relaxation of the plasma to the bulk
3. Permanent material modification

Free Electron Plasma Formation

Glasses are transparent to visible light and infrared radiation because they do not absorb those wavelengths; in other words there is no electron transition (from the valence zone to the conduction zone) to absorb of these wavelengths. So a laser beam with wavelengths on this spectrum normally travels through.

When the intensity is too great, non-linear absorption can happen and instantly promotes an electron from the valence zone to the conduction zone since the energy gap is much greater than the laser light. For nonlinearities to occur, the intensity of the laser beam must be similar in magnitude to the electric field of the valence electrons with the atoms nuclei, 10^9 Vm^{-1}. In terms of laser intensities, that would mean about 5 10^{20} Wm^{-2}. Naturally such intensities warrant a tight focus of the laser beam.

There are three mechanisms that can create this the promotion of electrons: multiphoton ionization, tunneling photoionization and avalanche photoionization. These three mechanisms can happen simultaneously, however, the probability of occurrence differs depending on the exposure conditions. The avalanche mechanism is mainly an aftermath of the first two mechanisms, which advance in time.

We speak of multiphoton absorption, when multiple photons are absorbed by an electron and elevated to the conduction band via virtual states. For this procedure to happen, the number of absorbed photons must have an energy sum bigger than or at least equal to the energy gap figure [1]. This can be described by the equation[5]:

$$E_g = n\,\hbar\omega \quad (2.2.1)$$

Where n is the number of photons needed to be absorbed to reach the energy threshold.

This mechanism is more probably to take place when we have relative low intensities of light, but higher light frequencies (but not enough to elevate the electron straightly to the conduct band).

The structural changes seem to have an intensity threshold rather frequency dependence. So that shows, multiphoton absorption is not the only mechanism taking place or there would be a different energy threshold for every material with a different band gap. This means that the next mechanism is taking place as well.

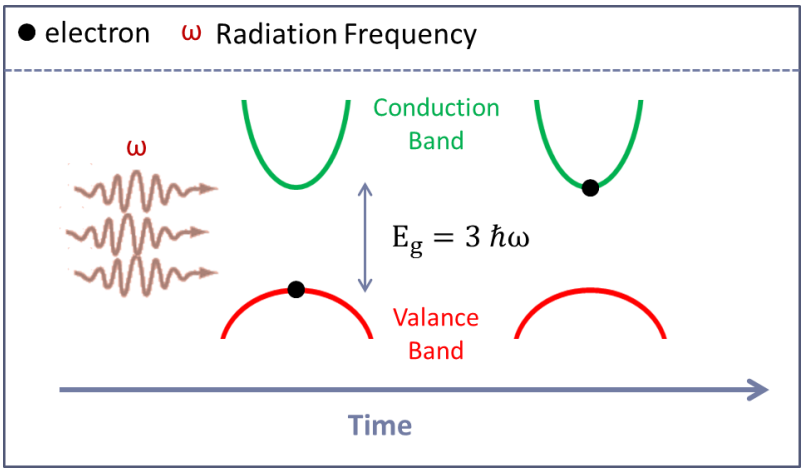

Figure 1 Schematic representation of multiphoton absorption process

The other mechanism taking place during the transition is tunneling ionization. In the presence of a strong electric field the energy band gap will bend and the valence band (VB) and the conduction band (CB) will have a similar energy. This causes tunneling effects and the electrons jump to the CB because of the quantum nature of electrons and the spreading of their wavefunctions figure [2].

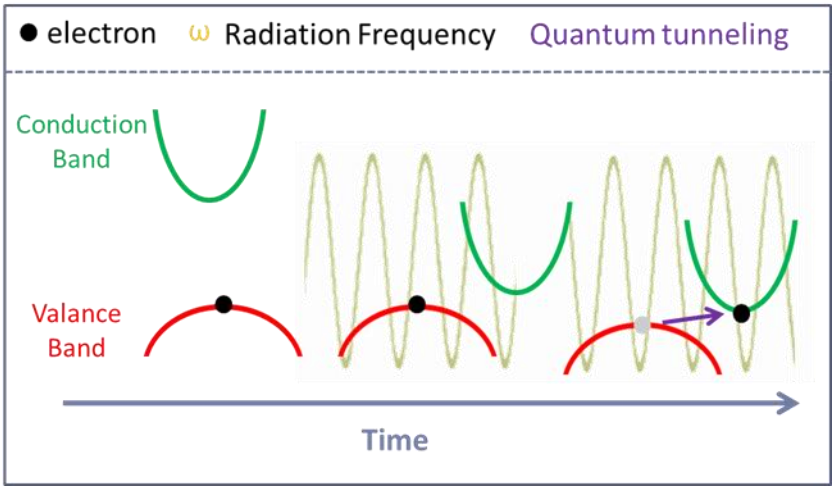

Figure 2 Tunneling ionization. Laser electric field distorts the energy bands, increasing the probability of a tunneling ionization

The third mechanism is called avalanche photoionization. After the elevation of an electron to CB, it is still capable of absorbing energy from the laser beam and getting to a further excited state. In such a case there is extra kinetic energy and it the electron can ionize another electron on the VB by collision and promote it to the CB. As long as laser light is present, ionizing can continue constantly.

The electrons that initiate the phenomenon are called seed electrons. Usually this the seed electron is caused by multiphoton ionization and tunneling photoionization or it is thermally induced, but that is not the case for fs pulses, because thermally induced phenomena occurs in picosecond scales.

While the avalanche is happening, the number of free carriers increases to the critical value of 10^{21} cm^{-3}. This happens because the electrons are constantly absorbing laser light as described in mechanisms 1 and 2 and producing extra electron in the CB. This plasma is resonant to the laser frequency and absorbing the remaining pulse. Figure [3]

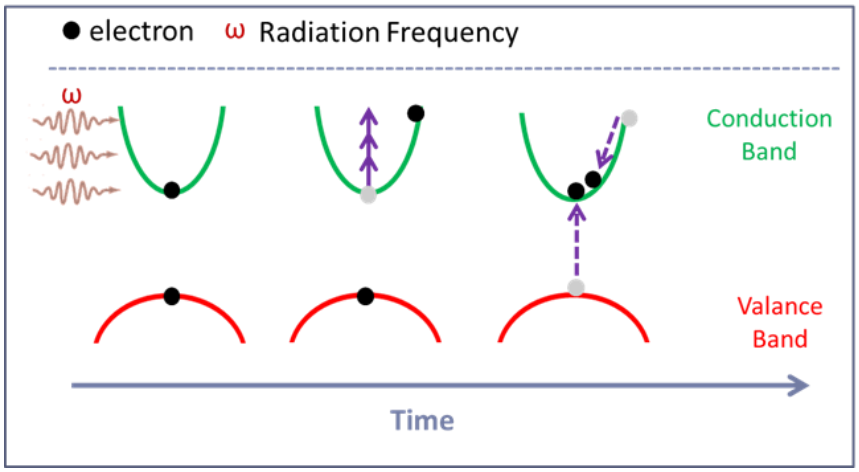

Figure 3 Schematic representation of avalanche ionization process, a seed electron in the CB absorbs additional energy increasing it's kinetic energy. By collision with VB electron it promotes them in the CB

The energy will be transferred around 10 picoseconds, long after the fs (10-100 fs) pulse has gone. This is why fs micromachining is advantageous compared to ps and ns pulses. The excited electrons have a smaller life span than electron-phonon scattering time (1 ps). So there is no time for ions excitation. This means the heat diffusion will be confined inside the focus volume and thereby increasing the precision of this technique.

Furthermore, since enough seed electrons are produced by the first two mechanisms, it is straightly applicable to large a number of materials without the need of impurities.

The first two mechanisms can be embedded into the same theoretical model. The Keldysh parameter describes which of those two mechanisms will dominate:

$$\gamma = \frac{\omega}{e}\sqrt{\frac{m_e c\, n\, \epsilon_o\, E_g}{I}} \quad (2.2.2)$$

Where:

- ω: laser frequency
- I: laser intensity
- m_e: effective electron mass
- e: electron charge

- c: speed of light
- n: linear refractive index
- ϵ_o electronic permittivity of free space

Depending on the value of γ, we can predict which mechanism will takes part place:

- γ>>1.5 Photoionization will be based mostly to on the tunneling effect.
- γ≈1.5 Photoionization will be based on a combination of both mechanisms.
- γ≈1 Photoionization will be based on multiphoton ionization.

Structural Changes

After the plasma creation at the point of focus, relaxation process will initiate causing permanent structural changes. So far there is no model to fully describe how this is happens since none of the models describes all different cases of refractive index modification. For fused silica an extended work can be found[12].

In general the absorbed energy from the free electron is transferred into the lattice in some ps. A shock wave will follow in a nanoscale time frame, exiting out the dense focus and in the microsecond scale the thermal energy diffuses out of the focal volume.

Those energies can induce melting or non-thermal ionic motions, which cause permanent structural changes.

The resulting structural changes can at least be grouped into three categories. We can determine the outcome generally by the amount of energy we deposit on the sample.

- Smooth refractive index change, usually increasing $\Delta n=10^{-3}$.
- Birefringent refractive index modification by nanosized modified areas (not smooth).
- Vacuum bubbles caused by micro-explosions.

Laser Repetition Rate

The descriptions below are limited to one pulse interaction, this means the repetition rate of the laser is much smaller than the thermal transfer phenomenon. So relatively speaking, there is enough time between each pulse to be considered an independent phenomenon repetition rates higher than 100 kHz this assumption is not valid anymore[8].

At higher repetitions rates the heat accumulates in the focus continuously until irradiation stops. So it is like a point thermal source is placed in the focus. The material melts continuously and so does the affected area. In other words the diameter of the affected waveguide constantly increases.

By controlling the writing speed, we control the number of pulses hitting a certain area. That is how we control the waveguide diameter. Of course in this case, the mechanism of structural changes is totally based in heat accumulating effects.

But since our laser system offers a 1 kHz repetition rate, this equals one pulse every one millisecond; each pulse occurs as an independent event.

1. Smooth Refractive Index

This was the first observed structural change; the refractive index induced is smooth and uniform. We fused silica with the following parameters: the energy threshold is 100nJ for a NA=0.6 objective lens and pulse duration of 100fs with a wavelength at 800nm. The irradiated area was examined and showed densification.

The exact mechanism is still under investigation. It is certain however that the increased densification is caused while the glass is cooling down. But the full mechanism is complex and it is uncertain to which amount the parameters contribute to the mechanism.

One of the major debates revolved around the speculation, if the creation of color centers could possibly cause the densification. This will be intercepted as, a change in the absorption spectra will cause a change in the refractive index.

Today research shows that the color center only plays a small part in the densification mechanism of the irradiated area and that it further depends on the type of glass.

2. Birefringent Refractive Index Change

If the energy directed at the bulk increases even further (about 150-500nJ), while still using the same parameters as described above, the changes induced inside the bulk will no longer be smooth. A waveguide written under such conditions in fused silica is called birefringence because

The densification does not occur smoothly in the whole volume of the irradiated area, but in subwavelength structures (i.e. periodic structures of changed and non-changed areas).

In the fused silica case it was shown that the orientation of the nanogratings was perpendicular to the writing laser polarization in all cases.

In 2003 it was explained that birefringence occurred due to periodic nanostructures that were caused by interference of the laser field and the induced electron plasma wave.

The periodicity of the nanostructures is about $(\lambda/2)n$ where, λ is the wavelength and n is the refractive index of the bulk. A successful model describing the formation of nanoplanes was developed by Taylor's research team.

3. Vacuum Bubbles

If additional energy is deposited on the bulk (higher than 500nJ), while the other parameters are still the same, the changes induced will be much more radical than before[9].

Free electrons will transfer energy back to the bulk in the form of a strong shock wave, resulting in high temperatures and great pressures that are greater than Young's modulus.

This effect is possibly created by coulomb repulsion between ions, since the ionic shielding has been reduced, and the outer electrons have been ionized.

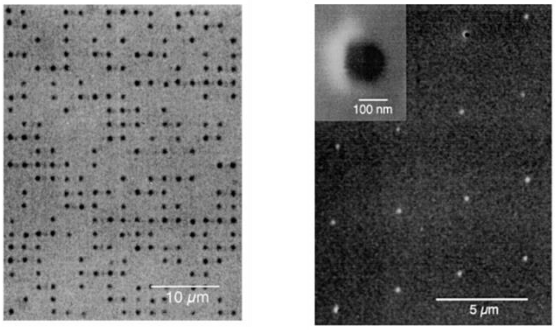

Figure 4 : a) demonstration of voids inside fused silica, written with fs laser. Optical microscope fails to give the true dimensions. b) with use of an electron microscope it's shown the true dimension is 200nm

The material from the core of the energy focus volume will be ejected and forced into the surrounding volume. That will leave a hollow core and a densified crust.

The resulting structure will be a vacuum bubble, which will have a much smaller refractive index in the center (vacuum) and a densified profile around the bubble bulk interface, resulting in an increased refractive index. The morphology of those vacuum bubbles differs, depending on the type of material that is used, the exposure time etc.

In the work of Glezer, Milosavljevic[10] it has been shown that the actual diameter of those voids was nanosized about 200nm. Although they used an objective of NA=0.65 and the laser wavelength was 750 nm, resulting in a focus size of about 1μm. It is believed the smaller size originates in the nonlinearities of the absorption, the excited region will be much smaller than the linear intensity distribution.

Such structures were only used only for optical memory so far. In this work we take advantage of the great refractive index changes up to 30 per cent and use them as scatterers. We can create these scattering media by positioning controlled voids inside the bulk. Image [4]

2.1.2 Adjustable Parameters - Writing Geometry

So far we have covered the mechanism of writing and the dependence on the structural changes of the energy we deposit. But there are some other variables worth mentioning in this chapter, which have a significant impact on creating a photonic lattice.

Focus

Since the changes in the material need big energy density in a volume, the place where the structural changes occur are at the focus of the beam. So we first have to put the volume focus of an objective and the confocal parameter under consideration.

To focus the beam, an objective is used in most applications; depending on the numerical aperture (NA) of this objective and the wavelength of the laser beam, a focus of a certain radius will be formed. The radius equals:

$$r = w_o = \frac{M^2 \lambda}{\pi\, NA} \quad (2.3)$$

Where M[1] is the beam quality factor, λ is the wavelength.

There is a diffraction limit of how well we can focus the beam because of the wave nature of light. This means, even if we focus in x-y direction the intensity to a radius as predicted by (2.3), in the z direction the intensity will be spread in a distance b.

$$b = z_0 = \frac{M^2 n\, \lambda}{\pi\, NA} \quad (2.4)$$

This parameter is almost w_o^2, that means it can rise to quite an asymmetry while writing a structure. This problem was instantly observed when the first waveguide was made in 1996 by Hirao, and it plays an important role in with the writing geometry, as will be shown in next chapter. Figure [5]

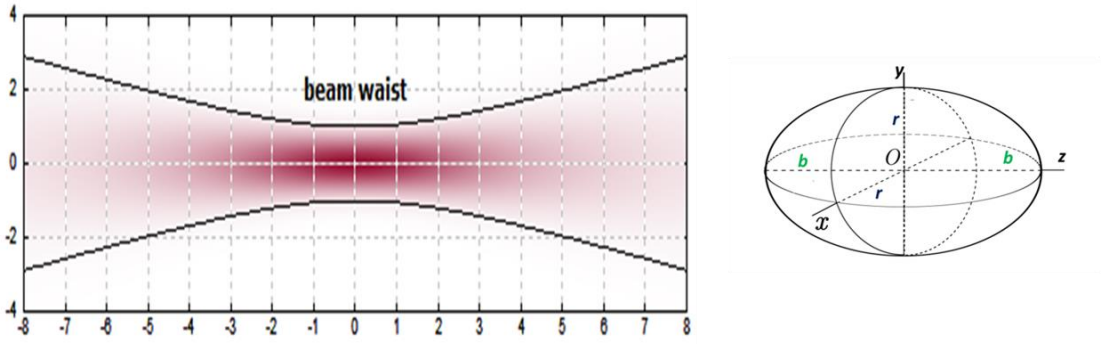

Figure 5 a) b : confocal parameter . 2r : focus diameter Here it's shown how the intensity is concentrated at the focus. b)The resulting volume is an ellipsoid with b as long axis and r as small radius. 2.x.b the 3d representation of the ellipsoid.

At high intensities the propagation of light diverges from its linear properties. This is happens because the electric field of the light becomes similar in magnitude to the atomic field, and no longer it's a minor perturbation.

Nonlinearity Threshold

This results in as a distortion of the refraction index of the medium, the higher the intensity is the higher is the value of the refraction index. This means a Gaussian profile, will have a higher value of refractive index at the center than at the wings. In other words, a positive lens refractive index is created and a self-focusing phenomenon initiates, this is called Kerr effect[8].

[1] Beam quality factor: a parameter for quantifying the beam quality of laser beams. It is defined as the beam parameter product (product of the beam radius in a focus and the far-field beam divergence) divided by λ / π, the latter being the beam parameter product for a diffraction-limited Gaussian beam with the same wavelength.

When self-focusing occurs a plasma formation will manifest at the center of the beam where the intensity is higher and a decrease of plasma formation as will occur if you move away from the center. This plasma density causes a decrease of the refractive index in the center and an increase of the values at the wings; exactly like a negative lens refractive index profile. So the beam will start to defocus again.
These two phenomena can be repeated for hundreds of meters but one has to be careful while writing a structure to work with lower intensities to initiate the Kerr effect figure [6].

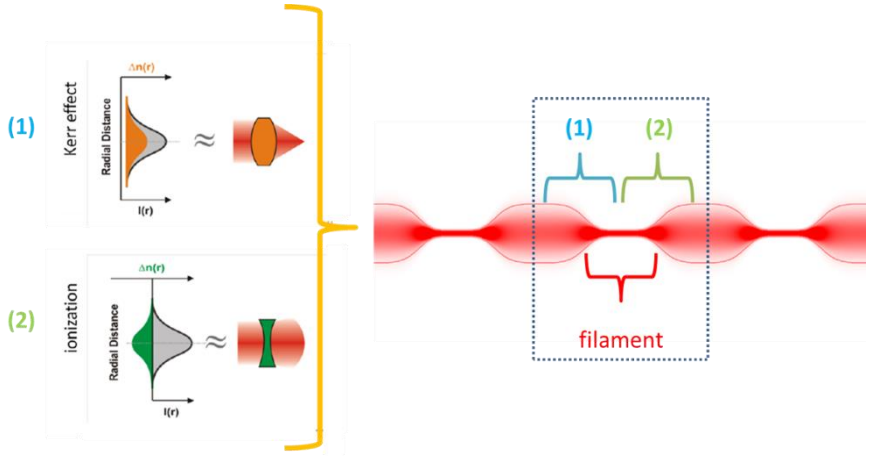

Figure 6 Pulse nonlinear propagation. 1) High intensities, will create a refractive index profile similar to a positive lens, which will selffocus the beam. 2) the self focused beam will create plasma that will make a refractive index profile similar to a negati

The threshold for self-focusing to occur can be derived from the relation:

$$P_c = \frac{3.77\,\lambda^2}{8\pi\, n_o n_2} \quad (2.5)$$

Where λ is the wavelength of the beam, no is the linear refractive index and n_2 is the non-linear refractive index. This value only has significance for high intensities. For fused silica the power threshold is ~1.8 MW. So we have to make sure that we do not reach such values, if we want a controlled writing.

Writing Geometry

Given the anisotropy of the focus, the confocal parameter is not identical with the focus radius, there is an asymmetry while writing a structure. This effect was immediately observed by Hirao's team in 1996[1]. They observed there was a strong asymmetry in the waveguide they wrote with the fs laser. So there are two ways to write a structure with laser micromachining today:

The first option is to move the sample parallel to the focus, giving it a symmetrical shaped spot and structure. Such a set-up is impractical (no comma) because the length of such structures cannot be longer than the working distance of the objective. And since most objectives have a working distance between several hundreds μm to just a few mm, this is quite limiting.

The other option is to move the sample transverse to the focus, but this will create an asymmetry in the direction of the beam. Depending the application this can be a drawback or not. Objectives with high NA compensate this asymmetry but the working distance is limited, which means the depth of writing. Image [7].

In this case MHz repetition rates (no comma) are generally immune to this asymmetry because the changes are induced by heat diffusion that travels symmetrical away from the focus, which on the end offers a symmetric result compared to kHz repetition rates systems.

Thankfully, two solutions were proposed to cure this asymmetry. Both rely on the use of non- Gaussian beams, as we will see in detail next.

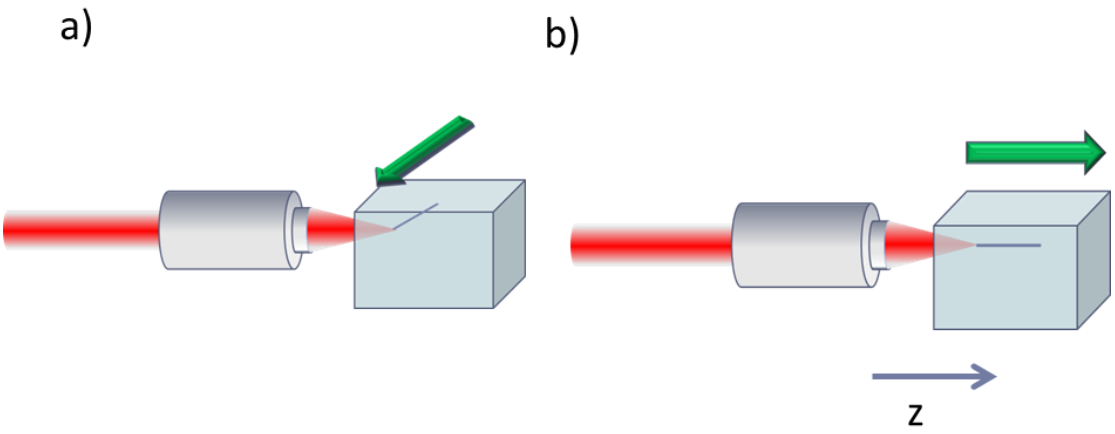

Figure 7 The different writing geometries. a) Although a symmetric structure, is very limited in the length. b) The most commonly used method, but giving an asymmetric result in z direction.

Asymmetry Therapy

Our research team usually does not work with those methods, but they are presented and explained here for completeness and because our team initially considered using them. There are a number of techniques, however, I will elaborate on the simplest and most practical one: the slit beam shaping method[11].

To make a symmetric cross section, you need to vary the beam waist ratio. But that means a ratio around 10 to offer a symmetric result. The easiest way is to put a slit right behind the objective.

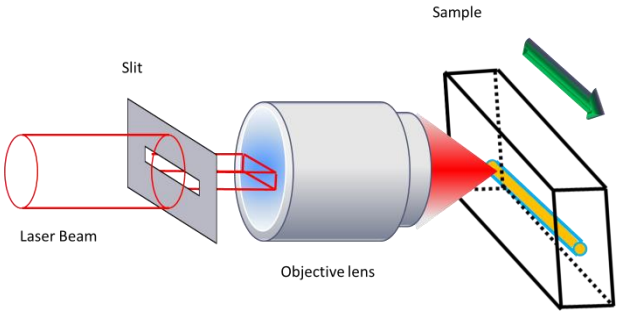

Figure 8 The slit method set-up. A slit just before the objective with the dimensions given from (2.6) is enough to cure the assymetry.

The slit is placed along the sample translation direction to reduce the NA of the focusing in the beam perpendicular to waveguide axis. The opening of the slit ought to have the size Ry:

$$R_y = \frac{NA}{n}\sqrt{\frac{\ln 2}{3}}R_x \quad (2.6)$$

Where Rx is the beam diameter that goes through the objective and n is the refractive index of the sample, Figure [8].

Additional Variables

Writing Speed

If one has the intention to create a waveguide or a similar structures, the speed at which the focus scans the sample is a very important factor. Every point of the sample must have been exposed to the necessary amount of pulses to initiate the desirable structural change.

We already covered that the repetition rate of a laser is important. If we work at the MHz regime, heat is accumulated in the focus volume. This results in much higher writing speeds compared to a kHz laser system.

So for a 1 kHz system the speed for a smooth waveguide ought to be 25 μm/s, which, compared to a 2 MHz system that can reach 1 mm/s, is a significant advantage. A way to evaluate the effective number of pulses N for the spot size is:

$$N = \frac{2w_o R}{v} \quad (2.7)$$

Where w_o is the focus radius, R is the repetition rate of the laser, and v is the velocity at which the sample is translated.

Pulse duration

The pulse duration is a significant parameter. Firstly, if it is longer than fs pulses, distorted structures will be the result. But even in the case of fused silica, it has been observed that losses of a waveguide are depending on the duration of a pulse for femtosecond scales. In contrast borosilicate glass is not effected from femtosecond pulses. But for subpicosend pulses (no comma) micromachining is sufficient. So we can choose from an array of different laser systems.

Polarization

There is a strong dependence on the polarization of the laser beam with fused silica. This seems to be cased from the nanogratings structures are formed in the middle of the energy regime. Once more in borosilicate glasses show no polarization dependence, since the nano sized gratings haven't been observed in any writing condition. It is believed that the heat accumulation suspends any dependence.

Wavelength

It has been shown that for larger wavelengths larger than 1.5 μm can offer a bigger processing window compared to the 800 nm systems. The energy process for the first case is 1 to 23 μJ compared to 0.5 to 2 μJ in the second case. Although there are certain advantages in the first cases, the implementation can be more complex.

Numerical Aperture of the objective

We already discussed the importance of the NA in the shape of focus. But two non-linear phenomena can occur at lower intensities than the intensities needed to induce structural changes in a medium.1 The first is self-focusing (occurs at 4MW is the case of fused silica), as we have covered above, and the second is white light generation. White light generation is otherwise known as supercontinuum generation. We speak of white light generation when an ultrafast laser pulses through a strongly non-linear device (a piece of bulk glass for instance) and the laser light is converted to light with a very broad spectral bandwidth. If the NA of the lens is less than 0.1 the two phenomena have intensity thresholds lower than the structural changes threshold. Those two phenomena disturb the writing control, resulting in structures no longer defined by the focus volume.

There are additional parameters for laser micromachining, like the Quill effect for example, but they are out of the scope of this thesis. The reader can look it up in the reference list for further information[5].

Reference

1. Davis, K. M., Miura, K., Sugimoto, N. & Hirao, K. Writing waveguides in glass with a femtosecond laser. *Opt. Lett.* **21,** 1729–1731 (1996).

2. Ehrt, D., Kittel, T., Will, M., Nolte, S. & Tünnermann, A. Femtosecond-laser-writing in various glasses. *J. Non. Cryst. Solids* **345-346,** 332–337 (2004).

3. Lee, C. Y., Chang, T. C., Wang, S. C., Chien, C. W. & Cheng, C. W. Using femtosecond laser to fabricate highly precise interior three-dimensional microstructures in polymeric flow chip. *Biomicrofluidics* **4,** 46502 (2010).

4. Eaton, S. M. *et al.* Femtosecond laser microstructuring for polymeric lab-on-chips. *J. Biophotonics* **5,** 687–702 (2012).

5. Osellame, R. C. G. R. R. *Femtosecond Laser Micromachining Photonic and Microfluidic Devices in Transparent Materials*. (Springer Berlin, 2014).

6. Ventura, M. J., Straub, M. & Gu, M. Void channel microstructures in resin solids as an efficient way to infrared photonic crystals. *Appl. Phys. Lett.* **82,** 1649 (2003).

7. Submitted, T. *et al.* Pmma microfluidics technology: development and characterization. (2010).

8. Gattass, R. R. & Mazur, E. Femtosecond laser micromachining in transparent materials. *Nat Phot.* **2,** 219–225 (2008).

9. Glezer, E. N. & Mazur, E. utlrafast - laser driven micro-explosion in transparent materials. (1997).

10. Glezer, E. N. *et al.* Three-dimensional optical storage inside transparentmaterials. *Opt. Lett.* **21,** 2023–2025 (1996).

11. Ams, M., Marshall, G. D., Spence, D. J. & Withford, M. J. Slit beam shaping method for femtosecond laser direct-write fabrication of symmetric waveguides in bulk glasses. *Opt. Express* **13,** 5676–5681 (2005).

12. Papazoglou, D. G. & Tzortzakis, S. Physical mechanisms of fused silica restructuring and densification after femtosecond laser excitation [Invited]. Opt. Mater. Express 1, 625–632 (2011).

2.2 Scattering

In general scattering can be defined as the procedure when a type of radiation is constrained to change its linear propagation because of an existent inhomogeneity inside a medium. This even includes even the beams reflected from a surface, when they deviate from the Reflection law (Snell's law). Those inhomoginities are called scatterers or scattering centers.

When multiple scattering occurs the interaction tends to be normalized by the number of random events, so the final path of the radiation looks like a deterministic distribution of the radiation intensity. When light travels through mist for example, multiple scattering will be similar to diffusion. This is why media that cause multiple scattering events are called diffusers.

Since this thesis is about light scattering, we will focus on light scattering phenomena. Although scattering is a wave nature phenomenon, one can come across it wherever there is wave propagation.

Coherent light exhibits additional post-scattering behavior because of its interference phenomena. When coherent light undergoes scattering multiple times, interference of the scattered light will occur, and the resulting light distribution is called speckles[1].

Coherent backscattering is an amplified case of backscattering when coherent light is scattered multiple times by a medium and it is attributed in to weak localization[2].

Electromagnetic Scattering

There are a number of scattering events when it comes to electromagnetic radiation. When there is not much scattering or there is no energy transfer, it is called elastic. Usually Rayleigh or Mie scattering belong into this category. However, we will only work with inelastic scattering in this thesis. Brillouin, Raman, inelastic X-ray and Compton scattering usually involve an energy transfer. The cases of light scattering can be grouped, depending on a dimensionless parameter.

$$\alpha = \frac{\pi D_p}{\lambda} \quad (2.2.1)$$

Where D_p is the circumference of a particle, λ is the wavelength. Depending on the value of α:

α<<1 Rayleigh Scattering

Raleigh Scattering happens when light is scattered by a body much smaller than wavelength of the light. Typically we consider the scatterer is a sphere, gaseous or liquid. Scattering is categorized as a Raleigh scattering when its size is 0.1λ of the light wavelength.

α≈1 Mie Scattering

When the size of the scatterer is no longer much smaller than the wavelength, usually we use Mie scattering theory. This model can be used for ellipsoids as well, but there is no close

form for arbitral scattered geometries. In general in Mie scattering we have more forward remission compared to Rayleigh Scattering.

α>>1 Geometrical Scattering.

When the ratio between the diameter of the scatterer and wavelength is bigger than 10, laws of geometric optics are not sufficient to describe the propagation through the scatterer.

2.2.1 Single Scattering

When light goes through an inhomogeneous medium, we can see its diffusion. Light spreads through the volume, carrying no information what's on the back. This is the aftermath of multiple scattering events, which, as we have already mentioned, can either be Rayleigh or Mie scattering. First we will cover single scattering, before we move on to multiple scattering behaviors, which is the sum of multiple single scattering events.

So it is best to start the discussion about scattering by explaining how light propagates. Light is well known to be an electromagnetic wave and can therefore be described by the Maxwell equations. There are four equations and they correlate electric field evolution with the magnetic field, together giving the light propagation.

$$\nabla \cdot E = \frac{1}{\epsilon_0}\rho \quad (2.2.2)$$

$$\nabla \times E = -\frac{\partial B}{\partial t} \quad (2.2.3)$$

$$\nabla \cdot B = 0 \quad (2.2.4)$$

$$\nabla \times B = \mu_0 J - \epsilon_0 \mu_0 \frac{\partial E}{\partial t} \quad (2.2.5)$$

The formulas describe the electromagnetic propagation in free space. So equation (2.2.2) actually says, we need some charge to produce an electric field, and will turn up to coulomb law of electric force for a static point charge[3].

The second equation (2.2.3) proves that the electric field flux is correlated with the time evolution of the magnetic field.

Equation (2.2.4) demonstrates there are no magnetic monopoles (at least for the time being).

And (2.2.5) shows that the flux of the magnetic field is correlated with the electric field time evolution. (Most times the factor $\mu_o J$ is zero, which means the electric currents act as a magnetic field sources).

With some mathematic tricks, we can break the correlation of the two fields and isolate each field to a wave propagation equation.

$$\nabla^2 \boldsymbol{E} = -\epsilon_0 \mu_0 \frac{\partial^2 \boldsymbol{E}}{\partial t^2} \quad (2.2.6)$$

$$\nabla^2 \boldsymbol{B} = -\epsilon_0 \mu_0 \frac{\partial^2 \boldsymbol{B}}{\partial t^2} \quad (2.2.7)$$

So the last two equations describe two propagating waves, with speed $c^2 = \frac{1}{\epsilon_0 \mu_0}$. So what is left now is to see how these waves propagate while meeting variations of the electromagnetic constants ($\epsilon_0 \mu_0$). When that happens the values of the waves differ from their usual values in a vacuum, this is due to scattering and absorption phenomena (depending the material).

To keep things simple, we ignore the magnetic wave for the time being (since it usually only weakly interacts with matter), and only consider one solution (2.2.6). In case of a planar wave we use the complex representation.

$$E_i(\boldsymbol{r}) = \hat{\boldsymbol{e}}_{\boldsymbol{i}} e^{ik\hat{\boldsymbol{i}}\cdot\boldsymbol{r}} (2.2.8)$$

Where $\hat{\boldsymbol{i}}$ is the vector of propagation and $\hat{\boldsymbol{e}}_{\boldsymbol{i}}$ is the vector of electric field polarization. The amplitude of the electric field is considered to be one, as can be seen in figure (2.2.2).

So when this planar wave meets a scatterer, an object with different electric constants than vacuum, it will scatter away from that object. This object it will act as a point source, creating a new spherical wave of the form $\frac{e^{ik\boldsymbol{R}}}{R}$ where **R** is the distance of the scatterer in space. But the actual electric field getting away from the source will not necessarily be a spherical wave. To describe the field after scattering, we need two new notions: scattering amplitude and scattering cross section.

Therefore the electric field will have this form:

$$E_i(\boldsymbol{r}) = \boldsymbol{f}(\hat{\boldsymbol{s}}, \hat{\boldsymbol{i}}) \frac{e^{ik\boldsymbol{R}}}{R} \quad (2.2.9)$$

The function $\boldsymbol{f}(\hat{\boldsymbol{s}}, \hat{\boldsymbol{i}})$ is called scattering amplitude (SA). It is a vector quantity since the polarization of the electric field may change after scattering. The SA is dependent on the observation angle $\hat{\boldsymbol{s}}$ and the incident direction $\hat{\boldsymbol{i}}$.

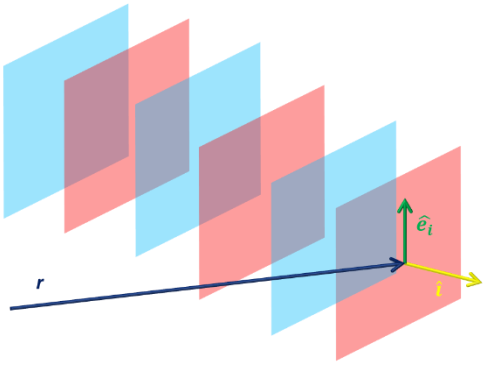

Figure 9 A planar propagation in 3D space, $E_i(\boldsymbol{r}) = \hat{\boldsymbol{e}}_{\boldsymbol{i}} e^{ik\hat{\boldsymbol{i}}\cdot\boldsymbol{r}}$ Where $\hat{\boldsymbol{i}}$ it's the vector of propagation and $\hat{\boldsymbol{e}}_{\boldsymbol{i}}$ it's the vector of electric field polarization. The amplitude of the electric field, it's considered to be one. (red is positive max value, blue maximum negative value)

The power of the incident P_i and scattering wave P_s are:

$$P_i = \frac{|E_i|^2}{2Z_0} \quad (2.2.10)$$

$$P_s = \frac{|E_s|^2}{2Z_0} \quad (2.2.11)$$

Where $Z_0 = \sqrt{\frac{\mu_0}{\varepsilon_0}}$ is the complex resistance of the medium. Taken all together, the power that goes through an elementary surface dS in a distance R_z from the scatterer is $P_s dS$. Since $dS=R^2 d\Omega$ the energy will be $R^2 d\Omega P_s$. All these factors define the differential scattering cross section dσ, where:

$$P_i d\sigma = R^2 d\Omega P_s \quad (2.2.12)$$

Therefore:

$$\sigma_d(\hat{\boldsymbol{s}}, \hat{\boldsymbol{i}}) \equiv \frac{d\sigma}{d\Omega}(\hat{\boldsymbol{s}}, \hat{\boldsymbol{i}}) = |\boldsymbol{f}(\hat{\boldsymbol{s}}, \hat{\boldsymbol{i}})|^2 \quad (2.2.13)$$

And if we integrate ~~for~~ all angles, we can find the total scattering cross section.

$$\sigma_s = \int_{4\pi} |\boldsymbol{f}(\hat{\boldsymbol{s}}, \hat{\boldsymbol{i}})|^2 d\Omega \quad (2.2.14)$$

And along there is backscattering cross section.

$$\sigma_b(\hat{\boldsymbol{i}}) = 4\pi \frac{d\sigma}{d\Omega}(\widehat{-\boldsymbol{i}}, \hat{\boldsymbol{i}}) \quad (2.2.15)$$

The scattering cross section has surface units, but is quite different from the object's surface in general. As we will see in later paragraphs, the scattering cross section is dependent on the wavelength of the radiation.

We'll consider a dielectric scatterer of finite volume V. Its dielectric constant is ε(r), where r index means it can vary inside the scatterer. Ampere's law insider a medium will have the form (Maxwell's equation depart from the form they were presented above, because the response of the dielectric must be taken into account).

$$\boldsymbol{\nabla} \times \boldsymbol{H} = i\omega\varepsilon \boldsymbol{E} + \boldsymbol{J_{eq}}(\boldsymbol{r}) \quad (2.2.16)$$
$$\boldsymbol{J_{eq}}(\boldsymbol{r}) = i\omega\varepsilon_0(\varepsilon_r - 1)\boldsymbol{E} \quad (2.2.17)$$

Where factor J_{eq} describes a current which could exist inside the volume of the scatterer. Such a current acts like a source of electromagnetic waves, and is defined by the vector potential:

$$\boldsymbol{A}(\boldsymbol{r}) = \frac{\mu_0}{4\pi} i\omega\varepsilon_0 \int_V \frac{e^{-ikR}}{R} [\varepsilon(\boldsymbol{r}') - 1]\, \boldsymbol{dr}' \quad (2.2.18)$$

Where R=|r-r'| the distance from the origin. The evaluation of the electric field requires the flux of the vector potential:

$$\boldsymbol{E} = \boldsymbol{\nabla} \times \boldsymbol{\nabla} \times \frac{\boldsymbol{A}}{i\omega\varepsilon_0\mu_0} \quad (2.2.19)$$

The operator will cast on the r variable, when the observation point P is very far away from the scatterer **r>>r'**:

$$\nabla\left(\frac{e^{-ikR}}{R}\right) \approx \left(\frac{e^{-ikr}}{r}\right) \approx -ik\hat{\boldsymbol{r}}\frac{e^{-ikr}}{r} \quad (2.2.20)$$

Returning to (2.2.19) evaluate the electric field, one determines that:

$$\boldsymbol{E} = -\frac{k^2}{4\pi}\int_V \frac{e^{-ikR}}{R}[\varepsilon(\boldsymbol{r}') - 1]\hat{\boldsymbol{r}} \times (\hat{\boldsymbol{r}} \times \boldsymbol{E}(\boldsymbol{r}'))\, \boldsymbol{dr}' \quad (2.2.21)$$

Working on the far field approximation, we set $|\boldsymbol{r} - \boldsymbol{r}'| \approx r - \boldsymbol{r}' \cdot \hat{\boldsymbol{r}}$ for the numerator and $|\boldsymbol{r} - \boldsymbol{r}'| \approx r$ for the denominator, so (2.2.21) becomes:

$$\boldsymbol{E} = -\frac{k^2}{4\pi}\frac{e^{-ikr}}{r}\int_V [\varepsilon(\boldsymbol{r}') - 1]\hat{\boldsymbol{r}} \times (\hat{\boldsymbol{r}} \times \boldsymbol{E}(\boldsymbol{r}'))\, \boldsymbol{dr}' \quad (2.2.22)$$

The integral variable will undergo a modification $\hat{\boldsymbol{r}} \times \left(\hat{\boldsymbol{r}} \times \boldsymbol{E}(\boldsymbol{r}')\right) = \boldsymbol{E} - \hat{\boldsymbol{r}}(\hat{\boldsymbol{r}} \cdot \boldsymbol{E})$**.** We already showed that the electric field will have the form of form of (2.2.9) after scattering; therefore we can have a close form for the SA:

$$\boldsymbol{f} = -\frac{k^2}{4\pi}\int_V e^{-ik\boldsymbol{r}'}[\varepsilon(\boldsymbol{r}') - 1]\hat{\boldsymbol{r}} \times (\boldsymbol{E}(\boldsymbol{r}') - \hat{\boldsymbol{r}}(\hat{\boldsymbol{r}} \cdot \boldsymbol{E}(\boldsymbol{r}')))\, \boldsymbol{dr}' \quad (2.2.22)$$

The last equation, gives the SA as a function insider the scatterer, which is yet to be evaluated. At this point one can go forward and use the Rayleigh method[4].

2.2.1.1 Rayleigh Scattering

Single scattering phenomena are distinguished depending on the size of the scatterer compared to the wavelength of the propagating radiation. When the scatterer is smaller than the wavelength Rayleigh scattering (RS) occurs[4], [5].

We are all accustomed to Raleigh scattering in our daily lives, since it is the main mechanism that makes our sky blue. RS depends on $\sigma \sim 1/\lambda^4$, therefore the shorter wavelength of the visible light will be scattered mostly by the molecules of the atmosphere, which are roughly a few nm in size. So sun light that travels through the atmosphere is diffusing on the whole atmosphere making the sky appear blue.

Building on the equation (2.2.22), we now know that the scatterer is a dielectric sphere, with a radius r and with a dielectric constant ε_r, inside an electric field $\boldsymbol{E} = E_0\hat{\boldsymbol{z}}$**.** To find the electric field inside the sphere, one needs to solve the Laplace equation (2.2.2).

The potential in such a case V(r) will be: $\nabla^2 V = 0$, solving the problem in spherical coordinates.

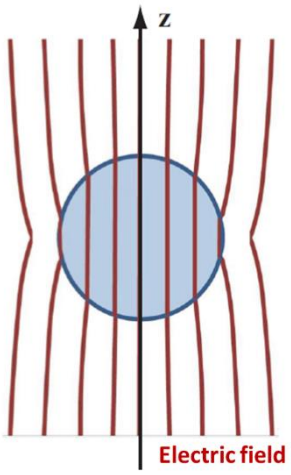

Figure 10 :The electric field lines insider a dielectric sphere.

$$\nabla^2 V = \frac{1}{r^2}\frac{\partial}{\partial r}\left(r^2\frac{\partial V}{\partial r}\right) + \frac{1}{r^2\sin\theta}\frac{\partial}{\partial\theta}\left(\sin\theta\,\frac{\partial V}{\partial\theta}\right) = 0 \ (2.2.23)$$

Where ϕ dependence is considered to be zero because of the symmetry problem. Dividing the variables, this means the potential has the form V(r,θ)=R(r)P(θ) , expressed in simpler terms:

$$\frac{1}{R}\frac{d}{dr}\left(r^2\frac{dR}{dr}\right) = -\frac{1}{P\sin\theta}\frac{d}{d\theta}\left(\sin\theta\frac{dP}{d\theta}\right) \ (2.2.24)$$

We separate the two parts by equaling them with a constant value k. We can do this since each part of the equation is depended on a different variable.

$$-\frac{1}{P\sin\theta}\frac{d}{d\theta}\left(\sin\theta\frac{dP}{d\theta}\right) = k \ (2.2.25)$$

We can consider k to be an integer, k=(n+1)n , for the n=0,1,2 the solutions will be the first Legendre polynomials.

Continuing with the R depended part:

$$\frac{1}{R}\frac{d}{dr}\left(r^2\frac{dR}{dr}\right) = n(n+1) \rightarrow \frac{d}{dr}\left(r^2\frac{dR}{dr}\right) = n(n+1)R \ (2.2.27)$$

This differential equation has as solutions r^n and $r^{-(n+1)}$. Consequently the solution of Poisson equation will have the general form

$$\psi_1 = r^n P_n(\cos\theta) \ (a) \text{ and } \psi_1 = r^{-(n+1)}P_n(\cos\theta) \ (b) \ (2.2.28)$$

For the first order solution (n=1) we have the solution for the inside and outside of the sphere.

$$V_{in} = A_{in} r\cos\theta + B_{in}\frac{1}{r^2}\cos\theta \ (a)$$

$$V_{out} = A_{out} r\cos\theta + B_{out}\frac{1}{r^2}\cos\theta \ (b) \ (2.2.29)$$

Employing boundary conditions, the potential must be zero at infinity, the above result;

$$V_{in} = Ar\cos\theta \ (a)$$

$$V_{out} = -Er\cos\theta + \frac{B}{r^2}\cos\theta \ (b) \ (2.2.30)$$

One more boundary condition, its potential must be level on the sphere, so:

$$Aa = -E_0 a + \frac{B}{a^2} \ (2.2.31)$$

And the electric deposition D must be perpendicular on the surface and it must be constant. For the radial contribution, the form is:

$$D_r = -\varepsilon \frac{\partial V}{\partial r} \quad (2.2.32)$$

So next step is to evaluate the inside and the outside of the sphere, assuming:

$$D_{r,in} = -\varepsilon_0 \varepsilon_r A cos\theta \quad (2.2.33)$$

$$D_{r,out} = \varepsilon_0 \left(-E_0 \cos\theta - \frac{2B}{r^3} \cos\theta \right) \quad (2.2.34)$$

Concluding that:

$$A = -\frac{3E_0}{\varepsilon_r + 2} \ \ and \ \ B = \frac{\varepsilon_r - 1}{\varepsilon_r + 2}$$

So the electric field inside the sphere will be

$$\boldsymbol{E_s} = \frac{3}{\varepsilon_r + 2} \boldsymbol{E_0} \quad (2.2.35)$$

Rayleigh Approach

Now having done the necessary math we can go on and generate Raleigh scattering. We use the calculations above, with the difference that the outer field is on z direction and the amplitude is one.

$$\boldsymbol{E_i} = \hat{\boldsymbol{z}}\, e^{-ikx} \quad (2.2.36)$$

Using equation (2.2.35), the electric field inside the scatterer will be:

$$\boldsymbol{E_s} = \frac{3}{\varepsilon_r + 2} \boldsymbol{E_i} \quad (2.2.37)$$

We take the SA from the equation (2.2.22):

$$\boldsymbol{f} = \frac{k^2}{4\pi} V \frac{3(\varepsilon_r - 1)}{\varepsilon_r + 2} \left(\hat{\boldsymbol{z}} - \hat{\boldsymbol{r}} (\hat{\boldsymbol{r}} \hat{\boldsymbol{z}}) \right) \quad (2.2.38)$$

V is the volume of the sphere. The differential cross section will be according to (2.2.13)

$$\frac{d\sigma}{d\Omega} = \frac{k^4}{(4\pi)^2} \left| \frac{3(\varepsilon_r - 1)}{\varepsilon_r + 2} \right|^2 V^2 \sin^2\theta \quad (2.2.39)$$

And the total cross section:

$$\sigma = \int \frac{d\sigma}{d\Omega} d\Omega = \frac{128\pi^5 a^6}{3\lambda^4} \left| \frac{3(\varepsilon_r - 1)}{\varepsilon_r + 2} \right|^2 \quad (2.2.40)$$

2.2.1.2 Mie Scattering

Mie scattering is also known as the Lorenz–Mie solution or the Lorenz–Mie–Debye solution[4,5] . When the scatterer is comparable to the wavelength or a bit larger, we use the Mie theory to describe its propagation. There are no approximations here, so the spherical Bessel function will be required. The scatterer is considered to be spherical or ellipsoid. The general wave equation like (2.2.6) is

$$\nabla^2 u = \frac{1}{c^2}\frac{\partial^2 u}{\partial t^2} \quad (2.2.41)$$

Separating the time dependent part with the spatial coordinate part as we did in (2.2.16), we take two different equations: the Helmholtz equation and the harmonic time dependence

$$\nabla^2 u + k^2 u = 0 \quad (2.2.42)$$

$$\frac{\partial^2 u}{\partial t^2} = -\omega^2 u \quad (2.2.43)$$

Where we replaced k=ω/c and k is the wavenumber. The general solution to the Helmholtz equation is spherical harmonics will be the solutions to each of the three differential equations below.

$$\left(\frac{d^2}{d\varphi^2} + m^2\right)\Phi(\varphi) = 0 \quad (2.2.44)$$

$$\left[(1-\chi^2)\frac{d^2}{dx^2} - 2x\frac{d}{dx} + \left(l(l+1) - \frac{m^2}{1-x^2}\right)\right]P_l^m(x) = 0 \quad (2.2.45)$$

$$\left[z^2\frac{d^2}{dz^2} + 2z\frac{d}{dz} + \left(z^2 - l(l+1)\right)\right]j_l(z) = 0 \quad (2.2.46)$$

Equation (2.2.44) has as solutions exponentials $e^{\pm im\varphi}$ where m=0, $\pm 1, \pm 2$ …

Equation (2.2.45) has the first and second type polynomial Legendre as a solution, where x=cosθ and l=0,1,…

Equation (2.2.46) is solved by spherical Bessel functions of the first and second type, $j_l(kr)$ and $n_l(kr)$

To sum up, the general solution of Helmholtz equation (2.2.42) is:

$$u(r,\theta,\varphi) = \sum_{l=0}^{\infty}\sum_{m=-l}^{l}[a_{lm}j_l(kr) + b_{lm}n_l(kr)][c_{lm}P_l^m(\cos\theta) + d_{lm}Q_l^m(\cos\theta)][c_{lm}\cos m\varphi + f_{lm}\sin m\varphi] \quad (2.2.47)$$

Where $a_{lm}, b_{lm}, \ldots f_{lm}$, are constants that are defined by the boundary conditions. In the case of scattering u(r,θ,ϕ) it is the electric field (or the magnetic field). Using the above equations, we can evaluate the SA and CS of scatterer. The actual solutions are difficult to

calculate and when multiple scatterers exist, it is impossible to solve just with numerical solutions.

One important result of Mie scattering is the existence of resonances. Those resonances are not only depending on the wavelength, but also the size of the scatterer. Therefore, it can be used as a tool to measure the size of a particle.

Mie and Rayleigh scattering differ in many ways. Mie scattering is roughly depended on the wavelength, this is why f.e. light that is scattered from droplets appears as a white/gray color that means it's been scattered all the colors same way. Additionally, more light will travel through in Mie than in Rayleigh scattering. In general the bigger the scatterer, the

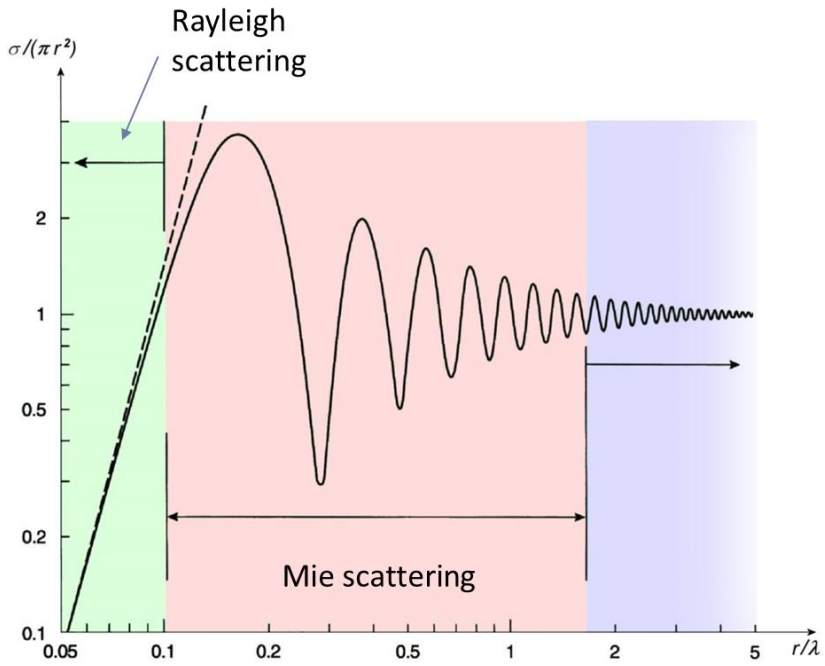

Figure 11 Scattering regimes. Every color define a different response of light for the size of the scatterer compared to the wavelength

more light will pass through.

On the figure [11] we can see that the regions of scattering.

2.2.2. Multiple Scattering

So now that we have covered the basic single scattering theory, particularly how light propagates when there is only one scatterer, we can we move on to the regime where multiple scattering occurs. When multiple scattering occurs, the density of the scatters is too high and the one scattering event is connected with the many other scattering events. The resulting image of light propagating through is a halo of light, diffusing in the whole volume of the material. Hiding any information of the interior structure or what is behind the medium.

But how can we quantify the regime of scattering we face? The question depends on the density of the scatterers existing inside a volume of smooth refractive indexes (Air, glass etc). So we need to know the volume of a scatterer v_s , their total number N_s and the volume V at which they are dispersed. So we conclude the density of scatters is:

$$\rho = \frac{N_s v_s}{V} \quad (2.2.48)$$

So from the values defined by the above equation, we can conclude the regimes we are working with:

- ρ<0.1% Single scattering regime.
- ρ~ 1% Equation of transfer needs to be solved.
- ρ>>1% Diffusion regime, the model best used is diffusion approximation. But on this regime, biological tissues exist. Plus the modern application of wavefront shaping and use of wavefront shaping are referred on this regime.

I will continue with describing the basic models that are used, including the diffusion approximation and how some variables that occurs (scattering free path, scattering coefficient etc.) and there will be some qualitative analysis of wave equation in mesoscopic regimes.

We begin with the diffusion approximation first, but this means we first have to take a look at the transport theory (TT). It was developed by Chandrasekhar (~1960) and gives satisfactory results for low scatterer s distribution ρ~1. In the framework of TT the wave nature of light is ignored, it deals only with energy transport. At the limit of high density of the scatterers, diffusion approximation of TT is implied to describe light behavior traveling through the scatterer. In general the interference phenomena are excluded from this model, although there are modifications on this framework to introduce interference. The simulations that make use of diffusive theory are usually Monte Carlo simulations.

There is an approach to describe light propagation through scattering called analytical theory. We begin with Maxwell equations (2.2.2)-(2.2.5) and by introducing scattering and absorption behavior we obtain correlation and variance functions, statistical quantities in integral and differential form. This approach is really hard to be solved, since it must be solved for every scatterer. But in today's computing it is possible to obtain light behavior in a well-defined scattering medium with Finite difference time domain algorithms (FDTD).

These two theories (TT and AT) describe the same phenomena in a different ways. So bridges exist between the two theories. So a Fourier transform of specific intensity used in TT (we will define that below) exist between mutual coherence function in AT (also explained below)[4].

.

2.2.2.1 Transport Theory of Radiation (Basic Notations)

In order to describe a scattering medium properly, one does not only have to consider the density of the scatterers but also the scattering free path (minimum distance between to scattering events), and the scattering coefficient etc. These parameters are defined through an approximation of the Transport Theory of radiation the diffusion approximation. Before we see this approximation, we need to cover the basic notation or TT and define the main function of description. We no longer talk in terms of electric and magnetic field here, but of specific intensity.

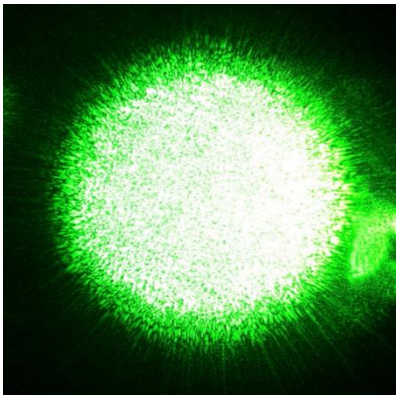

Figure 12 Speckle pattern.

TT was first initiated in 1903 by Schuster, and used to be called radiative transfer theory as well. A statistical differential equation was later formulated by Chandrasekhar in 1950. It deals directly with energy propagation through a scattering medium (tenuous distribution)[4], [5] [6].

Specific intensity.

The main quantity of studying in TT is called specific intensity, radiance or brightness and in modern literature is called spectral radiance. For its definition, we consider a wave of energy propagating at point **r** in a medium.

The wave carries frequency ω, phase ϕ, and amplitude A. All these quantities while propagating inside the medium vary thought time, with the result that the power flux vector (pointing vector in terms of electromagnetic wave) varies through time in terms of magnitude and direction.

For a random direction **s**, we can find the average power flux intensity for a frequency band Δv around v and within a unit solid angle ω. This is called specific intensity **I(r,s)** and its dimension are $Wm^{-2}\ sr^{-1}\ Hz^{-1}$.

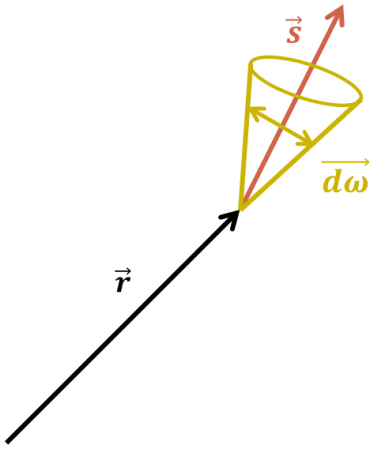

Figure 13 Wave propagating in a medium. At position r , we define the specific intensity for a direction s the average power flux intensity for a frequency band Δv around v and within a unit solid angle ω

Power Flux

The next required quantity is flux. The amount of power dP flowing within a dω solid angle, through an elementary area dα oriented in a direction of unit vector $\mathbf{s_o}$ in a frequency interval (v,v+dv) is therefore given by :

$$d\boldsymbol{P} = \boldsymbol{I}(\boldsymbol{r}, \hat{\boldsymbol{s}}) \cos\theta \; d\alpha \; d\omega \; dv \quad (2.2.49) \text{ (Watts)}$$

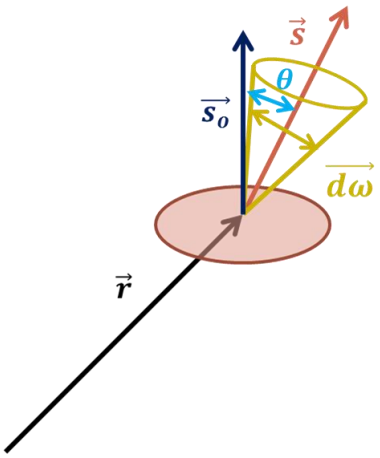

*Figure 14 Power Flux definition. Having defined specific intensity, we measure how much power for **s** direction is propagating through and are a da on the direction s_0.*

Total Flux

The total flux emitted by a surface da of a large surface A can be defined as the summing of the specific intensity for each angle of the direction **s** to the vector of the differential surface da, $\mathbf{s_0}$. ($0 \leq \theta \leq \frac{\pi}{2}$)

$$\text{Where: } \boldsymbol{F}_+(\boldsymbol{r},\widehat{\boldsymbol{s_o}}) = \int_{2\pi_+} \mathbf{I}(\boldsymbol{r},\widehat{\boldsymbol{s_o}})\,\hat{\mathbf{s}}\cdot\widehat{\boldsymbol{s_o}}\,d\omega \quad (2.2.50.a) \text{ and } \hat{\mathbf{s}}\cdot\widehat{\boldsymbol{s_o}} = \cos\theta$$

There is also the backward flux density F_ , for flux propagating on the opposite direction.

$$\boldsymbol{F}_-(\boldsymbol{r},\widehat{\boldsymbol{s_o}}) = \int_{2\pi_-} \mathbf{I}(\boldsymbol{r},\widehat{\boldsymbol{s_o}})\,\hat{\mathbf{s}}\cdot(-\widehat{\boldsymbol{s_o}})\,d\omega \quad (2.2.50.b)$$
$$\text{(Here } \frac{\pi}{2} \leq \theta \leq \pi)$$

The quantities F+ and F_ have the dimensions of Wm-2 Hz-1. The total flux density is defined as the difference of those two variables, or in a more compact way as:

$$\boldsymbol{F}(\boldsymbol{r}) = \int_{4\pi} \boldsymbol{I}(\boldsymbol{r},\hat{\boldsymbol{s}})\hat{\boldsymbol{s}}\,d\omega \quad (2.2.51)$$

And this is the net flux for surface A.

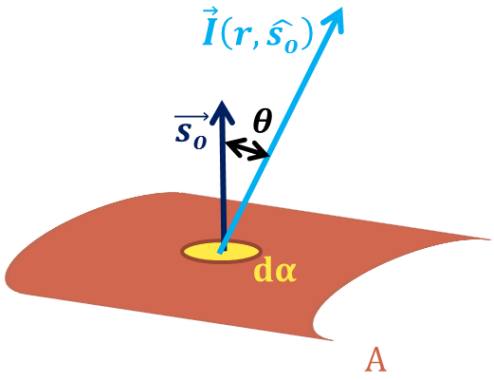

Figure 15 Total flux definition. Having defined specific intensity, we measure what is the net power flux propagating through and are a da.

Energy Density

The final quantity to define is energy density, u**(r)** at **r.** This means the amount of energy that passes a small area da in dt, at an angle dω within the (v, dv) will be I da dω dv dt, (I is specific intensity).
The volume this energy occupies will be da(c dt). Therefor du is defined as:

$$du(\boldsymbol{r}) = \frac{I\, da\, d\omega\, dv\, dt}{da\, c\, dt} = \frac{\boldsymbol{I}(\boldsymbol{r}, \hat{\boldsymbol{s}})\, d\omega}{c} \quad (2.2.52)$$

So integration in all angles is:

$$\left(\boldsymbol{r},\ \right) = \frac{1}{c} \int_{4\pi} \mathbf{I}(\boldsymbol{r}, \widehat{\boldsymbol{s_0}})\, \hat{\boldsymbol{s}} \cdot d\omega \quad (2.2.53)$$

If there is isotropic radiation, this means there is no dependence on the direction of s then the power radiated from da for a random s direction will be equal to:

$$P = (I\ da) \cos\theta = P_0 \cos\theta \quad (2.2.53)$$

To conclude our analysis we will look at the differential equation of specific intensity. Every major physics problem is a differential equation in need to be solved. For example in Newtonian mechanic F=ma, in quantum mechanics it is the Schrödinger equation etc. Working on this framework we need to define and work on the differential equation.

For convenience, we consider a cylindrical elementary volume with a unit cross section and length ds. Then specific intensity I(r,s) is incident upon it. The volume will contain ρds particles (ρ is number density, particles density). Every particle will absorb σ_αI and scatters σ_sI power. So while radiation propagates in, there will be a reduction:

$$d\boldsymbol{I}(\boldsymbol{r}, \boldsymbol{s}) = -ds(\sigma_\alpha + \sigma_s)\boldsymbol{I} = -\rho ds\, \sigma_t \mathbf{I} \quad (2.2.54)$$

But there will be some increase of power because other particles will scatter along s and an estimation is needed for this contribution.
The incident flux density through a small angle dω is S_i=**I(r,s')** dω' . The particles will scatter the flux. For a given direction **s** at a distance R from the particle the density flux will be:

$$S_r = \frac{[f(\boldsymbol{s}, \boldsymbol{s}')]^2}{\boldsymbol{R^2}} \boldsymbol{S_i} \quad (2.2.55)$$

f**(s,s')** is the scattering amplitude, from the equation (2.2.22). So the scattered specific intensity on **s** direction will be:

$$\boldsymbol{R^2} S_r = |f(\boldsymbol{s}, \boldsymbol{s}')|^2 \boldsymbol{S_i} = |f(\boldsymbol{s}, \boldsymbol{s}')|^2 \boldsymbol{I}(\boldsymbol{r}, \boldsymbol{s}') d\omega' \quad (2.2.56)$$

We add the incident flux for every possible **s'** direction to the **s** direction.

$$\boldsymbol{R^2 S_r} = \int_{4\pi} \rho |f(\boldsymbol{s}, \boldsymbol{s'})| \boldsymbol{I}(\boldsymbol{r}, \boldsymbol{s'}) d\omega' \boldsymbol{ds} \quad (2.2.57)$$

We make use of the phase function, which equals with:

$$p(\boldsymbol{s}, \boldsymbol{s'}) = \frac{4\pi}{\sigma_t} \left| f\ (\boldsymbol{s}, \boldsymbol{s'}) \right|^2 \quad (2.2.58)$$

Adding all the contributions in one equation (plus one possible internal source contribution) results in the equation of transfer:

$$\frac{d\boldsymbol{I}(\boldsymbol{s}, \boldsymbol{s'})}{ds} = -\rho\ \sigma_t I(\boldsymbol{r}, \boldsymbol{s}) + \frac{\rho\sigma_t}{4\pi} \int_{4\pi} p(s, s') \boldsymbol{I}(\boldsymbol{r}, \boldsymbol{s'}) d\omega' + \varepsilon(\boldsymbol{r}, \boldsymbol{s}) \quad (2.2.59)$$

The particle density and size can differ with distance, so $\rho\sigma_t$ and p can be functions of **r.** A length variable can be defined τ, called optical length. At value 1, the intensity will be reduced 1/e, determined by equation (2.2.54).

$$\tau = \int \rho \sigma_t ds \quad (2.2.60)$$

Where τ is optical distance before I exponential diminish (free path).

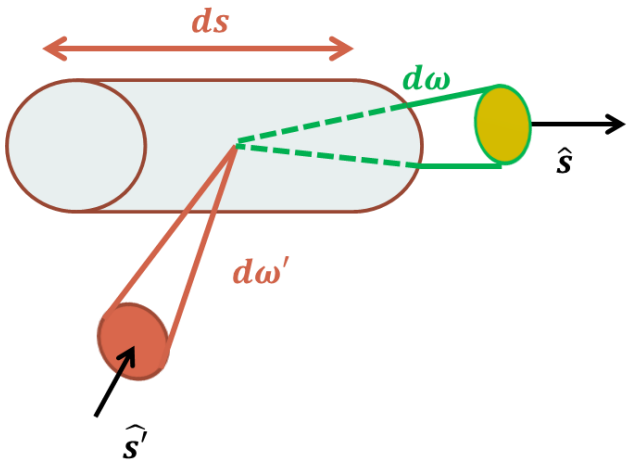

Figure 16 Total flux definition. Having defined specific intensity, we measure what is the net power flux propagating through and are a da

Diffusion Approximation

However, the above equation (2.2.58) of radiation transfer fails to describe the propagation of light in a highly scattering medium (density of scatterers more than 1%). If this is the case, someone has to move on to diffusion approximation and repair the damage.
Since RTE has six depending variables (x,y,z,θ,ϕ,t) it is impractical to be solved exactly. In diffusion approximation the medium is considered to be almost non-absorbing and after some sufficient scattering events, it is considered as isotropic.

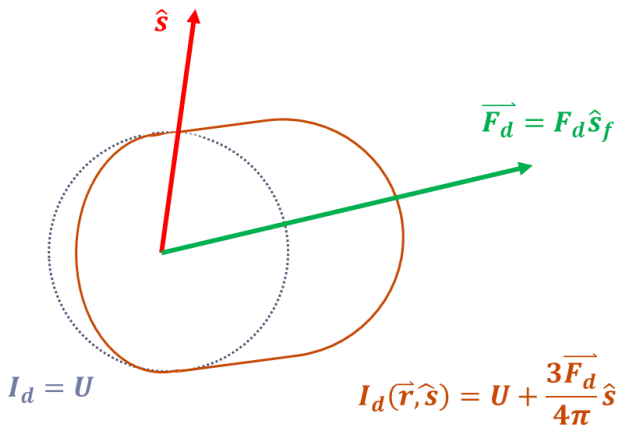

Figure 17 The diffuse intensity Id in diffuse approximation

The total specific intensity propagating through a medium will be:

$$I(\boldsymbol{r},\boldsymbol{s}) = I_d(\boldsymbol{r},\boldsymbol{s}) + I_{ri}(\boldsymbol{r},\boldsymbol{s}) \quad (2.2.61)$$

Where $I_{ri}(\boldsymbol{r},\boldsymbol{s})$ is the parameter of losses, the well-known follows Beer's law:

$$I_{ri}(\boldsymbol{r},\boldsymbol{s}) = I_i(\boldsymbol{r_0},\boldsymbol{s})\, e^{-\tau} \quad (2.2.62)$$

And $I_d(\boldsymbol{r},\boldsymbol{s})$ describes the scattering intensity given by transport equation:

$$\frac{d\boldsymbol{I_d}(\boldsymbol{s},\boldsymbol{s'})}{ds} = -\rho\,\sigma_t \boldsymbol{I_d}(\boldsymbol{r},\boldsymbol{s}) + \frac{\rho\sigma_t}{4\pi}\int_{4\pi} p(s,s')\boldsymbol{I_d}(\boldsymbol{r},\boldsymbol{s'})d\omega' + \varepsilon(\boldsymbol{r},\boldsymbol{s}) + \varepsilon_{ri}(\boldsymbol{r},\boldsymbol{s}) \quad (2.263)$$

A source term describing the reduced intensity I_{ri}

$$\varepsilon_{ri}(\boldsymbol{r},\boldsymbol{s}) = \frac{\rho\sigma_t}{4\pi}\int_{4\pi} p(\boldsymbol{s},\boldsymbol{s'})\boldsymbol{I_{ri}}(\boldsymbol{r},\boldsymbol{s'})d\omega \quad (2.2.64)$$

We assume that the diffuse intensity will be scattered almost uniformly in all directions. But there must be a favorable direction, otherwise the net energy flux would be zero. This means:

$$I_d(\boldsymbol{r},\boldsymbol{s}) \approx U_d(\boldsymbol{r}) + c\boldsymbol{F_d}(\boldsymbol{r}) \cdot \boldsymbol{s} \quad (2.2.65)$$

Where c is a constant, which is found to be 3/4π. And the diffuse flux will be:

$$\boldsymbol{F_d}(\boldsymbol{r}) = \int_{4\pi} \boldsymbol{I_d}(\boldsymbol{r},\boldsymbol{s}) \cdot \boldsymbol{s} d\omega = \boldsymbol{F_d}(\boldsymbol{r})\boldsymbol{s_f} \quad (2.2.66)$$

$U_d(\mathbf{r})$ is the average diffuse intensity.

$$U_{\boldsymbol{d}}(\boldsymbol{r}) = \frac{1}{4\pi}\int_{4\pi} \boldsymbol{I_d}(\boldsymbol{r},\boldsymbol{s})d\omega \quad (2.2.67)$$

Integrating the scattered intensity over all 4π of soling angle we get:

$$\boldsymbol{\nabla F_d}(\boldsymbol{r}) = -4\pi\,\rho\,\sigma_\alpha\,\mathrm{U}(\mathbf{r}) + 4\pi\rho\sigma_\mathrm{s}\,\mathbf{U_{ri}} + \mathbf{E}(\mathbf{r}) \quad (2.2.68)$$

$$\mathrm{U_{ri}} = \frac{1}{4\pi}\int_{4\pi} \mathbf{I}_{ri}(\mathbf{r},\mathbf{s})d\omega \quad (2.2.69)$$

$$\mathrm{E(r)} = \int_{4\pi} \varepsilon(\boldsymbol{r},\boldsymbol{s})d\omega \quad (2.2.70)$$

$U_d(\mathbf{r})$ is the average diffuse intensity.

$$U_{\boldsymbol{d}}(\boldsymbol{r}) = \frac{1}{4\pi}\int_{4\pi} \boldsymbol{I_d}(\boldsymbol{r},\boldsymbol{s})d\omega \quad (2.2.71)$$

Where specific intensity is the one we approximate with:

$$I_d(\boldsymbol{r},\boldsymbol{s}) \approx U_d(\boldsymbol{r}) + c\boldsymbol{F_d}(\boldsymbol{r})\cdot\boldsymbol{s} \quad (2.2.72)$$

Returning to scattered intensity equation:

$$\left(\boldsymbol{s}\cdot\boldsymbol{\nabla}U_d\right) + \frac{3}{4\pi}\boldsymbol{s}\,\boldsymbol{\nabla}\left(\boldsymbol{F_d}\cdot\boldsymbol{s}\right) = -\rho\sigma_\mathrm{t}\mathrm{U_d} - \frac{3}{4\pi}\rho\sigma_\mathrm{t}\left(\boldsymbol{F_d}\cdot\boldsymbol{s}\right) + \rho\sigma_\mathrm{s}\mathrm{U_d} + \frac{3}{4\pi}\rho\sigma_\mathrm{t}\left(\boldsymbol{F_d}\cdot\boldsymbol{s}\right)\mathrm{p}_1 + \varepsilon_\mathrm{ri} + \varepsilon \quad (2.2.73)$$

Where p_1 represents the average forward scattering minus the backward scattering of a single particle.

$$\mathrm{p}_1 = \frac{1}{4\pi}\int_{4\pi} p(\boldsymbol{s},\boldsymbol{s}')\boldsymbol{s}\cdot\boldsymbol{s}'d\omega' \quad (2.2.74)$$

The Phase function can be approximated with various simpler functions.

If we multiply with **s** and integrate all over 4π, we obtain

$$\boldsymbol{\nabla}U_d = -\frac{3}{4\pi}\rho\sigma_t(1-p_1)\boldsymbol{F_d} + \frac{3}{4\pi}\rho\sigma_\mathrm{t}\left(\boldsymbol{F_d}\cdot\boldsymbol{s}\right) + \int_{4\pi}\varepsilon(\boldsymbol{r},\boldsymbol{s})\boldsymbol{s}d\omega + \int_{4\pi}\varepsilon_{ri}(\boldsymbol{r},\boldsymbol{s})\boldsymbol{s}d\omega \quad (2.2.75)$$

$\sigma_t(1-p_1)$ The transport cross section σ_{tr}.

Combining and eliminating flux density,

$$\boldsymbol{\nabla} \cdot \boldsymbol{F_d}(\boldsymbol{r}) = -4\pi\,\rho\,\sigma_\alpha\,\mathrm{U}(\mathbf{r}) + 4\pi\rho\sigma_\mathrm{s}\,\mathrm{U}_\mathrm{ri} + \mathrm{E}(\mathrm{r}) \quad (2.2.76)$$

will result in a differential equation of U_d.

The differential equation of U_d is the fundamental steady state diffusion equation.

$$\boldsymbol{\nabla^2} U_d(r) - \kappa_d^2 U_d(\boldsymbol{r}) = -3\rho\sigma_s\rho\sigma_{tr}U_{ri}(\boldsymbol{r}) - \frac{3}{4\pi}\rho\sigma_{tr}E(\boldsymbol{r}) + (\boldsymbol{r}) + \frac{3}{4\pi}\nabla \cdot \int_{4\pi} \varepsilon_{ri}(\boldsymbol{r},\boldsymbol{s})\boldsymbol{s}d\omega + \frac{3}{4\pi}\nabla \cdot \int_{4\pi} \varepsilon(\boldsymbol{r},\boldsymbol{s})\boldsymbol{s}d\omega \quad (2.2.77)$$

Where $\kappa_d = 3\rho\sigma_\alpha\rho\sigma_{tr}$

This equation is called fundamental steady state diffusion equation, it describes the average diffuse intensity $U_d(\boldsymbol{r})$ combining with appropriate boundary conditions concludes the mathematical formalism.

2.2.2.2 Multiple Scattering Theory with Analytical Theory

The last approach, analytical theory (AT) solves the Maxwell equations by implying statistical implements. This work was made by a number of scientists, starting in 1931 with Ryde and Cooper, to 1977 with Ishimaru. This approach is a link between TT and AT. It considers the correlation of the field, a very important phenomenon in the mesocopic regime. Although AT can include time depended media, we will skip this part, since it is out of the scope of this work[4].

We consider a distribution of scatterers, r_1, r_2, r_3,..., r_N in a volume V. A scalar field ψ^α at r_a. The point r_a is a point inside the medium. The Helmholtz equation is:

$$(\nabla^2 + k^2)\psi = 0 \quad (2.2.78)$$

Where k is the wavenumber $k=2\pi/\lambda$ for the surrounding medium. The ballistic part (the non scattered field, We consider the field reaches r_a before there is any scattering.) incident wave function is defined as φ_i^a. The field ψ^α at r_a, since the fields can be super positioned, will be the ϕ_i and the contribution U_s^a from all the N particles consisting the medium.

$$\psi^\alpha = \varphi_i + \sum_{s=1}^{N} U_s^a \quad (2.2.79)$$

Where U_s^a

$$U_s^a = \{u_s^a \Phi^s\} \quad (2.2.80)$$

Equation (2.2.80) describes the wave emitted from the scatter S to the position r_a. Φ_s is the incident wave on the scatterer S. The quantity u_s^a is the scattering characteristics of the scatterer S to the direction r_a.

The {} denotes that this is no real product. In a far field approximation, r_s-r_a>>0 and Φs are approximated like a planar wave propagating for a given direction i.

$$\Phi^s = e^{i\boldsymbol{k}\boldsymbol{r}} \quad where\ \boldsymbol{k} = k\hat{\boldsymbol{i}} \quad (2.2.81)$$

Then using the far filed approximation, u_s^a is:

$$u_s^a \approx f(\hat{\boldsymbol{q}}, \hat{\boldsymbol{i}})\frac{e^{ikr}}{r} \quad with\ r = |r_a - r_s| \quad (2.2.82)$$

q is a unit vector in the direction of $\boldsymbol{r_a} - \boldsymbol{r_s}$ and $f(\hat{\boldsymbol{q}}, \hat{\boldsymbol{i}})$ the scattering amplitude for the scatter S.

Φs on the other hand can be the contribution of the initial beam and the scattering field from the rest of the scatterers. So it will have a form similar to equation (2.2.79).

$$\Phi^S = \Phi_i^s + \sum_{t=1,\ s\neq t}^{N} U_t^s \quad (2.2.83)$$

Combining (2.2.79) and (2.283) we can derive the field for r_a.we

$$\psi^\alpha = \varphi_i \ + \sum_{s=1}^{N} u_s^a \left(\Phi_i^s + \sum_{t=1,\ s\neq t}^{N} u_t^s \Phi^t \right) \rightarrow$$

$$\psi^\alpha = \varphi_i \ + \sum_{s=1}^{N} u_s^a\, \varphi_i^s + \sum_{s=1}^{N} \sum_{st=1,\ s\neq t}^{N} u_s^a u_t^s \varphi_i^t + \ldots \quad (2.2.84)$$

The first term on equation (2.284) describes the incident wave. The second term is the contributions from the scatters, but only from the initial wave. The terms after that describe the contributions from each scatterer. These fields come about from the scattered fields scattered back to the scatterer. The specific term for this is ~~the~~ double scattering.

In general (2.2.48) is the sum of two groups. The first describes multiple scattered light from all the whole medium. It is clear from the sheer number of contributions how difficult it is to compute that. The second group measures the contributions of multiple scattering light from the same scatter back and forth.

An approach to solve the problem was introduced by Twersky, which neglects the second group. This approach is valid in cases with little backscattering (Mie regime). There are many complicated methods to solve each problem. Today the use of the numerical approaches such as the Monte Carlo simulations for the diffusion equation or the Finite Difference Time Domain (FTDT) can give us the exact electric field evolution[7],[8].
For this reason, we skip any other details and move on to some general responses and quantitative values describing a scattering medium, focusing on the mesoscopic regime.

2.2.2.3 Scattering of Light in the Mesoscopic Regime

The definition of the mesocopic regime usually ranges between a few μm to some mm. In terms of electron diffusion, mesocopic regime is the intermediate between molecules to bulk, where inelastic scattering is not dominant. In general with light waves, this cover bulks, where coherent light travels through the medium and and still retains its coherence and phase memory, we can observe what is known as a speckle pattern[9].

Speckle pattern is that grainy pattern of light; TT describes how the intensity is spreading while propagating through a scattering medium. But what we actually see with coherent

light is that the halo is composed of light grains. This grains are local of constructive interference of light. Different light wave fronts meet at a specific point and since are in a phase, constructive interference occurs. The speckle pattern it's correlated over a distance l no matter how much the wave travels.

Although we cannot see what is behind the medium, the information actually is scrambled inside that speckle pattern. With the use of wavefront shaping techniques, exploiting interference phenomena (memory effect) or algorithms, image reconstruction behind a scattering medium has been achieved these days.

The strength of a scattering medium is usually described by the mean free path l_s.
It describes the average distance light travels inside a scattering medium before it undergoes a scattering event.
Another quantity usually used, is called scattering coefficient, which is linked by the equation[10] (2.2.85)

$$l = \frac{1}{\mu_s} \quad (2.2.85)$$

The scattering coefficient is linked by the equation (2.2.59)

$$\mu_s = \frac{\rho\sigma_t}{4\pi} \quad (2.2.59)$$

And by the evaluating this factors, one can measure it experimentally.

Another interesting parameter is Thouless time of the medium τ. The medium is considered to be non-absorbing and the energy is transmitted from one edge to the other. These parameters describe how much time light spent inside the medium, so another important parameter is the medium thickness L.

$$\tau = \frac{L^2}{l_s v_e} \quad (2.2.60)$$

Where v_e is the energy velocity (in this case the light speed inside the medium). Thouless time is connected to the average speckle size and the bandwidth of each speckle.

On this regime we are considering the light propagating as a wave, so we use the wave equation from (2.2.6):

$$\nabla^2\Psi(r,t) = \frac{n^2(r)}{c^2}\frac{\partial^2\Psi(\boldsymbol{r},t)}{\partial t^2} \quad (2.2.61)$$

Where n(r), this means variations of refractive index include the scattering events. It can be shown by using the Green function of a system that there is a specific number of modes that light can travel through in a medium with constant n or n(r) [].
But a more simple approach can create the same result, by thinking how many wavelengths can be spaced in a medium with area A.

$$N_s = \frac{2\pi A}{\lambda^2} \quad (2.2.62)$$

That means for a visible light we can have 10 million of modes per mm^2. This means that if a wave crosses this medium, it will be coupled to these modes, so the wave inside the medium will be the linear combination of these media. In other words, these modes are the eigenfunctions of the transmission matrix of the medium.

$$E_m^{out} = \sum_{n=1}^{N} t_{mn}\, A_n\, e^{i\varphi_n} \quad (2.2.63)$$

But those modes can support a certain bandwidth, which is dependent on Thouless time. Which means, in every mode waves of specific bandwidth can couple inside.

$$\delta\omega = \frac{1}{\tau} \quad (2.2.64)$$

Eventually the total number of independent modes that transverse inside the medium for a given wave with bandwidth of ΔΩ will be:

$$N_f = \frac{\Delta\Omega}{\delta\omega} \quad (2.2.65)$$

Concluding that the product $N_s N_f$ is the number of the total independent modes that can be transmitted in a given medium for a given spectrum.

The average speckle size, it has been shown, will on average have a size:

$$\delta x \approx \frac{\lambda}{2\, n(r)} \quad (2.2.66)$$

This was shown in the work of Vellekoop, Lagendijk and Mosk. Where they proved the shape of the speckle is predicted by the van Cittert-Zemike Theorem[11]. We close the discussion here, and continue in section 2.4 with the applications on wavefront shaping through scattering media.

Reference

1. Hecht, E. *Optics*. (Addison-Wesley, 2002). at <http://books.google.gr/books?id=7aG6QgAACAAJ>

2. Lagendijk, A., Tiggelen, B. Van, Wiersma, D. S. & Anderson, P. W. Fifty years of Anderson localization. (2009).

3. Griffiths, D. J. *Introduction to Electrodynamics*. (Prentice Hall, 1999). at <http://books.google.co.in/books?id=M8XvAAAAMAAJ>

4. Ishimaru, A. *Wave Propagation and Scattering in Random Media*. (Wiley, 1999). at <http://books.google.gr/books?id=wAZnuHdEKL0C>

5. Wang, L. V & Wu, H. *Biomedical Optics: Principles and Imaging*. (Wiley, 2007). at <http://books.google.gr/books?id=RKukklVYAY4C>

6. Cheong, W. F., Prahl, S. A. & Welch, A. J. A review of the optical properties of biological tissues. *Quantum Electron. IEEE J.* **26,** 2166–2185 (1990).

7. Gedney, S. D. *Introduction to the Finite-Difference Time-Domain (FDTD) Method for Electromagnetics*. *Synthesis Lectures on Computational Electromagnetics* **6,** 1–250 (2011).

8. Choi, W., Mosk, A. P., Park, Q. H. & Choi, W. Transmission eigenchannels in a disordered medium. *Phys. Rev. B* **83,** (2011).

9. Sheng, P. *Introduction to Wave Scattering, Localization and Mesoscopic Phenomena: Localization and Mesoscopic Phenomena*. (Springer, 2006). at <http://books.google.gr/books?id=u7l4f65OnSUC>

10. Mosk, A. P., Lagendijk, A., Lerosey, G. & Fink, M. Controlling waves in space and time for imaging and focusing in complex media. *Nat. Photonics* **6,** 283–292 (2012).

11. Vellekoop, I. M., Lagendijk, a., Mosk, a. P. & LagendijkA. Exploiting disorder for perfect focusing. *Nat Phot.* **4,** 320–322 (2010).

2.3 Optical Properties of Biological Tissues

In this part we explore the optical properties of a biological tissue. Biological tissues are complex optical media and they have both absorption and scattering properties. A lot of effort is put into bio-imaging systems currently; different areas of the electromagnetic spectrum are used and each effort offers different advantages[1].

For big biological tissues for example X-rays can be used to give maximum imaging depth with a great spatial resolution. But X-rays deliver no information on the functionality of an organism, and it also cannot be used for imaging in soft tissues. Additionally, X-rays are classed in the high energy radiation spectrum and endangers the viability of biological tissue[1].

Figure 18 A demonstration of the light scattered from a finger and low absorption

Magnetic Resonance Imaging (MRI) is a technique that unites most of the advantages: Non-ionizing, high contrast even for soft tissues and it offers insight into the functionality of the tissue. But the data acquisition is slow and the costs for usage and maintenance are extremely high.

The ultrasonic imaging systems offer satisfactory results, but the contrast is not high enough for biological samples of millimeter- sized organisms such as insects and flies, which are routinely used in biological research.

Optical imaging systems are non-ionizing, low in cost and offer excellent tissue functionality. The spatial resolution of the imaging techniques is unfortunately compromised because of the scattering. Although absorption from tissues is a significant parameter, there is an operation (red light) where absorbance is compensated satisfactorily enough. But the tissues are complex, clusters of cells and interfaces, or as we say in the terminology of optics, randomly distributed refractive index interfaces with high refractive index differences. The result is that light is scattered on this interfaces and the light that propagates is diffused while propagation and imaging information is lost.

But there are also a lot of advantages to justify our persistence on working with visible light and trying to compensate scattering phenomena. For a start, it is non-ionizing, so it is a safe way to image biological tissues without harming the tissues. The response spectrum (absorption, florescence) can give out the information of the composing elements of the tissue or functionality.

There is a number of additional information one can obtain by bio imaging, it is possible to distract information from scattering in different cell parts (in that particular sense, absorption and scattering are not always unwelcome phenomena), the Doppler Effect can inform us about the liquid flow inside a tissue etc.

There is a number of therapies that employ light irradiation. It is imaginable for example that a cancerous cell concentration could be accurately irradiated with the use of adaptive optics.

A biological tissue in general strongly scatters; absorption of only 400nm to 1350 nm wavelengths is in some sense weak. The scattering mean free path (the distance between two scattering events) is more or less 100μm.

On the other hand absorption length (the length before the initial beam intensity falls on 1/e of the initial value) is 10 to 100mm. So we see a 2 to 3 magnitudes difference.

The result of these two phenomena is the diffusion of light while propagating inside a biological tissue. We can all witness this phenomenon with light traveling through our finger.

Absorption.

Although we have covered scattering events in detail, but we have said almost nothing about absorption. This phenomenon describes the quantum effect when electrons elevate to higher atomic states from their initial state by absorbing a quanta of the light that propagates through[2].

The elevation to a higher permitted state is called excitation and can only happen (in the linear regime) only when the radiation that propagates through with frequency v corresponds to the photon energy equal to the energy difference between the excited state and the ground state. The equation reads as follows:

$$hv = E_f - E_i \quad (2.3.1)$$

The excited electron will not remain in this state indefinitely, it will return to the ground state and there are several possibilities how this can happen. So while radiation with frequency v that satisfies such a transmission propagates through the medium then its intensity will fall when it come out the medium because of the lost quanta due to absorption.

The excited electron will return to the ground state by either emitting a photon (if it's the same energy is called luminescence and if the photon has lower energy, fluorescence or phosphorescence) or by heat emission.

We can deduce very important information about the structure of the state of the tissue from these spectra. In general luminescence lasts for some femtoseconds; fluorescence lasts some nanoseconds; phosphorescence on the other hand can last from some milliseconds to some seconds.

If the photon, while interacting with molecules, is not involved in any energy exchange, then we speak of elastic scattering. If there is an energy transfer, i.e. the remitted photon has a higher or lower energy, we call it inelastic scattering. Raman scattering is a case of inelastic scattering. Inelastic scattering is a very important tool to help analyze the chemical composition in the irradiated structure.

Absorption is described by the absorption coefficient μ_α, which is the probability of a photon to be absorbed by a medium per unit path length, so the dimension of this value is cm^{-1} . If we have a single absorber (like a single scatterer e.g.), its capacity to absorb is described by the absorption cross section σ_α. Although this is related to geometric cross section σ_g (The

actual size of the absorber) it can have much higher values. This difference is described by the absorption efficiency for a specific wavelength:

$$\sigma_\alpha = Q_a \sigma_g \quad (2.3.2)$$

So if a medium consists of a distinctive number of absorbers the total absorption is described by the absorption coefficient:

$$\mu_\alpha = N_a \sigma_\alpha \quad (2.3.3)$$

Which can be used for the Beer-Lamberts law:

$$I(x) = I_0 e^{-\mu_\alpha x} \quad (2.3.4)$$

So transmittance can be easily defined as:

$$T(x) = \frac{I(x)}{I_0} \quad (2.3.5)$$

If someone wants to examine the absorbance properties of biological tissues, there are

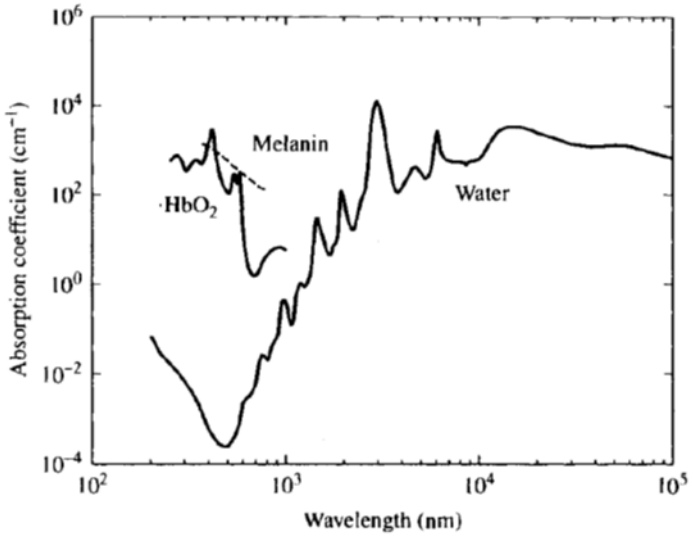

Figure 19 The absorption from the three main absorbers of human tissue. Hemoglobin, which shows different absorption if it's oxide. Melanin and water. There is a low absorption in red. [Image from [2]]

three major absorbance factors to consider as we can see in figure [19]:

- Hemoglobin (the absorbance is different for oxygenated and deoxygenated forms as we can see in image 2.3.2)
- Melanin
- Water

Each one covers a different part of the wavelength spectrum, which leaves an operation window at the red spectrum, where the absorbance is lowest. This is why optical tomography is working in the red spectrum.

We do not cover all the absorption properties but only the scattering properties of a tissue in the paper. So the next step is to introduce the proper absorption coefficient on the artificial structure.

This selection is justified by the fact that the absorbance is relatively small compared to scattering phenomena in the Mesoscopic regime.

Scattering properties of Biological Tissues

A biological tissue is composed of cells compactly placed next to each other, with compact sub-cell structures inside (nuclei, mitochondria). In the intercellular space a lot of proteins exist like collagen with significant dimensions and sufficient density to produce Rayleigh scattering.

The total amount of the scattering is described by the scattering coefficient μ_s , which is – as already mentioned - the probability of a photon to be scattered inside a medium per unit path length. The inverse of the scattering coefficient is called scattering mean free path l_s, as we saw already. Like previously demonstrated we can connect the scattering cross section with the geometric cross section and create a parameter called scattering efficiency Qs. Those quantities coexist in the equation:

$$\mu_s = N_s \sigma_s \quad (2.3.6)$$

Where

$$\sigma_s = Q_s \sigma_g \quad (2.3.7)$$

A similar relation to Beer-Lambert law can be defined, showing how much of the light is diminished from the initial direction.

$$T(x) = e^{-\mu_s x} \quad (2.3.8)$$

So taking into account absorption and scattering, one can define the total interaction coefficient or extinction coefficient:

$$\mu_t = \mu_\alpha + \mu_s \quad (2.3.9)$$

In conclusion because of their general complexity we can sum up the properties of ~~the~~ biological tissues with ~~those~~ two parameters (μ_α and μ_s). So there generally is no necessity to use the same compounds or exact structure to recreate a biological tissue, especially for ~~the~~ scattering properties. So if one can create a controlled artificial scattering structure, it is possible to have the same or similar values as in the desired biological tissues.

Today there is a vast library of data, having fully characterized every kind of tissues, both μ_α and μ_s. This means, one can find the optical properties of the desirable tissue. At this point it is essential to mention that in order to experimentally measure μ_α and μ_s there are various methods and models to use. Each method has its weaknesses, in particular regarding the absolute value, and often they are difficulties with the implementation.
All the models are based in diffusion theory, which we covered in section 2.2.2.2.

Although for this master thesis no actual measurements of optical properties took place due to limitation of time, we are nevertheless going to discuss the theoretical framework of measuring the optical properties of a scattering medium and mention some important points and limitations.

The simplest method for example is the Kubelka-Munk method, which is favored by scientists for its simplicity both in experimental measurements and numerical simulations. Although there are a number of assumptions, it still generates satisfactory results in most cases. In this framework we describe the propagation of a uniform, diffuse irradiance (or specific intensity) through a one-dimensional slab with no reflection at the boundaries.

One measures the transmittance and reflection of a sample which are linked to the coefficients μαKM and μ_{sKM} experimentally (the KM index intents to show that although these quantities have the same dimensions with the TT coefficients, they are different quantities. But there is a direct relation between the two models). Unfortunately this model fails to describe the laser light propagation inside a tissue even after certain modifications in the model.

If one wants to measure the scattering properties of a medium there is a number of direct and indirect methods to do so. Using the direct methods, one evaluates Beer-Lambert law attenuation and uses a goniophotometric device to evaluate the phase function (2.2.58).

Indirect methods use measured quantities like the Kubelka-Munk index that are related to the transport theory model and are usually adjusted with algorithms to fit the measured data. These techniques are very complex, but if someone is interest in them and wants to learn more, one should take a look at Wai-Fung's work in 1990 for a preliminary introduction of those methods.

So is there a general model to reproduce the scattering properties of a biological tissue? The answer is yes! Although each type of tissue exhibits quite different optical behavior, there is a way to model each type of tissue in a simple way.

Studies have shown that the scattering properties of a tissue can be reproduced with two models, either a mixture of spheres with different sizes or layers of fluctuating refractive indexes. These models where reproduced numerically and adjusted to the experimental data.

In the sphere model the properties can be reproduced either by a pure Mie scattering (the scatterer is bigger than the wavelength) or by a mixture of Mie and Rayleigh scattering (sub-wavelength scatterers).

Two equations of equal significance can reproduce the reduced scattering coefficient of ~~a~~ biological tissue. The reduced scattering coefficient μ'_S (cm^{-1}) is linked to the scattering coefficient through the anisotropy g[2]:

$$g = 1 - \frac{\mu'_S}{\mu_S} \quad (2.3.10)$$

Anisotropy is the characterization of the medium in terms of the relative forward versus backward direction of scattered light. A significant parameter when the medium is observed with a microscope. Anisotropy is defined in the Radiation Transport Theory as the phase function integral for the whole space; we have seen this quantity already in equation (2.2.74):

$$g = \int_{4\pi} p(s,s')\,(s\cdot s')d\omega' \quad (2.3.11)$$

Although the reduced scattering coefficient is not the only parameter to fully reproduce a biological tissue, it is a sufficient enough model to reproduce at least seven types of tissues[3].

1. Skin
2. Brain
3. Breast
4. Bones
5. Fatty tissues
6. Fibrous tissues
7. Soft tissues

The measured data in the scientific literature can be simulated by two equations:

$$\mu_S' = a\left(\frac{\lambda}{500\ nm}\right)^{-b} \quad (2.3.12)$$

The equation is normalized to a reference wavelength λ=500nm. The parameter α is a dimensionless parameter, unique for each type of tissue. Corresponding to experimental data, the factor b is called “scattering power” showing the dependence of μ'_S to the specific λ.
The other alternative is:

$$\mu_S' = a\left(f_{Ray}\left(\frac{\lambda}{500\ nm}\right)^{-4} + (1-f_{Ray})\left(\frac{\lambda}{500\ nm}\right)^{-b_{Mie}}\right) \quad (2.3.13)$$

In this case we take into account the Rayleigh contribution for the specific wavelength. The parameter α’ is the actual value of μ'_S for λ=500nm again. There are two contributions, one for each type of scattering, for Rayleigh scattering this is $f_{Ray}\left(\frac{\lambda}{500\ nm}\right)^{-4}$ and for Mie scattering this is $(1-f_{Ray})\left(\frac{\lambda}{500\ nm}\right)^{-b_{Mie}}$. It is clear that the sum of the weights for each contributing will be 1 in total.
An example of the fitting can be seen in this figure:

Both equations for the range 400 to 1300 nm create equally good results. The parameters α and α’ for soft tissues needs extra care, since they demonstrate great variability.

On the example shown in figure, we observe better fitting of the (2.3.13) compared to (2.3.12) this is because skin is reach to collagen (~70nm) that exhibit rich Rayleigh scattering.

The parameters b and b_{Mie} there are cases which have low divergence and bigger for other cases. For further details one should follow the work of Steven Jacques where equivalent equations for absorption exist.

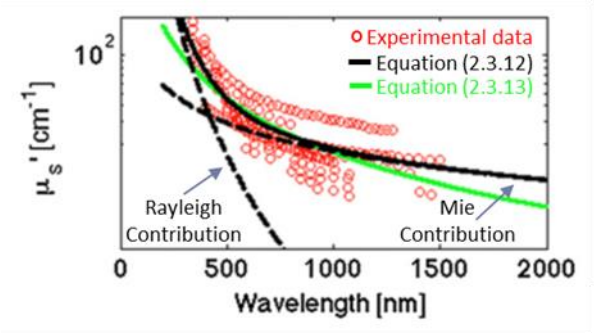

#	a (cm^{-1})	b	a' (cm^{-1})	f_{Ray}	b_{Mie}	Ref.
Skin						
1	48.9	1.548	45.6	0.22	1.184	Skin
2	47.8	2.453	42.9	0.76	0.351	Skin
3	37.2	1.390	42.6	0.40	0.919	Skin
4	60.1	1.722	58.3	0.31	0.991	Skin
5	29.7	0.705	36.4	0.48	0.220	Skin
6	45.3	1.292	43.6	0.41	0.562	Dermis
7	68.7	1.161	66.7	0.29	0.689	Epidermis
8	30.6	1.100	na	na	na	Skin

Figure 20 The fitting of the experimental data with equations. The fitting is satisfactory in both equations.

The advantages of generic tissue are clear, treatments, bio-imaging techniques and treatment protocols could be tested safely in such tissues. Additionally the physics in a stable scattering medium could be further explored (biological tissues change rapidly in time).

Reference

1. Wang, L. V & Wu, H. *Biomedical Optics: Principles and Imaging*. (Wiley, 2007). at <http://books.google.gr/books?id=RKukklVYAY4C>

2. Cheong, W. F., Prahl, S. A. & Welch, A. J. A review of the optical properties of biological tissues. *Quantum Electron. IEEE J.* **26,** 2166–2185 (1990).

3. Steven, L. J. Optical properties of biological tissues: a review. *Phys. Med. Biol.* **58,** R37 (2013).

2.4 Wavefront Shaping

In this last part we will explore the wavefront shaping field. The field was born in 2007 when Vellekoop and Mosk[1] managed to focus light behind a strongly scattering medium. This was done with the use of a spatial light modulator (SLM - for further details one has to go to experimental part of this thesis).

Since then a number of applications have flourished by using a scattering medium as a control element instead of a handicap. Most of the applications rely on the use of a SLM. After all, with the use of an active wavefront control, a scattering medium does not seem to be a barrier, but a desirable optical circuit element since it can offer a lot options.

Some of the highlights of this field are presented here. Although only focusing behind a scattering medium will be presented in detail because it is the technique that was used by us. But since the final goal is imaging through a strongly scattering medium, such as a biological tissue, we will contemplate what has been done in this field as well.

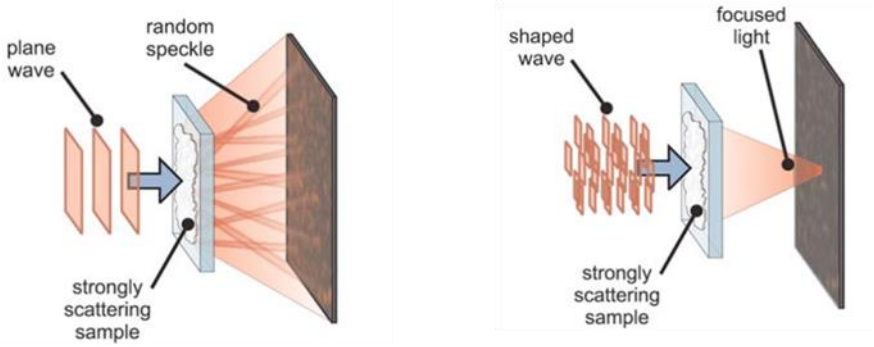

Figure 21 Experimental Demonstration of focusing. the Speckl pattern before optimization and after optimization , Photo from COPS group Twente

2.4.1 Focusing

Focusing behind a scattering medium was the foundation stone of wavefront shaping[1],[2],[3],[4]. The idea was simple, use a SLM to couple the light that propagates through a scattering medium with the eigenchannels of the system. Since the absorption is insignificant, the light that travels through a scattering medium is expected to channel with the natural channels of the medium, as we described in the previous section (equation 2.2.62 to 2.2.65).

For a non-optimized regular beam the coupling will not be sufficient and the energy is spread to different paths, resulting in a speckle pattern and spreading of intensity on the back of the scattering medium.

But if an optimized wavefront is used, the light will couple with the eigenchannels with transfer values close to 1. And more importantly, it will couple with eigenchannels that favor the transmission to the desired location. If that is possible, the random speckle pattern on the back of the scattering medium is expected not only to change, but a sharp spot will form where it is desired and the background noise will be considerably diminished. A perfect focus cannot be achieved unfortunately because of the natural experimental limitation of today's equipment.

The set-up was simple, as can be seen in the schematic in figure []. A SLM can induce a specific phase in a small portion of a light beam. This can create a well-shaped beam profile, since small areas of μm dimension have the desired phase. The SLM is controlled with a computer. If the SLM screen is inactive it works as a mirror (if it is the reflectance type). As we can see on the photo, the beam focused on a scattering medium. At first a TiO2 paint was used because it is a strongly scattering and low absorbing substance.

A CCD camera is placed on the other side of the scattering medium, observing the speckle pattern. Then a random mask is sent to the SLM from the computer. A random mask means each pixel has a random value of phase that will be induced in each point in the wavefront. Then a different speckle pattern is observed for each mask. We changed the masks until we found the optimum mask to supply us with a speckle on the desired location the optimum mask then is used as the optimum initial condition.

Having determined the optimum mask, we scan each pixel to find out what value will optimize the intensity in the desired location. Then the algorithm saves the change and moves for the next one until the whole SLM is scanned. When procedure is finished, a sharp focus will be observed and the surrounding speckle pattern will diminish compared to the first one.

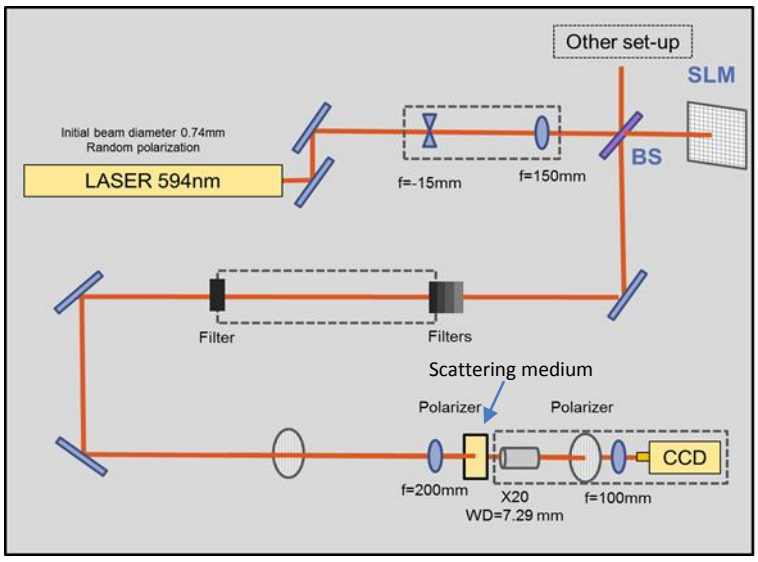

Figure 22 Set-up for focusing experiment, full details in section E3.

This focus is a result of constructive interference in the various eigenchannels of the medium. Since the scattering is a linear effect and deterministic (when the sample is stable in time), the resulting field will be the linear superposition of the incident field transformed by the transmission matrix of the medium (equation 2.2.63). Each pixel of the SLM then acts as an individual field that will be coupled with the transmission matrix, so this is the equation[5],[6]:

$$E_m = \sum_{n=1}^{N} t_{mn} A_n e^{i\varphi_n} \quad (2.5.1)$$

Where N is the number of pixels we use from the SLM. A_n and ϕ_n are the amplitude and phase of light of the particular segment. Finally t_{mn} is the transmission matrix element. So the code optimizes the summing of (2.5.1), making the terms on the right hand to be in phase.

This method is called iterative algorithm and it not the only way to achieve a focus behind a scattering medium. Other methods include the measurement of the transmission matrix, an excellent method that also makes use of a SLM. Optical phase conjugation uses a hologram written in a photorefractive crystal or digital phase conjugation that also uses a SLM instead of a crystal. Finally, the newest method is the opto-acoustic method, TROVE (the evolution of the TRUE method).This is a very promising methods for focusing behind a scattering medium.

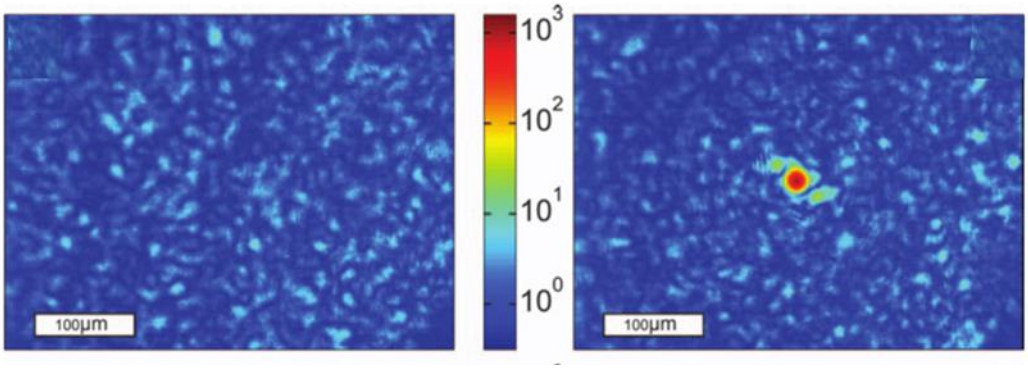

Figure 23 Photo from the initial Speckle pattern and the focus achieved after optimization[1]

2.4.2 Pulse Reconstruction after Multiple Scattering

The next big achievement in this regime was the reconstruction of a distorted ultrafast pulse after propagating inside a scattering medium. With the use of a SLM it is possible to repair spatial and temporal distortion of an ultrafast pulse caused by a scattering medium.

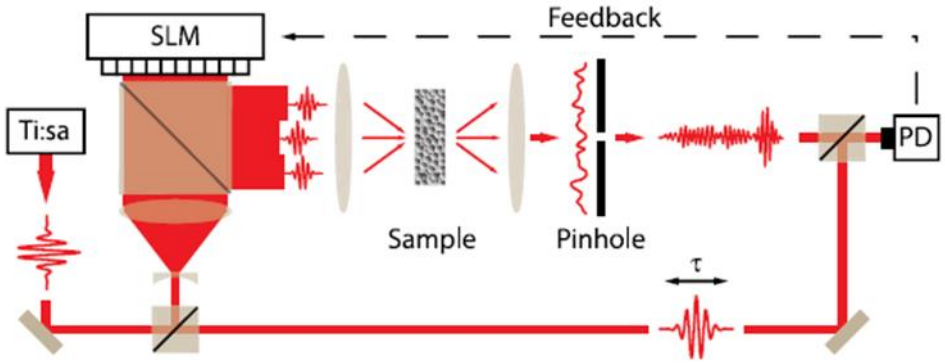

Figure 24 The experimental set-up from reference [7] , the optimization focus used here is a pin hole

The philosophy of the set-up is similar; the desired point was a pinhole or a fluorescent screen. The algorithm was optimizing the mask to maximize the signal of fluorescence or the light that was going through the pinhole. For further details one should take a look at the literature list of this thesis. On the figure [24] the set-up by Aulbach, J., Gjonaj, B., Johnson, P. M., Mosk, A. P. & Lagendijk,[7],[8] is presented.

In a similar work by Ori Katz[9] they showed that the more complex the medium is, the more temporary control we can have when we reconstruct the pulse.

2.4.3 Spectral Control with Wavefront Shaping

It was also shown that a scattering medium can be used as a spectrum analyzer, if instead of a CCD a spectrometer and a multispectrum source (an ultrafast pulse e.g.) are used. After that the readings of the analyzer are read by the computer while an optimization code is running in order to maximize the signal for a specific wavelength.

The set-up is presented in image [25], a work by Small, E., Katz, O., Guan, Y. & Silberberg, Y.

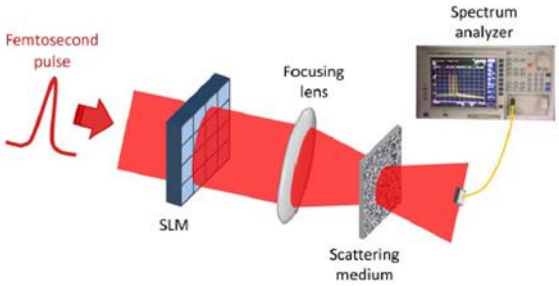

Figure 25 the signal to be optimized on this work, it's from a spectrum analyzer

2.4.4 Non-Invasive Imaging through a Scattering Medium

The same groups that have developed the previous methods have successfully created a set of techniques to surpass the scattering effects, by exploiting the memory effect. It is Memory effect because the speckle pattern stays stable, if the illumination of an object is shifted for a small radius.

Although the use of a SLM is not a necessity for these imaging techniques, it remains a field of wavefront shaping since there are possibilities of combining the use of a SLM with exploitation of memory effect.

The speckle illuminating the object might appear random, but it contains correlations that can be exploited. In particular the angular correlation known as the memory effect.

The group COPS from University of Twente achieved imaging through a scattering medium by exploiting the correlations[10]. There was a fluorescent object on the back of the scattering medium. A laser beams goes through the scatterer, and the speckle pattern illuminates the

object. A CCD is reading the fluorescent signal and an algorithm can reconstruct the image through the memory effect.

The total amount of transmitted fluorescence can be measured; it retains the information on the overlap between the object's fluorescent response, O(r), and the speckle intensity, S(r), where r is the vector of the spatial coordinates.

Rotating the incident beam over small angles θ does not change the resulting speckle pattern but only translates it over a distance Δr<θd. We call memory effect the fact that the speckle pattern is stable if we rotate the initial beam for small angles. The pattern will not change, but it will move in space.

The researchers at the University of Twente scanned the fluorescent object in this manner. For each angle the speckle pattern illuminated a different part of the object. This meant a different fluorescent single for each angle and eventually the whole object will be illuminated. The intensity of the fluorescence correlates with the laser speckle pattern. And through this relation they could reconstruct the image.

Therefore, the total measured fluorescence as a function of the incident angle is given by:

$$\mathrm{I}(\theta) = [\mathrm{O} * S](\theta)$$

An algorithm will de-correlate the above measured intensity and the image of the fluorescent object can be achieved. The scattering medium for this experiment was 50μm thick.

A different set-up was used, exploiting a SLM and the memory effect. In this version the light was behind the scattering medium. The scattered light was collected on a SLM. Then the algorithm optimized the wavefront until a focus was achieved. That was the image of a point source. So the SLM scattering medium was used as a lens. Then by exploiting the memory effect, they scanned an object in front of the light source and behind the scattering medium. Eventually a successful image reconstruction was achieved[11].

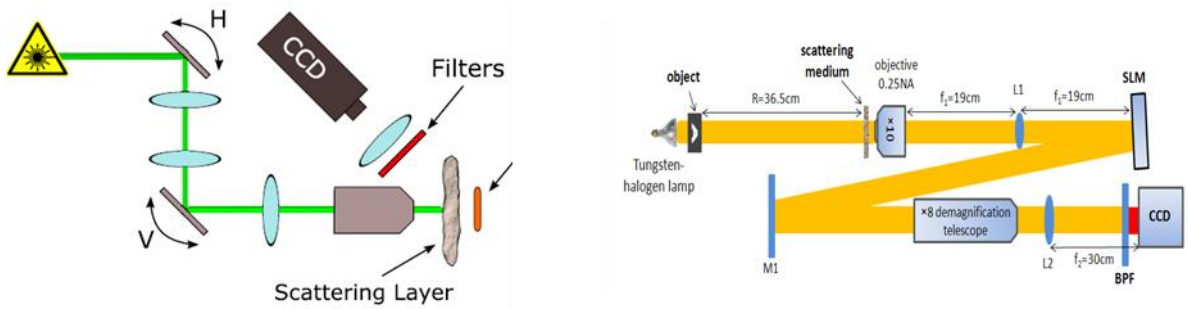

Figure 26 two experimental demonstrations, from [10,11]. In the first case by rotating the speckle pattern one can deduce the image behind the scattering medium, On the next case, the scattering medium is used as a lens, combined with a SLM

Very recently scientists in Paris achieved image reconstruction after a scattering medium with only a single photo. They showed that the whole information is scrambled just in one photo. The autocorrelation of the image of scattered light is identical to the autocorrelation of the object itself. An algorithm is connected with the two images; the algorithm is an iterative Fienup-type. For further details on this check the reference literature list[12].

References

1. Vellekoop, I. M. & Mosk, A. P. Focusing coherent light through opaque strongly. *Opt. Lett.* **32,** 2309–2311 (2007).

2. Vellekoop, I. M., Lagendijk, a., Mosk, a. P. & LagendijkA. Exploiting disorder for perfect focusing. *Nat Phot.* **4,** 320–322 (2010).

3. Popoff, S. M., Lerosey, G., Fink, M., Boccara, A. C. & Gigan, S. Controlling light through optical disordered media: transmission matrix approach. *New J. Phys.* **13,** 123021 (2011).

4. Dobisz, E. A. *et al.* Scattering Optics resolve Nanostructure. **8102,** 810206–810211 (2011).

5. Choi, W., Mosk, A. P., Park, Q. H. & Choi, W. Transmission eigenchannels in a disordered medium. *Phys. Rev. B* **83,** (2011).

6. Vellekoop, I. M. & Mosk, A. P. Universal Optimal Transmission of Light Through Disordered Materials. *Phys. Rev. Lett.* **101,** 120601 (2008).

7. Aulbach, J., Gjonaj, B., Johnson, P. M., Mosk, A. P. & Lagendijk, A. Control of Light Transmission through Opaque Scattering Media in Space and Time. *Phys. Rev. Lett.* **106,** 103901 (2011).

8. McCabe, D. J. *et al.* Spatio-temporal focusing of an ultrafast pulse through a multiply scattering medium. *Nat Commun* **2,** 447 (2011).

9. Katz, O., Small, E., Bromberg, Y. & Silberberg, Y. Controlling Ultrashort Pulses in Scattering Media. *Opt. Photonics News* **22,** 45 (2011).

10. Bertolotti, J. *et al.* Non-invasive imaging through opaque scattering layers. *Nature* **491,** 232–234 (2012).

11. Katz, O., Small, E. & Silberberg, Y. Looking around corners and through thin turbid layers in real time with scattered incoherent light. *Nat Phot.* **6,** 549–553 (2012).

12. Katz, O., Heidmann, P., Fink, M. & Gigan, S. Non-invasive single-shot imaging through scattering layers and around corners via speckle correlations. *Nat. Photonics* (2014). doi:10.1038/nphoton.2014.189

Experiment

E.1 Introduction

Since this master thesis is an experimental work, here in detail the practical details will be covered. For this work, I had to master two techniques;

1. Laser Micromachining
2. Wave front shaping a focusing experiment.

Each one will be covered individually. In both parts, I also needed to create codes to run the experiments, either by producing coordinates for the structures or for SLM to create a focus behind a scattering media. On the last part we have the outcome from the two techniques, meaning focusing through artificial scattering media.

E.2 Laser Micromachining

The micromachining set-up was constructed in the UNIS lab, (Ultrafast Nonlinear Interactions and Sources). We will start by covering the parts of the set-up we used.

The laser system is an amplified Titanium Sapphire system, with an output of 1kHz pulses. Each pulse has a duration of approximately 35 fs with central wavelength of 800nm. The energy of each pulse is 2.3mJ approximately. We use only a small fraction of the initial beam on the set-up with the help of a polarizer.

In the image, we depicture our experimental set-up and explain the use of each part.

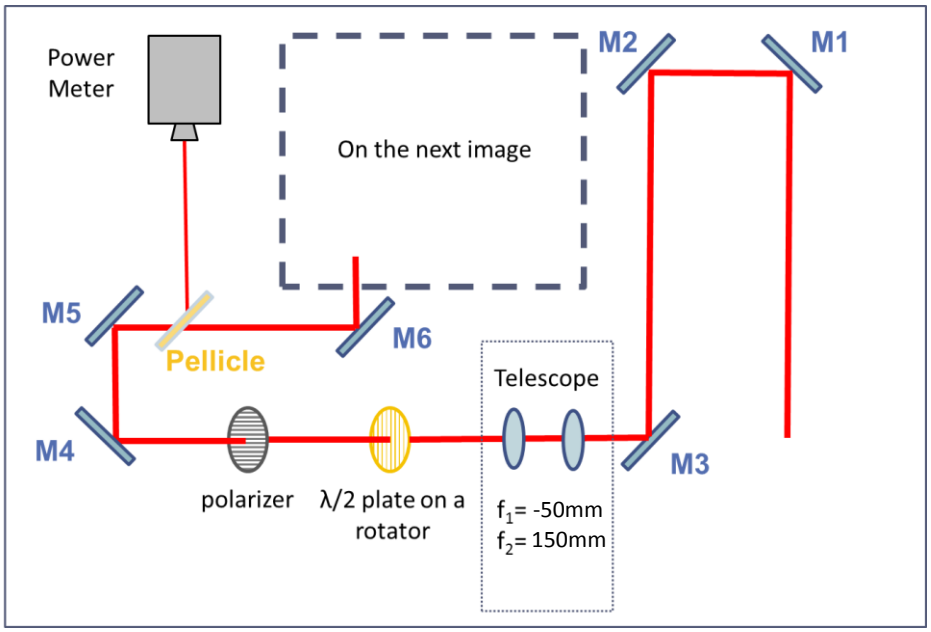

Figure 27 First part of writing Set-up

The beam enters our set-up, and two mirrors M1 and M2 are used to calibrate its position every day.

Telescope

After the beam reaches M2 it will go on to M3 and then it will be driven inside a telescope to reduce its size. This makes the intensity of the beam too low to cause Kerr effect or other non-linear phenomena that could happen for such a diameter.

The initial beam has a size:

Rx=1.4cm and Ry=1.6cm

The telescope should decrease the beam to dimensions:

$$m = \frac{f_o}{f_e} = \frac{f_1}{f2} = \frac{-50}{150} = 0.15 \ \ (E.2.1)$$

Which means we expect the initial beam to be 1/3 of the initial size. The actual shape of the beam after the telescope it has the size:

r_x=5mm and r_y=7mm.

Intensity Control

After the telescope, the beam will meet a λ/2 retardation plate. Those plates, made of birefrigent crystals, can change the linear polarization of the beam without the (significant) loss of energy. This plate works parallel with a linear polarizer. If the new polarization axis is perpendicular to the polarizer, very little energy will pass through (it can still be enough to induce changes, so filters are used for further reduction of the intensity). The λ/2 plate is mounted on a rotation stage. In conclusion the system polarizer - λ/2 plate works as an intensity control or energy control per pulse. The control should follow Malus' law for two polarizers:

$$I = I_o \cos^2 \theta \ \ (E.2.2)$$

Where θ is the angle between the axis of the polarizer and the λ/2 waveplate. We ~~tried it so to~~ checked the functionality of our system and the Joulemeter response, and we got satisfactory results, as one can see in figure [].

After that the beam will travel through M4 and M6. Then it will come across a pellicle. Pellicle is a thin plastic membrane which may be used as a beam splitter, with a reflection as low as 8 % and 92 % transmittance. The main beam will be driven by M7 into the recording set-up

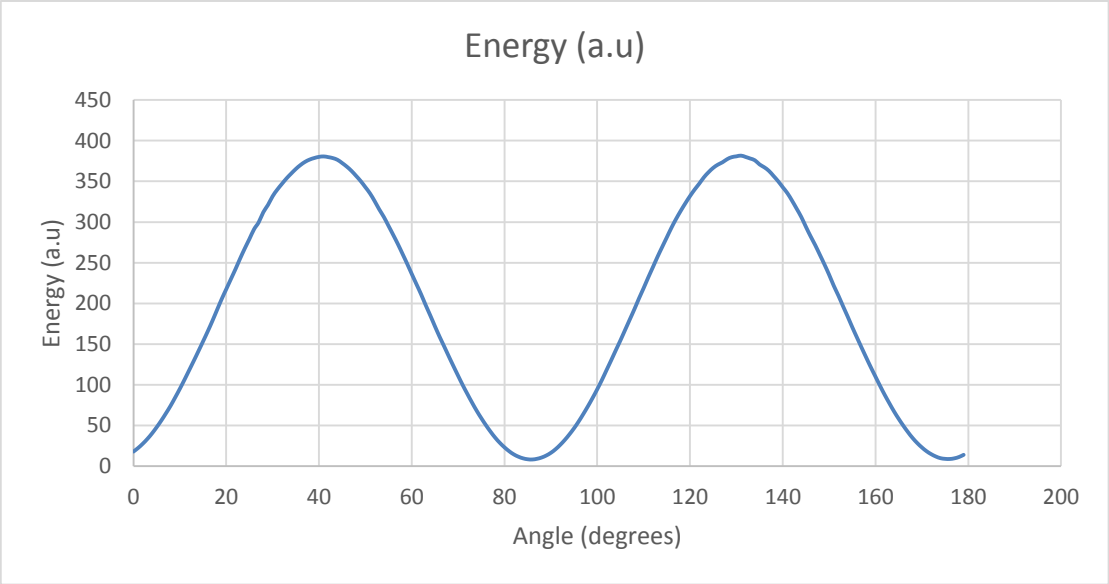

Figure 28 Graph Of intensity control response

while the low intensity part will be sent into the Joulemeter.

The Joule meter

The joulemeter we used is based on a pyroelctrical crystal. Pyroelectricity is the ability of certain anisotropic materials to generate an electrical voltage when they are heated or cooled.
Pyroelectricity can be seen as one of the side of a triangle with three vertices, each representing the three types of energy present in the material: mechanical energy, thermal energy and electrical energy. The side connecting the thermal and electric energies represents the pyroelectric effect. The side connecting the electrical and mechanical energies represents the piezoelectric effect. Finally, the side linking mechanical and thermal energies represents the thermo-electric effect of Peltier, Seebeck and Thomson. Below a temperature Tc, known as the Curie point, ferroelectric materials such as lithium tantalate, exhibit a large spontaneous electrical polarization. If the temperature of such a material is altered, for example by incident radiation, its polarization is then changed. This change in polarization may be observed as an electrical signal, if electrodes are placed on opposite faces of a thin slice of the material to form a capacitor. The sensor will only produce an electrical output signal when the temperature changes; that is, when the level of incident radiation changes. This process is independent of the wavelengths of the incident radiation and hence pyroelectric sensors have a flat response over a very wide spectral range.
For this purpose, there must be a calibration for each wavelength λ. The calibration of this

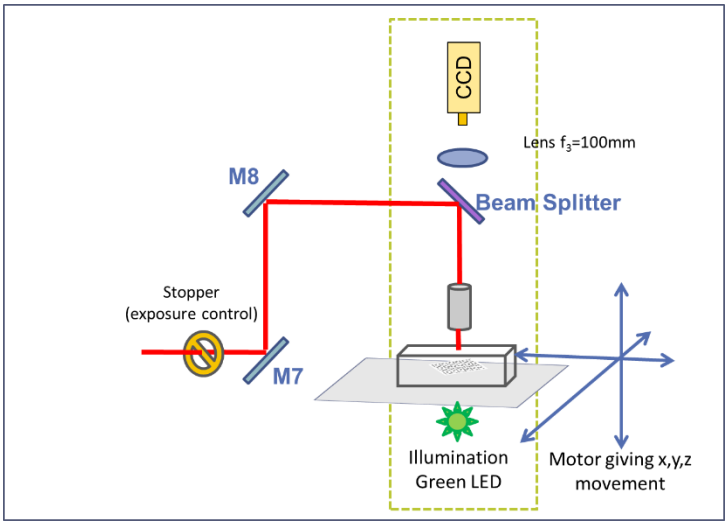

Figure 29 second part of writing system

unit was done for λ=1064nm so I recalibrate it for 800 nm. I used the whole laser beam and measured it with the power meter to be 2.29μJ.

Then by using the same telescope in my set up, I sent in in the Joulemeter, and reduced its energy by the use of a series of filters (ND 200, 200 and 100). I calculated the estimated drop in the energy to be 244,275 nJ. After that the measured value on the joulemeter was 13.10 J/V. By that I could deduce that the factor a E=aV , it is a =18.65nJ/V.

Shutter

Then the set-up continues in image []. It cannot be accurately pictured, but the set-up rises perpendicular, as can be viewed in image []. Before the beam goes into this part of the set-up, a shutter is placed to control the time exposure on the sample. By having a repetition rate of 1000 pulses per second, depending on the time the shutter is open, we can control how many pulses can be exposed on a specific point on the sample. This is a crucial parameter on creating voids; it seems that depending on the number of the pulses one can control the size of the void. Starting from 200 nm for 1 pulse and reaching to 1-2μm for around 1 second.

Then the beam will continue through a beam splitter. This beam splitter is used for two purposes. The first use is to send the beam on the sample. The second is to collect the light from the objective to the camera. This way we combine an observation system (the green dashed line in an image) with the writing system.

Observation Set-Up

After the beam splitter there is an objective lens. This lens focuses the beam inside the sample. Simultaneously, it works as an imaging system, so it collects the light from the place of focus, that way a direct observation on the area we induce changes can be made.

The light from the objective is collected from a positive lens, f_3=100nm and sent on a CCD camera on top to observe the procedure and help us examine the sample.

Writing set-up

As I have already mentioned, the laser beam is focused on the sample with the same objective lens we have used for imaging. In general we used two objective lenses:

Table 1 objective lens we used

Table 1			
Lens	NA	Magnification	Working Distance (mm)
1	0.70	X20	0.7
2	0.40	X40	0.7

We also worked with another set of experiments with an objective of NA=0.20 X8. For the initial structures we used the lens 2, but later on, to achieve smaller voids, we preferred the lens 1.

The estimated foci for those two lenses (and any given objective) for a Gaussian beam is given by:

The radius of the focus:

$$r = \frac{M^2 \lambda}{\pi NA} \quad (E.2.3)$$

Where M[22] is the beam quality, λ is the wavelength of the beam, NA is the numerical aperture of the objective.

The confocal parameter (the focus are not spherical but ellipsoids, as can be seen in image [2.1.5.1]:

$$b = \frac{M^2 n\lambda}{\pi NA^2} \quad (E.2.4)$$

From the equation (E.2.4) we can see that for NA close to one, the focus is spherical more or less. And this is the/one reason we preferred the lens 1 because the asymmetry is much better compensated.

The foci for the lenses we use, by using (E.2.3) and (E.2.4) and for a beam quality ~1.8 are estimated to be:

Table 2 size of focus for objective lenses

Lens	2 r (μm)	b (μm)	Volume of ellipsoid (μm3)
1	1.3	2.61	2.64
2	2.29	8.02	24.81

The above table shows the differences in shape between the voids those two lens can create. Although ~~the~~ lens 2 can offers a bigger coverage because scattering happens at the interface of the refractive index differences, we prefer to use smaller voids ~~but~~ with more refractive index interfaces. Moreover, the size of spots from lens2 are close to geometrical scattering, so we used lens 1 instead because it creates Mie scattering that we could easily adjust to Raleigh scattering.

Motors

Resuming the path of our beam, after the objective the beam will be focused on the working distance of the objective. There the sample is moved with Thorlabs motors Z820 model. Those motors can do repetitive movements of 200 nm, and the smallest possible step is 50 nm. In some codes we give coordinates steps integer products of 200nm. Their max speed is 700μm/sec. The error for each successive step is 0.2% (this means, if the step is x, then there will be an error in position 0.2x/100). Their operation length is 20 mm.

The samples are put in a holder, since they are transparent a green ~~led~~ or white led is used to illuminate and observe the procedure (monochromatic led helps to observe imperfections better than white light).

[2] A measure for how well a laser beam can be focused in certain conditions. The M² factor is defined as the beam parameter product divided by the corresponding product for a diffraction-limited Gaussian beam with the same wavelength.

Samples

The samples we have used are soda lime glass, microscope sample glasses. With dimensions of 75 mm X 2.5 mm X 1 mm. Both lenses can cover the whole thickness of the glass (because of the optical path inside the glass, but we will come on that later).

The soda lime glass usually has a refractive index n = 1.5172 for λ=800nm [], but the value can differentiate, depending on the impurities. In our case we evaluated with a simple method that the glasses we use have a refractive index n=1.6412 for λ=800 nm.

As one can see from table E.1 the working distance of the lens 1 and 2 is smaller than the thickness of the glass. But one can still use the whole thickness of the sample, which is 1mm.

This is possible because of the refractive index difference, the light propagates differently inside the glass and we can observe the distortion of linear propagation because of simple refraction. This means that the bottom surface of the objective seems to be only 0.6 mm away from the first (if we observed it through the glass). So when we enter the coordinates to build structures inside the glass we should take into account the z direction should be smaller and a correction should be made.

Eventually, when the beam with low energy to induce changes meets the interface glass air, it is reflected and can be seen in the CCD. We measure the difference of the two interfaces by when the beams is shown in our CCD camera, f.e. l_{opt}. Then by the simple relation:

$$l = l_{opt} n \quad (E.2.5)$$

We measure the refractive index in our set-up and we correct the coordinates in our structures.

Lab View Platform

The whole set-up is monitored by a lab view platform; a code was developed to help us control all the elements in our set-up, velocity, position, exposure time and energy. The program can read .txt files of specific format. In these files, we enter five coordinates, depending on if we want to create arrays of lines (usually for waveguides) or point by point movement (to create voids in specific position). In both functions, every coordinate is added to the reference point, which mean it ill be the point x=0,y=0,z=0 for the coordinates of the code.

For point by point writing the txt file should have 5 columns

- 1st column is the angle of the polarizer. We usually keep the value zero and we add it as a reference point to the desirable value.
- 2nd column is the y coordinate, added to the reference y value.
- 3rd column is the z coordinate, added to the reference z value.
- 4th column is the time exposure n milliseconds; we appoint how long the shutter will stay on this point here.
- 5th column is the x coordinate, added to the reference x value.

An example is set bellow:

0.000000	0.001000	0.030464	1000.000000	0.001000
0.000000	0.007352	0.030464	1000.000000	0.001000
0.000000	0.014022	0.030464	1000.000000	0.001000
0.000000	0.017966	0.030464	1000.000000	0.001000
0.000000	0.024663	0.030464	1000.000000	0.001000
0.000000	0.030376	0.030464	1000.000000	0.001000
0.000000	0.034218	0.030464	1000.000000	0.001000
0.000000	0.038692	0.030464	1000.000000	0.001000
0.000000	0.044107	0.030464	1000.000000	0.001000
0.000000	0.050958	0.030464	1000.000000	0.001000

On the straight array of the function the coding is similar but each line needs two command lines. The columns 1,2,3 and 5 describe the same coordinates. Column 4 is different however, it takes values of 0 and 1. Zeros stand for closing the shutter, and 1 for opening the shutter. In this case, if we want to build a line, we start by giving the first command line with the initial coordinates θ,x,y,z (the starting point in other words). At the same line we set the 4^{th} column to have the value 1. This means it goes to these positions and then opens the shutter.

The second command line describes the ending position, so again x,y,z,θ and the value 0. The meaning of this is: move to the new position and after you do that, close the shutter. An example is presented below:

0.000000	0.001000	0.030464	1000.000000	0.001000
0.000000	0.007352	0.030464	1000.000000	0.001000
0.000000	0.014022	0.030464	1000.000000	0.001000
0.000000	0.017966	0.030464	1000.000000	0.001000
0.000000	0.024663	0.030464	1000.000000	0.001000
0.000000	0.030376	0.030464	1000.000000	0.001000
0.000000	0.034218	0.030464	1000.000000	0.001000
0.000000	0.038692	0.030464	1000.000000	0.001000
0.000000	0.044107	0.030464	1000.000000	0.001000

0.000000 0.050958 0.030464 1000.000000 0.001000

Bare in mind, codes for giving coordinates and complying the above format were developed. The platform of programming language I chose was matlab because there is a variety of graphic tools preinstalled to inspect the resulting structures.

The codes that were made can cover different geometries complexities and the density of voids. Most of them are presented in the appendix.

E-T Mapping

Although the literature presents precise values to create the writing conditions, we need to adjust them to our set-up and sample. For this reason we have made an energy and time exposure mapping of response of the sample.

We made arrays of points, separated by 10 μm. This array has two axes x and y. As x increases, the time exposure increases as well from 50 ms to 1.500 ms. And on the y axis we increase the energy, by changing the angle from 0 up to 45 degrees, this means energy deposes from: 25 nJ up to 2μJ, figure [31,32].

The literature suggests that all the studies were based on single pulses. As it has been shown in section 2.1, the threshold value of energy for NA=0.65 for fused silica was 0.5 μJ. We observed that exposure time changes the size of the void. This was backed up by observation of E-T mapping in third harmonic generation microscopy. With this method we can observe the refractive interfaces and see that if the exposure time(~1 second ~100 pulses) is long enough, the voids are equal in size with the spot size.

The optical print of the voids in transmittance mode is black (this means no light passes through because of the high refractive index change. If it was a reflection, the illumination will be shown bright white then). We made small steps to check where there is overlapping. We observed a stop in overlapping at 2μm.

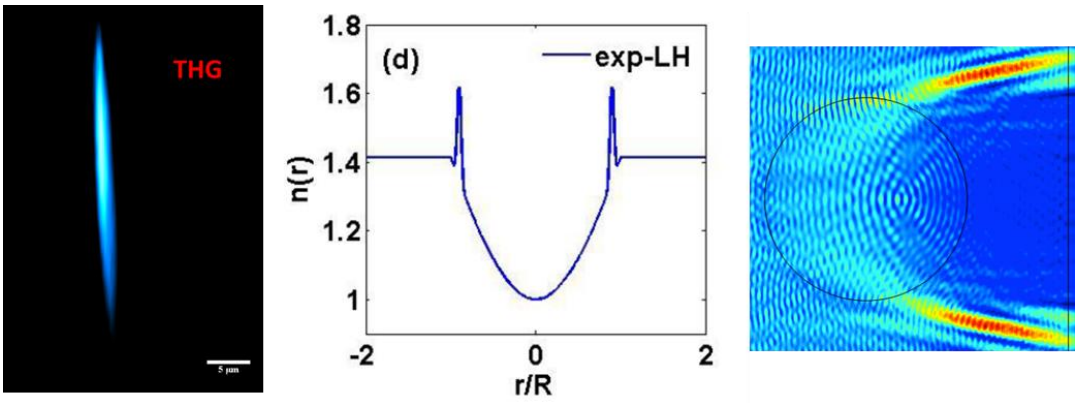

Figure 30 the voids we creat with THG microscopy. The refractive index profile and simulations with comsol how light propagates through.

A problem in both optical and THG microscopy is the resolution limit. The results are simply not good enough. In the future scattering measurements hopefully will be able to give an accurate value of their size and refractive index change.

So once again, to sum up, for E-T mapping we used NA=0.70 and we preferred to work with time exposures between 800-1000 ms and energy of 750nJ. And for ~~the~~ NA=0.40 we used the same time exposures, but the energy was 2.5 μJ.

The spots are structured with a void inside and a shell of denser materials, ~~the~~ portions of the material were just shot away and left the void. The expected refractive index profile is shown in image [30]. Comsol simulations show that those voids ought to work as a defocusing lens, and this is why they can be called an anti-Lunenburg lens (since they have

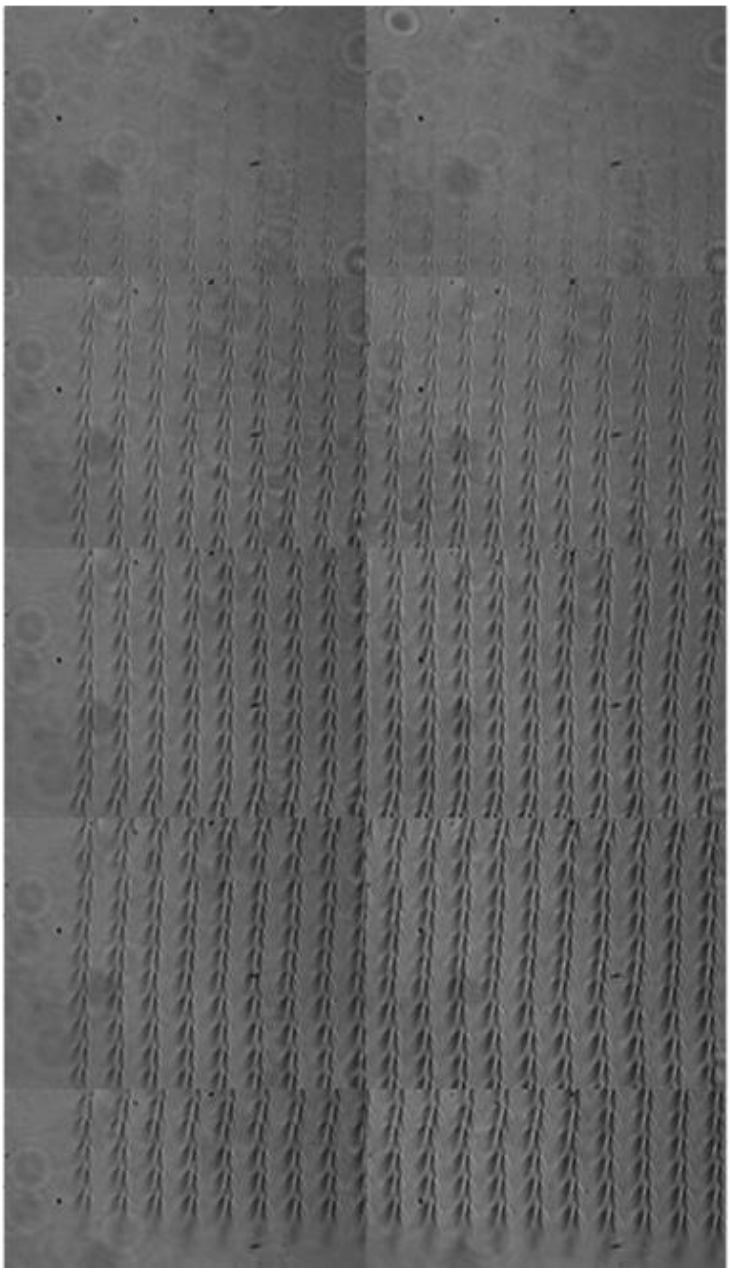

Figure 31 Energy mapping for NA=0.40, time expose in horiztal direction , energy in transverse

the inverse refractive index profile of the normal Lunenburg lens)

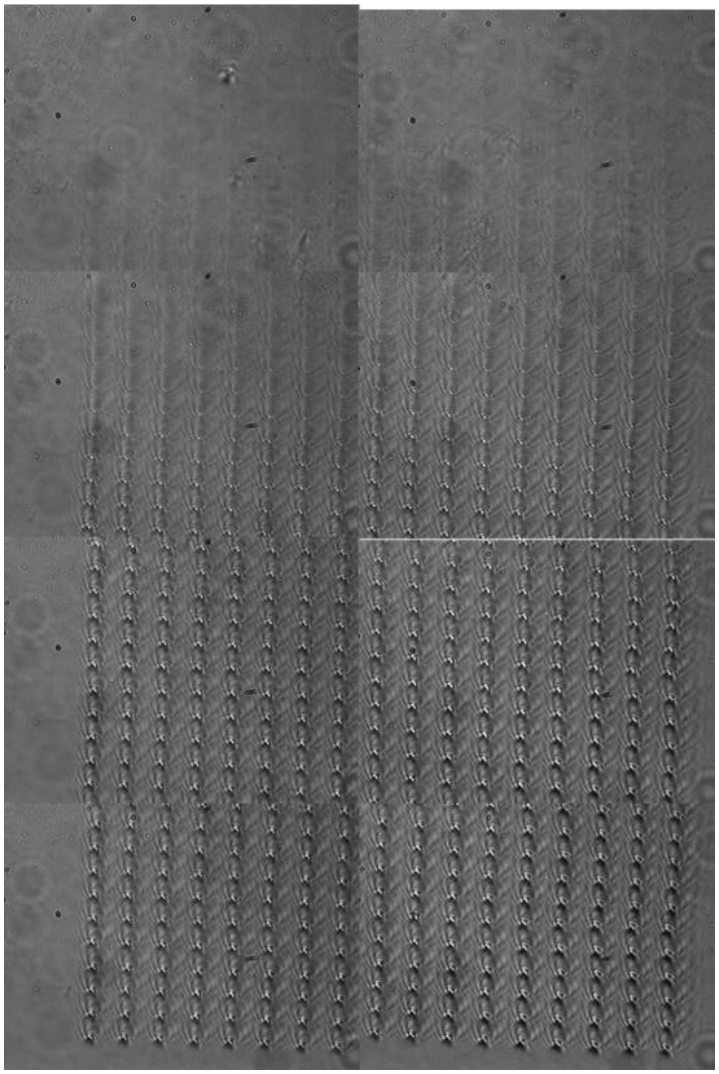

Figure 32 Energy mapping for NA=0.40, time expose in horiztal direction , energy in transverse

Imaging system

When we build a structure, the imaging system on the writing set-up is not optimized. All the structures are preferable to be observed in a distinct system with coherent illumination (laser light). So some of the observations were made by this small imaging system pictures in image [33].

It is rather simple, there is a helium neon laser from thorlabs, λ=633nm and random polarization. Since the beam quality is not clear and there is a lot of noise, a spatial filter is placed after the beam to clear the beam. It has been done with two lenses (f1 and f2).

Then from M2 the beam is sent into the objective to be focused inside the sample. Then an imaging system like the one we describe before it is used. The use of polarizers is necessary to handle of intensity.

The sample is on a moving stage with micrometer precision, that permits us to move the samples in x,y,z directions. The optical system is on another stage as well to move it on the z movement.

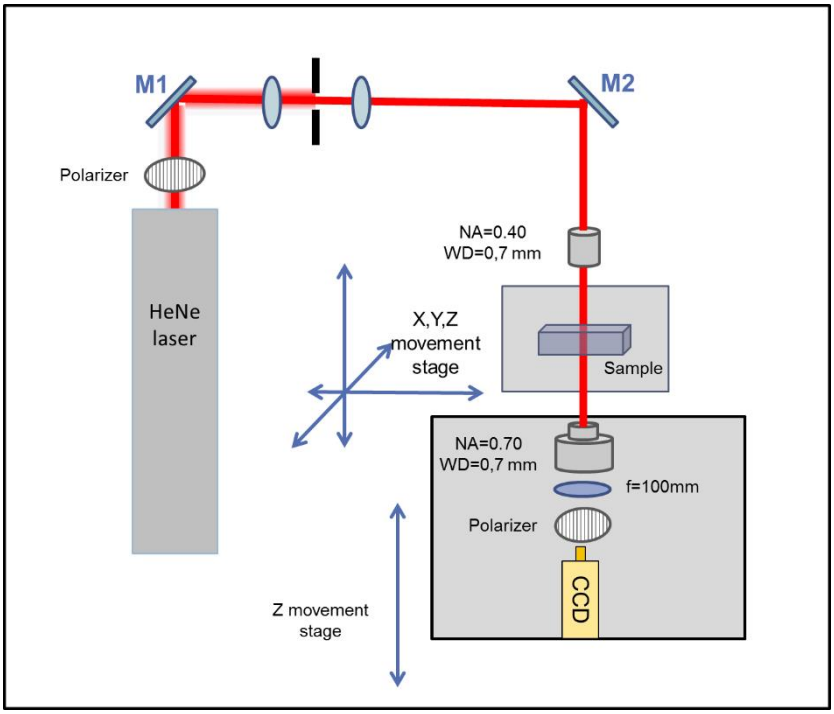

Figure 33 imaging system we use in UNIS lab

Testing

Having figured out optimized conditions for making a void in our set-up, we started with some test structures, to observe that our software, both labview and matalab (and the codes), work correspondingly right.

We observe the structures with the imaging system of wavefront shaping, which is described in the next section or in the small imaging system we have set up in our lab.

For a start, I created a code which will create a series of voids to form the logo of our lab UNIS. The size of this structure is 1X1 mm , and it is/ it has only one layer. The number of voids was 5050 spots. The graph representation can be seen in image and the image [34] of

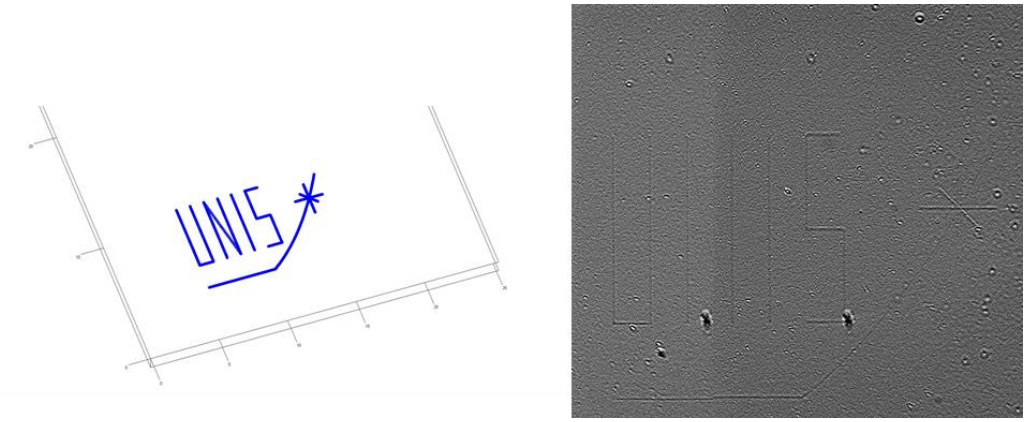

Figure 34 A test example, we wrote UNIS lab in a glass

the imaging system.

By that we can conclude that everything is operational and we can move on to more complicated structures.

Preliminaries Structures

A symmetrical structure was created and it was checked how it corresponds with coherent lighting. It has five layers each with 400 spots, 250x250 nm in the x and y direction, and it is separated each 20 μm figure[35].

A similar structure, with same dimensions and spacing was made. This time the spots were randomly positioned (a code generated random coordinates) and not symmetrical. We illuminated the structures with red and white light to observe differences. Finally most spectacular observations are made with laser illumination.

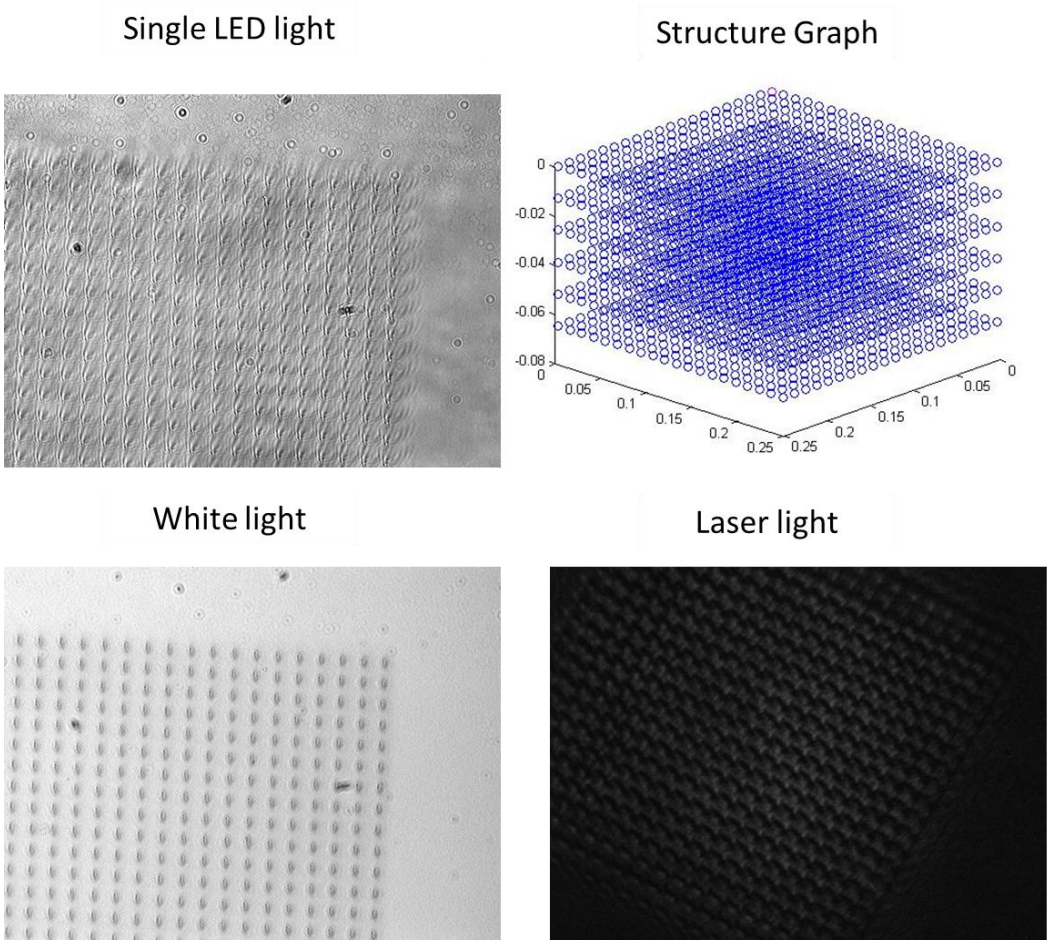

Figure 35 A symmetrical structure, doesn't give random pattern. a) led light b) the map c) white light d) laser light

We can observe the symmetrical ones gives no spectacular pattern. The white light illumination shows that the spots are well placed one behind the other and hide each other.

On the contrary the disordered structures, although we can see the shadows of the spots on the back in led light and white light, we find it much more fascinating in laser light, where a pattern of scattered light appears. It's unique for each type of disorder (it's deterministic) and more interestingly it's replicable with high precision.

This structure though, have very small density of scatterer to be consider highly scattering. It has a volume 250X250X100μm^3=6.25 10^6 μm^3. On the other hand the ellipsoids are 1.5 μm radius 8 μm confocal (long axis) and they number 5X400= 2000. Meaning each small void has a volume t=4/3 π r^{2}b =75.36 μm^3 so finally they cover a volume of T=150720 giving only a 2.4% coverage, figure [36].

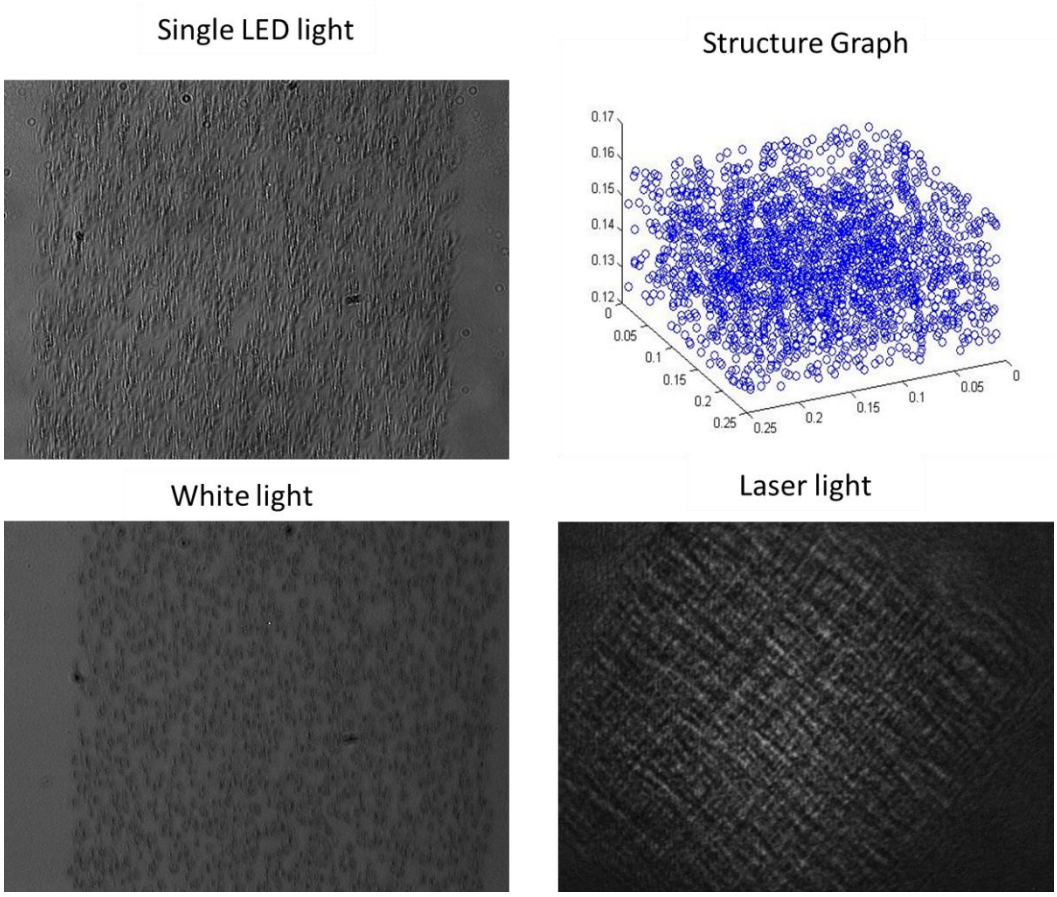

Figure 36 Same spacing and number of spots with the symmetrical. a) led light, b) the mapping fo the structure c) white light d) a raondom pattern is formed with laser light

Scattering media Geometries.

For strongly scattering media, which give us a speckle pattern when it's irradiated by laser light, one should reach the values of 30% or more as can be seen from the work of []. For this cause bigger structures and with varying geometries were made. A code was developed for each geometry with adjustable parameters.

Since each voids require more or less 4 seconds to be produced (and the time needed for the motors to change position), this limits the available time. So for this reason we mainly worked in structures of limited sides

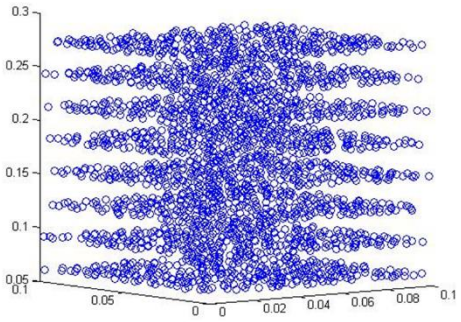

Figure 37 random layered structure

100X100μm but varying thickness.

There are 4 models of structures we have: completely random positions in layers, where x and y coordinates are randomly chosen to fit in frames of desirable size (like the one in image []). The problem with this code, there is an upper limit of random spots it can calculate. There is an overlapping check which evaluates new position to the spot if overlaps with a void. Unfortunately after ~31%. It's actually for a simple reason, when the voids are not laid neatly one close to the other, the leave much less free space for other spots to be placed. It's like a suitcase when the clothing are packed neatly more stuff can be crammed inside compared to a careless deposition. An example is shown in image [37]

Next we have the full 3D random deposition. Even in z coordinate we position randomly the spots, but in a specific window of values. On this case the code can cram more than 30%, because we have more freedom in the z direction. It can have values of 50 % or more. In this case the sort them by z direction. An example is shown in image [38]

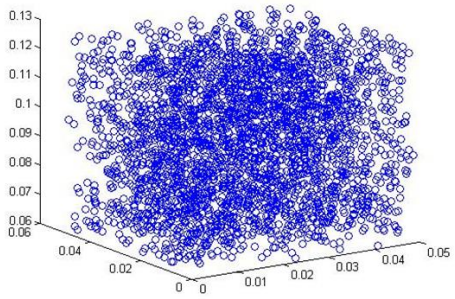

Figure 38 3D random geometry

The other one, it's identical to the one in the work of []. Rows of spots are created. The rows are spaced randomly to each other. And each row is placed randomly to the next one in the same plane. Although the density it's controllable, there is an upper limit to this geometry, meaning if the step it's too small it will be like voids one after the other. Example is shown in image [39].

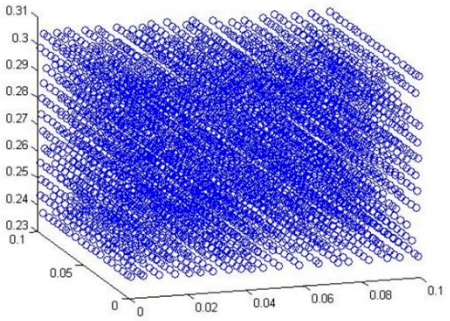

Figure 39 Layered structure in random spacing in rows.

Finally the last geometry is place voids one next to other and cover the whole layer. Even under this condition since they are spheroids, some space is left uncovered between the spots, reaching maximum 75%. But by placing layers of spots one after the other, doesn't make any difference from a symmetrical one. So we randomly remove voids from the full frame and reach a desirable value of density. An example is shown in image [40].

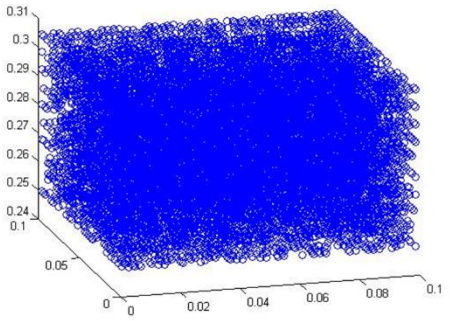

Figure 40 Full filled structure with random gaps

For the cause of this master thesis and my general work in the lab, many more codes are made, for randomly spaced arrays of lines, or photonic crystals coordinates. But since they don't necessarily fit on the cause of this work, are left out.

Examples of Build structures

During this time, there is a big number of structures of diverse parameters we build. It's pointless to present everything. So here are presented a few examples that were later checked in the wavefront shaping set-up. For a whole characterization, as mentioned before they ought to be check for their scattering coefficient, but unfortunately the time frame didn't let to happen. But the next thing is to characterize this geometries and check how they affect the transport coefficients.

In all above configuration speckle pattern was shown when irradiated with laser light. The problematic procedure, it's not only the density of voids required for a small volume, but the size of the volume itself. Comparing to Ti02 samples with Δn=100% that only few μm is enough to make it fully scattering and non-transparent, on this the case of glass Δn=30~62.5 % It requires more layers. But still the optimized conditions are under investigation.

Random position of Voids in layers

It was the first configuration we tried, especially in small density to study better the few scattering phenomena. For enough layers (up to 30 up to 40, each spaced 5μm) and about 150 spots per layer. In pictures [41,42] we can see the mapping of structure. And the photos

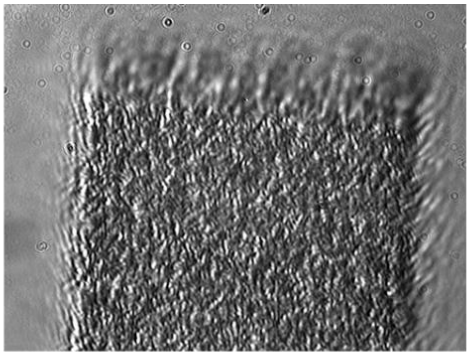

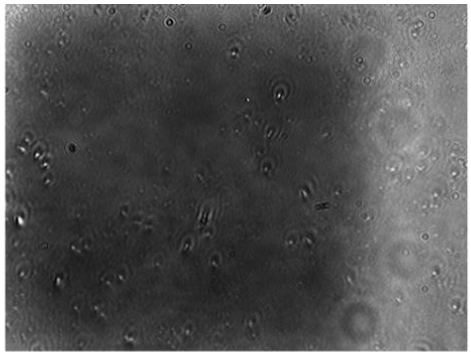

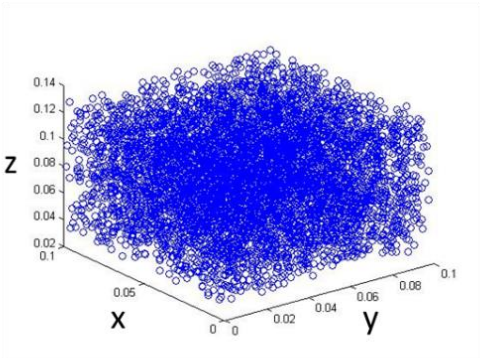

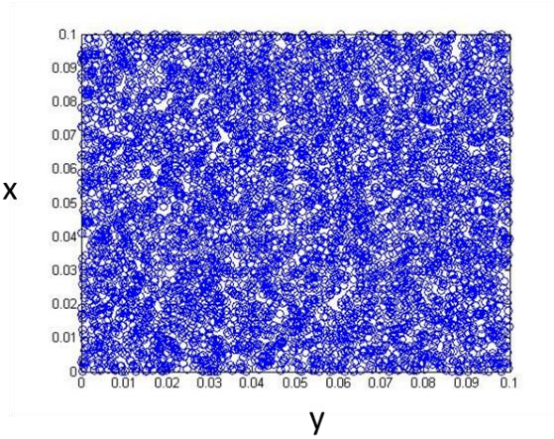

Figure 41 Structure with 40 layers, and random positions a) white light structure b) the shadow on surface c)the 3D map d) the spots in x,y axis of all layers

from

the observation system of our set up. The black shadow, it's the structure when looked from the surface of the glass. in last image, the cross section shows all the voids light will meet as it propagates through. Unfortunately as it can be seen in images [], that's not the right recipe for a strongly scattering medium. Although there is a speckle pattern present, which changes for different masks on the SLM, still it's not enough for some serious control, since most of the light that goes through remains ballistic. (the bright white dot in the center it's the focus from the objective.)

This structure it's only 160 μm thick, for the same geometry and many more layers the desirable speckle pattern ought to be present. Due limitation of time, this was not done at the moment this thesis was written. And the choice was the rather bigger time of creation compared to other geometries.

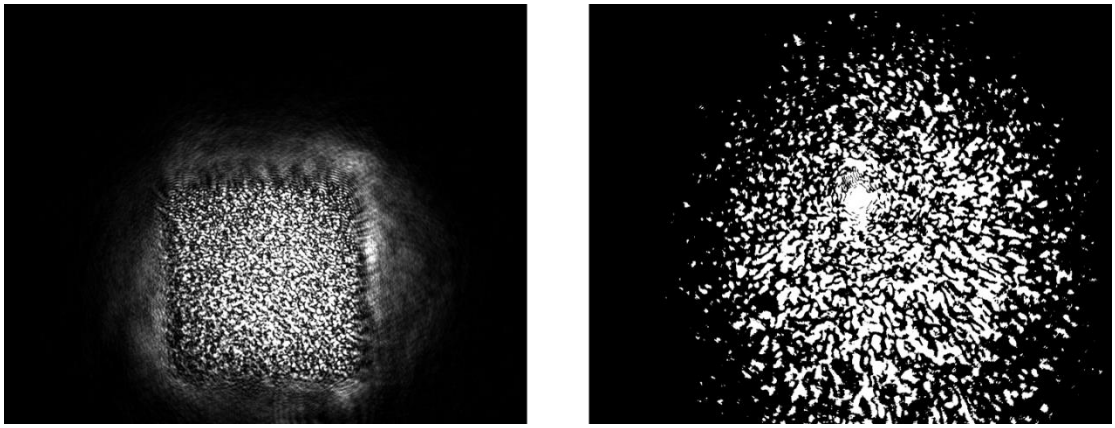

Figure 42 the same structure in lase light and the speckle pattern, still there is a lot of ballistic light to be exploit

Random Positioned Voids in volume

The next geometry, it's the completely random deposition of voids in specific volume. This geometry was the first to our experiment to present speckle pattern. But due limitation of time, wasn't fully explored.

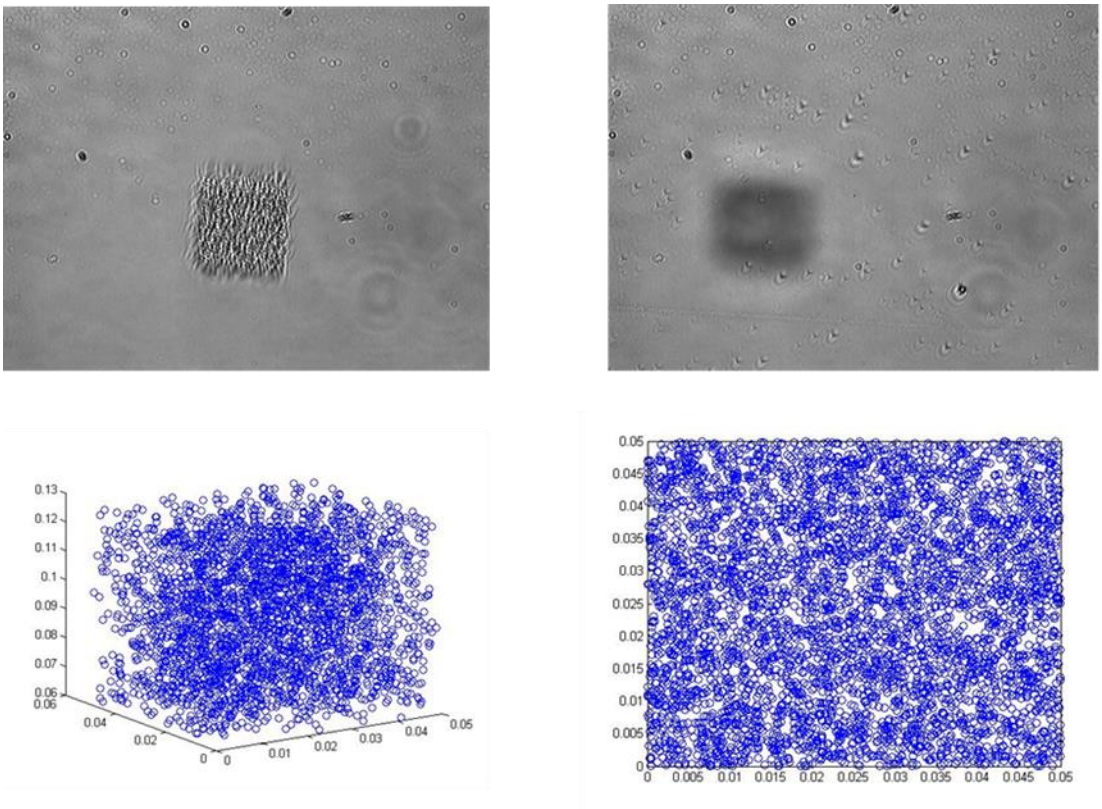

Figure 44 The 3D structure. In white light and shadow on the Surface. The 3D map and the spots in x,y dimensions

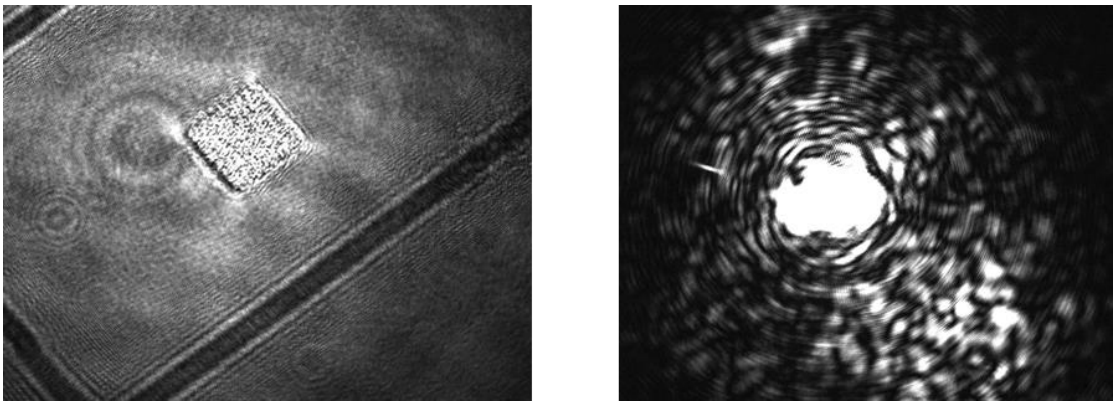

Figure 43 THe structure in laser light , as well we got speckle pattern but a lot of ballistic light as well

In general the best results for speckle pattern started at 100μm but not a patter we could exploit with wavefront shaping, because it's weak compared to ballistic light. This threshold seems to be kept in all the geometries, regardless if they are very dense or not (obviously there is a lower limit in the density as well). So it seems that for strong scattering material we should bear in mind that thickness of the structure it's more important, that make very dense layers. That's important to minimize the building time.

The structure as can be seen in images [42,43] show speckle pattern and a lot of ballistic light, which prevent it to be exploit. So again we see the necessity for extra thickness.

Randomly Spaced Voids in lines

This case was the most successful example, and the only one which had the chance to full develop and give an exploitable speckle pattern. In this case a structure that last almost 2 days to finish and dimensions 100X100X475 μm. In total it had 95 layers spaced with 5μm to each other. Each layer contained different number of spots, having an average number of 650 spots per layer.

Thankfully this structure was a success, and mostly because it had enough layers. Moreover it likely to be similar in optical behavior with a biological tissues, since the scatterers are

close to each other and spaced differently between them. Just like the cells are packed next

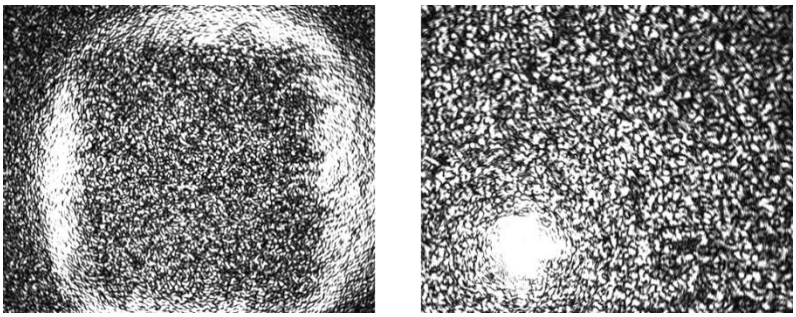

Figure 46 We can see the speckle pattern from the structure. This time was explotable.

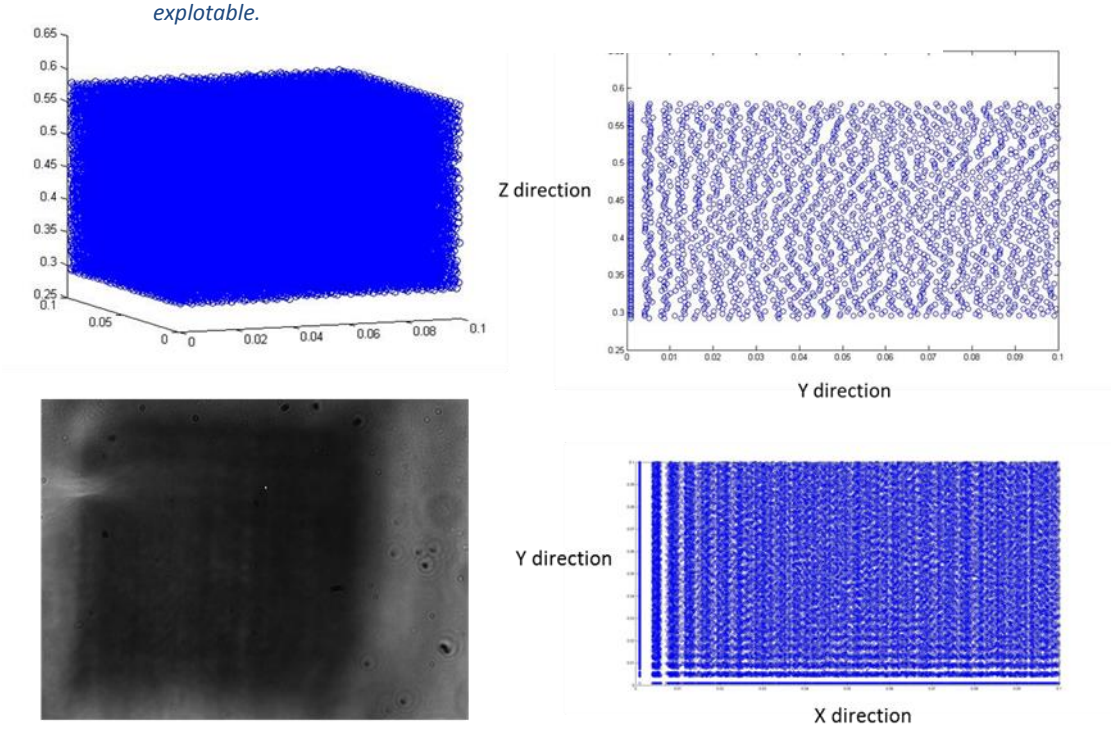

Figure 45 And the shadow from the surface. In the Graphs we can see how the voids are placed in the structure.

to each other.

From the mapping we can see how randomly are spaced the rows to each other, so the resulting structure to be fully covered by the spots to each point. The speckle pattern this time was much stronger and as we'll see later fully exploitable.

Fully covered layers and randomly placed gaps.

The last geometry, it can reach high densities, but really long times to be made. A structure up to 185 μm. Since each layer has about 1675 spots and each layer is spaced 5μm to each other. Unfortunately, the speckle pattern even for this geometry wasn't strong enough. This geometry, also can imitate the structure of a biology tissue. But it's take so much time to

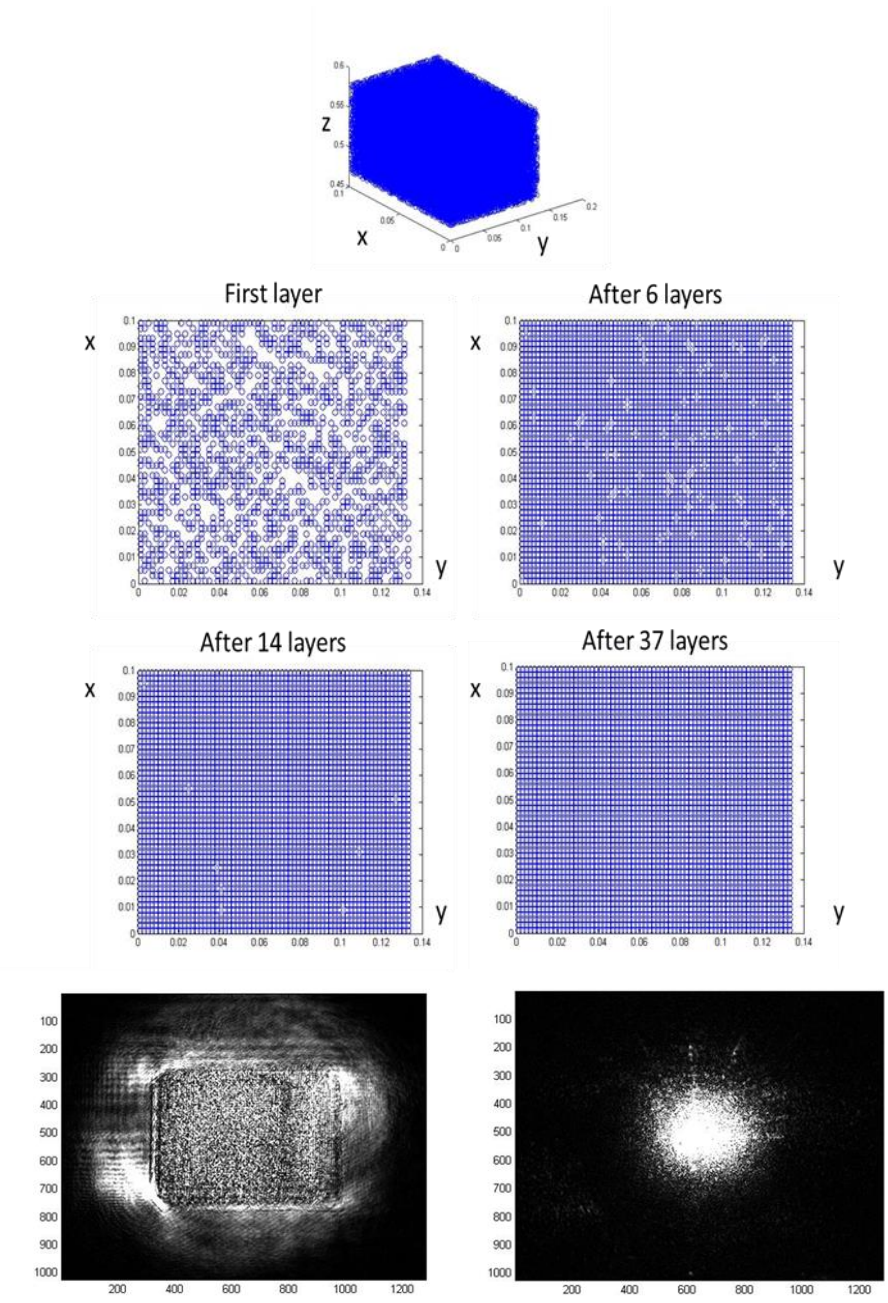

Figure 47 Although this case is a high density in voids the speckle pattern is weak due tje few layers

construct it, so for the time being, we will work with the rest geometries.

E.3 Wavefront Shaping

The main apparatus for this part of the experiment it is the SLM, which is connected to an imaging system as it can be seen in image [48].

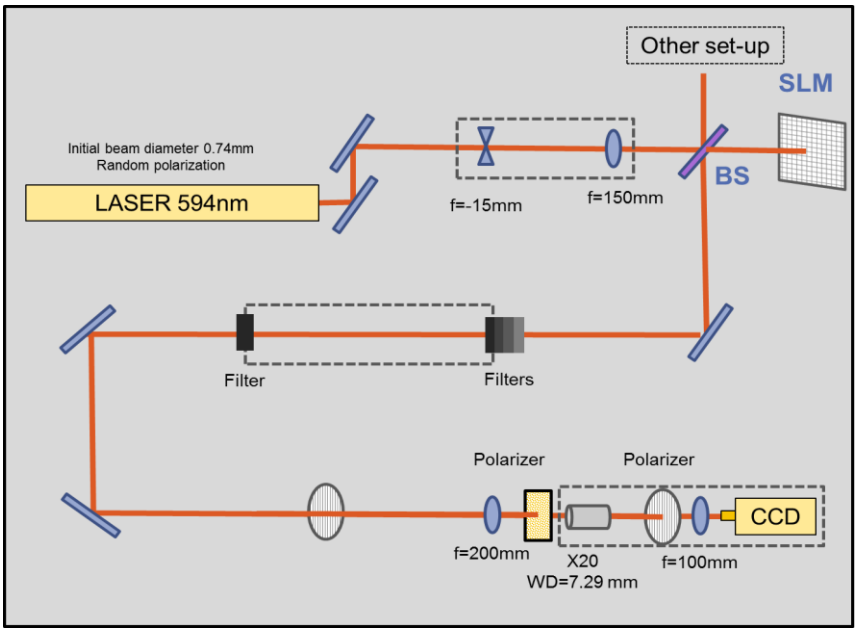

Figure 48 The wavefront set-up

But before we get to the in details about the set-up, some further words on what a SLM are needed.

SLM

Spatial light modulators, are devices that can modulate the phase of light that propagates through them or it is reflected by them. For this reason, SLMs are arrays of pixel, so each pixel can induce a phase change to only a small portion of the light beam. The quality of a SLM can be described, by the phase control on a wavelength (at least 2π phase modulation), the density of the pixels (fill factor) and the size of the pixel (the smaller they are, the smoother a beam profile we can get). Although for some applications simpler geometries are enough, the most popular ones, are square arrays of pixels, just like a common liquid crystal display LCD screen (actually most of them are LCDs).

The first SLMs developed in the 1980s where cumbersome, expensive and possessed only few dozen of 'pixels' which limited their applications to a few domains. They were particularly used in astronomy to compensate the optical aberration of

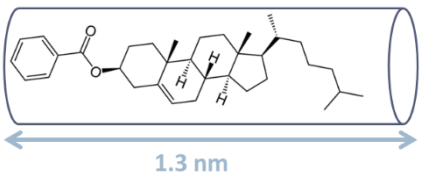

Figure 49 Liquid crystal shape and formula

the atmosphere.

Although today there is a number of SLM technologies, like deformable mirrors or the most commonly used, liquid crystals (LC). Liquid crystals were at first developed as a medicine for cancer, but soon it was observed that this liquid corresponds to electric fields or temperature changes.

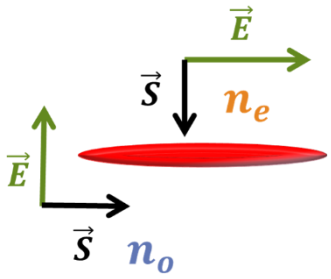

Figure 50 The refractive index for liquid crystals is different in respect light polarization with the axis of the crystal

The molecules composing such materials can be visualized as ellipsoids, with a single long axis about which there is circular symmetry in any transverse plane. The elongated structure of LC makes it an anisotropic image [50]. In particular to exhibit birefringence, or to have different refractive indexes for light polarized in different directions. LC have larger refractive indexes for optical polarization parallel to the long axis of the crystal (the extraordinary refractive index, n_e), and smaller uniform refractive index for all polarization directions normal to the long axis (the ordinary refractive index, n_o). Usually n_e-n_0=0.2 .

The interesting thing about LC is that if a voltage is applied, the LC are aligned to the direction of the applied voltage. Depending on how these LC are placed inside the cell in respect to the applied voltage, it can induce polarization swift or change the refractive index. In the latter case, by changing the refractive index for each cell to a desirable value, we can induce phase difference corresponding to:

$$\varphi = kx \rightarrow \varphi = \frac{2\pi n}{\lambda} x \quad (E.3.1)$$

Where x is the length of the cell where the light of wavelength λ travels through. And n is the refractive index the cell has acquired because of the voltage we have induced. There are three types of deposing the LC inside a cell:

I. Nematic,
II. Smectic,
III. Cholesteric

Each one corresponds for a different functionality. For phase- only- modulation an alternative form of nematic LCs are used called the parallel aligned nematic variety. In this case phase-only-modulation will occur for given polarization by changing the applied voltage (this means we change the refractive index inside the cell).

Since the SLMs are working exactly like a LCD screens, the same protocols of communication with a computer have been enforced. This means when a colorful image is pictured on a screen a map for the values of red green and blue (RGB) is made. For each color we have shades from 0 (absence) to 255 top bright, max value. So by combining 255 shades one can have 16,777,216 different colors. Each value from 0 to 255 corresponds to a fixed voltage applied to the pixel. A SLM works like a screen having only one available color. The actual color port a SLM uses is green, but we usually talk about gray levels for convenience reasons;

the shades of gray range from 0 to 255. This means there are 256 different voltages we can apply to each pixel, and for each value we can induce a specific phase swift.

SLM Calibration

For this experiment we acquired a Holoeye Pluto VIS/NIR/BB/TELCOM SLM with a huge spectrum response. Since it's covering the whole visible spectrum and infrared (IR) up to 1064nm, plus the wavelengths of telecommunication systems, 1520-1620nm (although that is IR too, I mention it separately because of its significance), the manufacturer have given the phase

Figure 51 Holoeye Pluto SLM device

swift for specific wavelengths only.

In our set-up we use a continuous work (CW) laser source from Throlabs with wavelength λ=594nm. This wavelength was not listed in the manual of the SLM, so we proceeded to calibrate the SLM. By doing the, we could deduce what phase swift we were inducing for each pixel value.

There is a number of available methods to calibrate a SLM. The most practical one, it's the double slit method, as it's pictured in image [52].

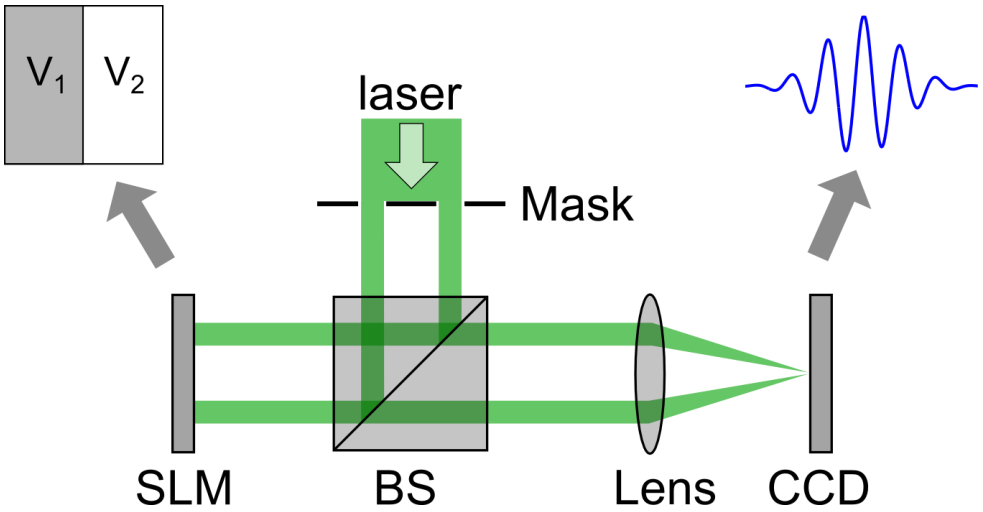

Figure 52 SLM calibration set-up www.wavefrontshaping.net

The laser beam is expanded and a double slit is used to have two separated and small collimated beams, in our set up those two holes of 1mm diameter size and spaced 2mm away from their centers. The SLM is divided in two parts where the pixel values are respectively V1 and V2. We make sure that the two beams are reflected on the two different parts of the SLM. After modulation by the SLM, we place a digital camera at the focal plane of the lens to observe the interference fringes. It is necessary to have fringes large enough so that there are as many pixels as possible in the interfering distance.

To measure the phase modulation, we fix the value of V_1 - for instance at the minimum pixel value - and vary the value $V_2 = V_i$ between the minimal and the maximal pixel value. When the relative phase between the two beams is modified, the fringes maximums of the fringes will be shifted by a distance δL_i δL. This can be obtained by calculating the correlation function between the first and the i^{th} image of the fringes and finding its maximum.

The phase variation can be derived from:

$$\Delta\varphi_\iota = 2\pi\frac{\Delta L}{\delta L_i} \quad (E.3.2)$$

The phase difference introduced by each shade on the SLM will be the distance of the two bright fringes to the distance of current and previous gray level fringe. We scan the phase difference induced for every shade of gray and finally we have a calibration plot how much phase difference we induce for specific wavelengths.

The set-up can been seen in image [53]. We used a f=40mm lens to focus the beam on the observation plane of our imaging system. The imaging system is compromised by a Thorlab camera U420 , a positive lens f=100mm and an objective lens, NA=0.70 , as it can be seen in

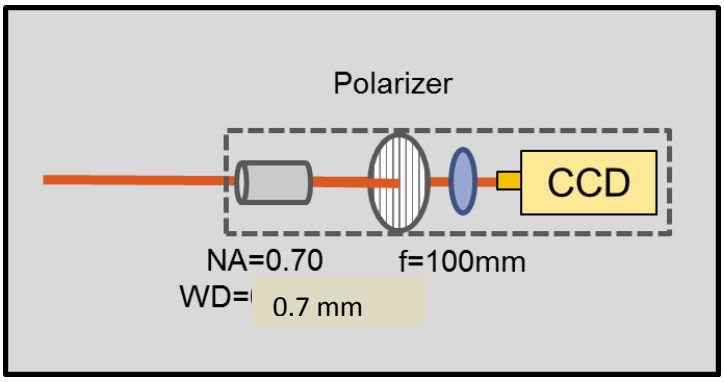

Figure 53 Imaging set-up , objective with CCD camera

picture [53].

Then a code changed the SLM in two parts, as it has been described above. The camera was recording the evolution of the fringes and saving them on the hard disc. At the end, a second

program created to deduce the graph bellow. The process time is relatively large, this is why the procedure was recorded and processed separately and not simultaneously.

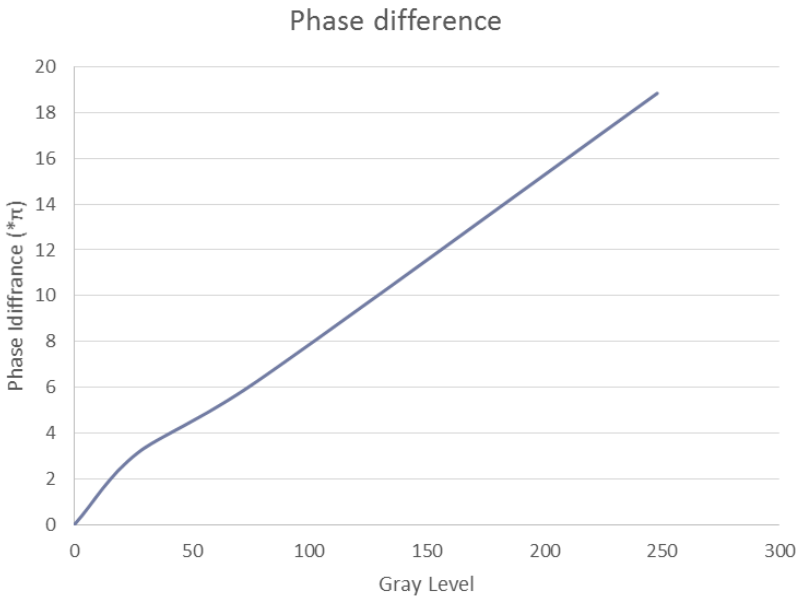

Figure 54 Calibration Plot of the SLM for 594 nm

We can deduce from the graph that the 2π phase difference is introduced for the value: 80. This information is useful when we will use our focusing code, because we can give more precise control from 0 to 2π phase swift for perfect focusing. In images [] we can see how the fringes are moving for different gray levels (pictured 0,45,57)

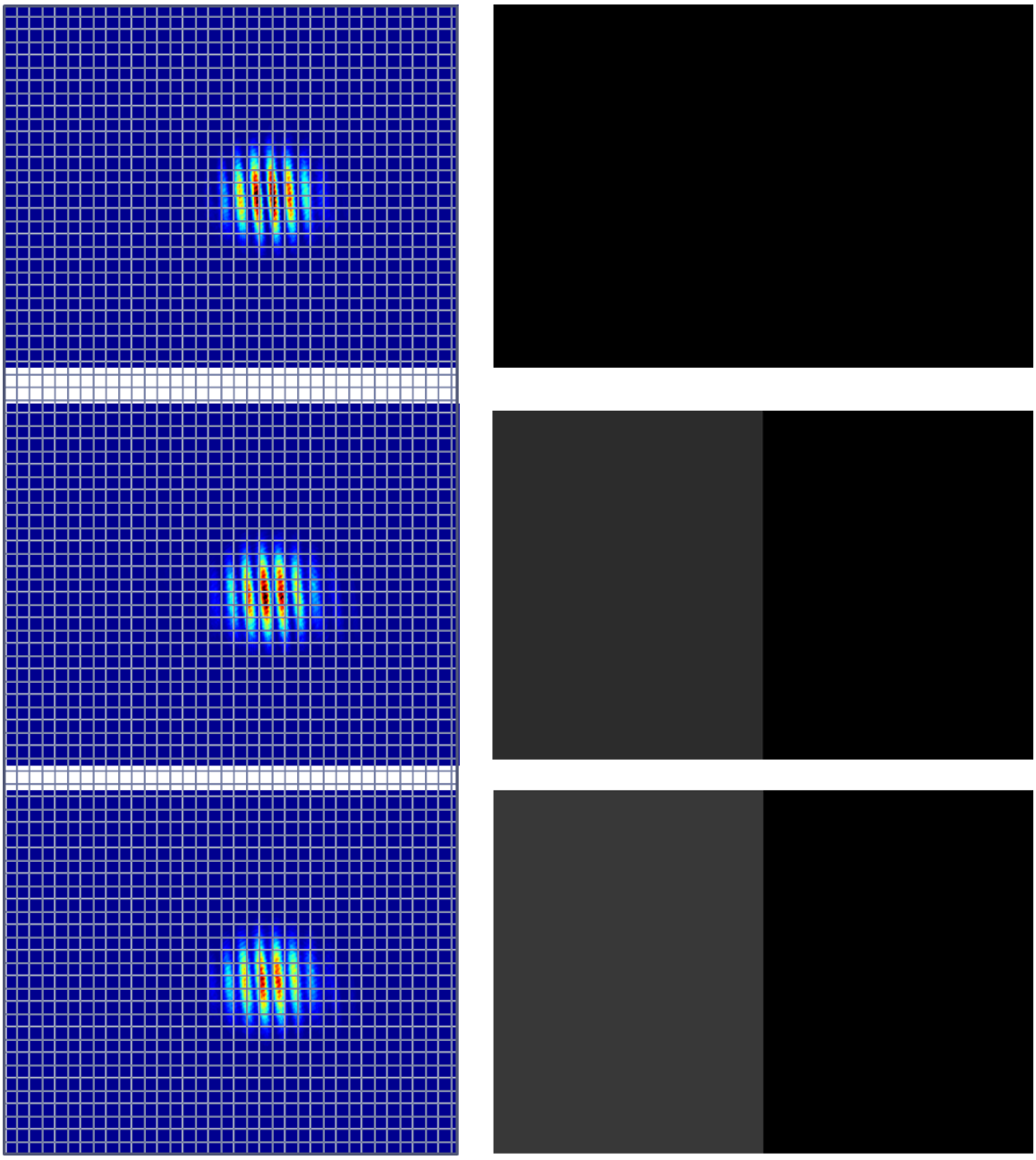

Figure 55 Movement of the fringes for different gray levels

Focusing

Focusing through a scattering medium, was the first application of the wavefront shaping. It requires a strong scattering medium which generates a speckle pattern after laser light propagates through it.

If the light is modulated by a SLM in a set up like the one in image [56], each pixel will introduce a different phase to each point of the beam. Making it possible for the beam to couple with the scattering medium in such way that it can be better transmitted through better.

Since scatterers are randomly located inside a scattering medium, means there is a random location of scatterers, the mask for the SLM (the phase pattern we need to introduce on it) to achieve such a goal, should be random as well.

The set-up is controlled with a computer connected with the SLM and reading the camera. The algorithm begins, by taking a photo with a white mask (a uniform mask in one shade). Then it will start producing random masks, with 30x30 megapixels (Arrays of the SLM pixels, 1 megapixel=30 actual pixel). The megapixels get random values from 0 up to 73 (where the phase is 2π swifted).

We usually start with 50 random masks, and the algorithm checks whether the intensity has increased to the desirable location for each pixel. After it has checked all the initial random masks, it chooses the one which produced the highest intensity in the desirable location (we create a new speckle pattern with a speckle on the location we desire).

Then an iterative part begins, which scan each pixel with step π to –π and checks if the intensity at the target increases. If it does, it keeps the change, differently it returns to the initial value. Doing this for each megapixel, we will get a tight focus, with some speckle artifacts around.

The way to check the quality of the focus, enhancement is used:

$$h = \frac{I_{optmized}}{I_{before\ optimization}} \quad (E.3.3)$$

Which is the ratio of the intensity at the end of the focusing algorithm to the intensity of the before optimization.

The set-up that was build is shown in image with details on image []. First the beam goes through a telescope to enlarge the size:

$$m = \frac{f_o}{f_e} = \frac{f_1}{f2} = \frac{100}{15} = 6.6$$

Although the resulting beam waist after the used of the telescope is just 6mm because it is cut with an iris. Then the beam meets a beam splitter to be sent to another set-up and on the SLM. The SLM it modulates the beam and reflects it back on the beam splitter. Half of the mean will follow the path to M3. The beam intensity is reduced further more with filters (Except the polarizers). The beam then goes through M4 and M5 to be filtered by a polarizer.

This polarizer can control the intensity of light further compared to the polarizer inside the imaging system; with such a set-up we can get rid of the ballistic light (as I have shown previously in section 2.2, light polarization gets elliptical when it is scattered).

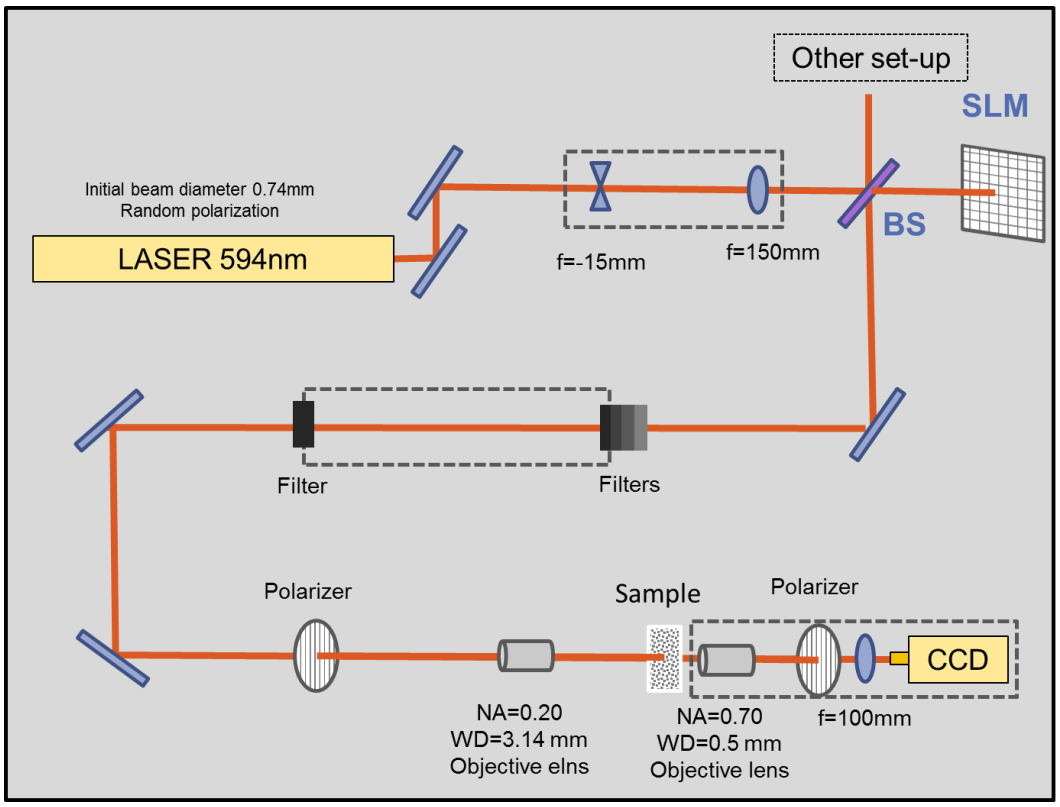

Figure 56 The wavefront Set-up

After the polarizer is focus by an objective lens. At the plane of focus, the sample is placed. We use an objective lens, to achieve the smallest possible focus, since the artificial structures are small in size.

Then the imaging system, that was described above monitors the scattered light. The set-up it's identical to most of the set-ups in literature of focusing by wavefront shaping. Having mount everything, before we try the artificial structures, we should check first if it complies well with other scattering media such as TiO_2 paint and commercial correction fluid.

TiO_2 Sample Preparation

We used TiO_2 sample, because of their low absorption and highly scattering properties. Powder of Ti02 was mixed in two different solutions, either distil water or ethanol. For each solution, we added different percentage of powder , 1, 2 or 4 % of the solution concentration.

Those liquid mixtures were left inside an ultrasound sonicator

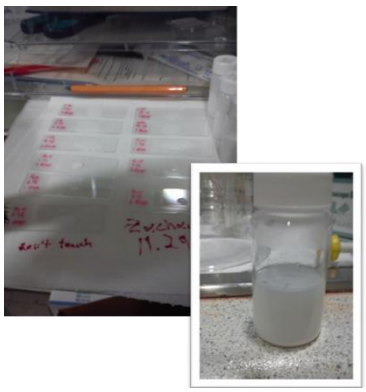

Figure 57 TiO_2 samples

for 30 minutes. After this the samples were a white liquids. We put 1,2 and 3 drops of each solution on small lab glasses (one for each). This had to be done very carefully in order for the drops to remain homogenous.

Then the samples were left to dry out for a day, a homogenous layer of white painting was left on the top. Each sample had a different concentration of scatterers, depending on the initial concentration and different thickness of the drops we used. All of them were used, so we could get some good focusing results.

Focusing

I have created a code that controls both the SLM and the camera. I ran some tests on those samples to examine the functionality of this code and to proof in principle that the set-up is functional.

I focused the beam on the sample and observed the speckle pattern with the imaging system. Then I moved back the imaging system (about 7 mm) and started a focusing experiment. There were several successful results for various positions, as can be seen in

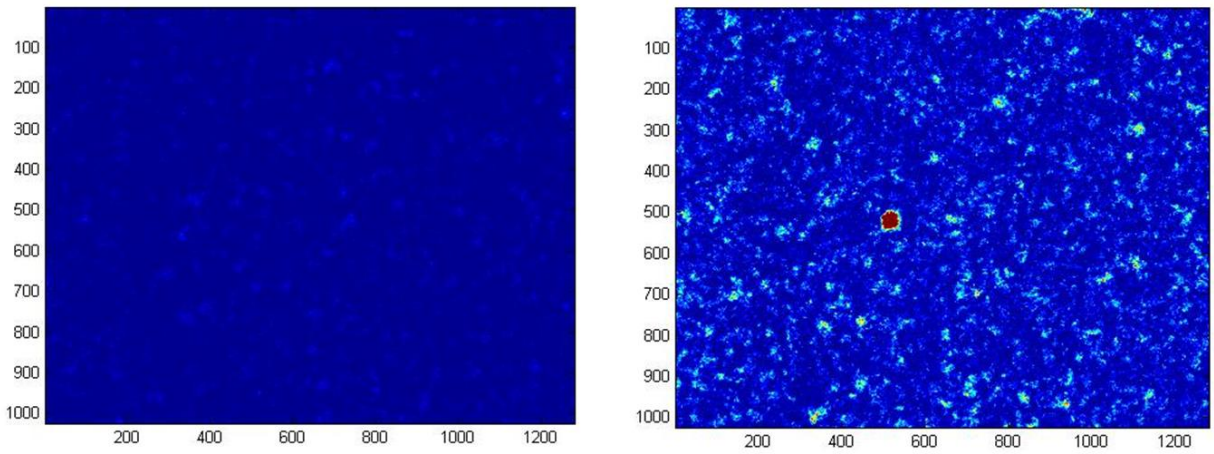

Figure 58 Initial Speckle pattern and the image after optimization in random position

below graphs.

In the images we can see the speckle pattern of a white mask ((this means no optimization). And next to it, the optimization was achieved and we successfully created a focus on the desirable location.

In images [58] the mask, the camera frame and the enhancement for each optimization step can be seen. We did it again for another position, to prove again the repeatability and functionality of the concept. And it was done successfully as can be seen in images [59]. I leave out the rest of data and tries (both with $Ti0_2$ and correction fluid), since they replicate same results.

Afterwards the road is open to check the response in our artificial structures.

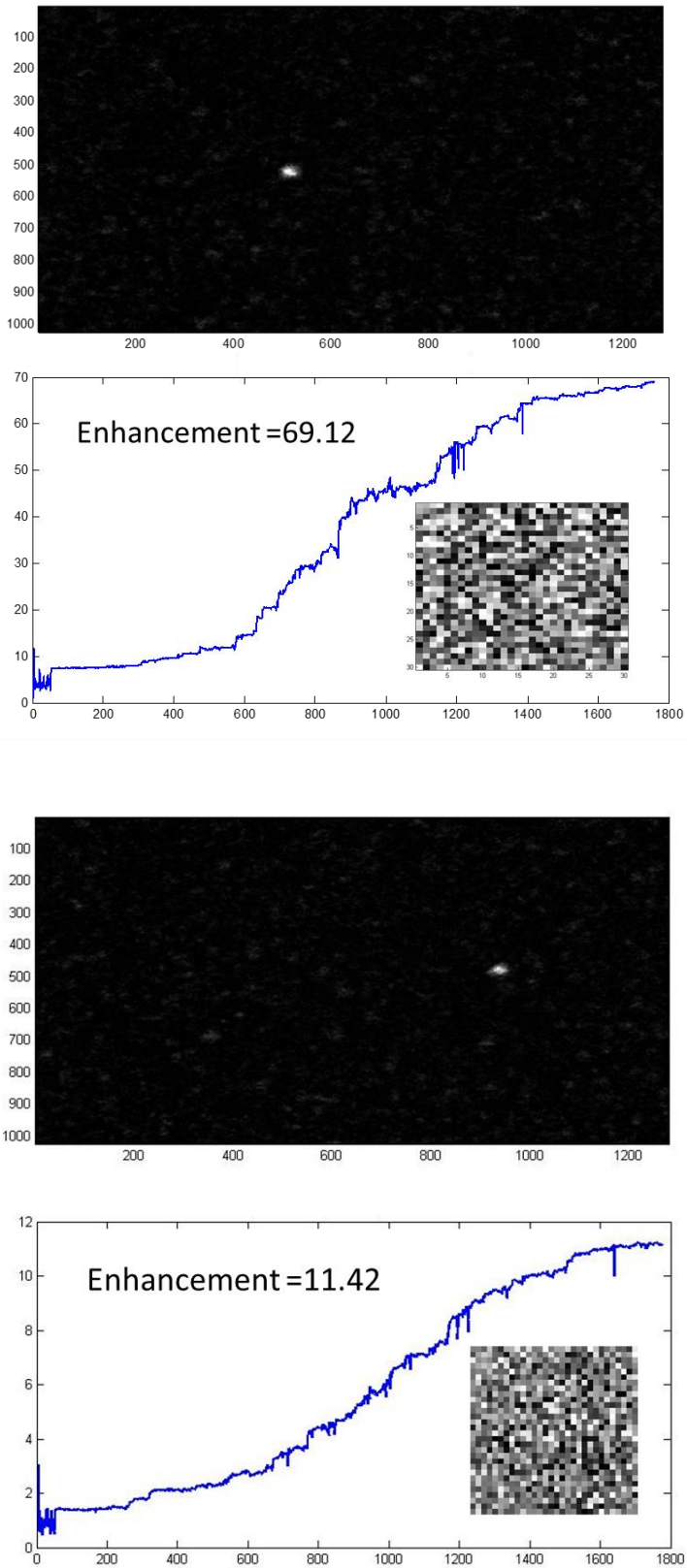

Figure 59 The optimization of TiO_2 in various position, each time successful

E4. Taming light propagation through scattering media

In this last section, we will combine the methods described before. We will use our artificial scattering structures and see if it is possible to have a focus on the back. The preliminaries test, showed that although there is a speckle pattern for structures around 100μm along the axis of light propagation, the values to have wavefront control seems to be around 500μm.

Because of limitation of time only one structure that was built that met all the criteria, but at least gave satisfactory results.

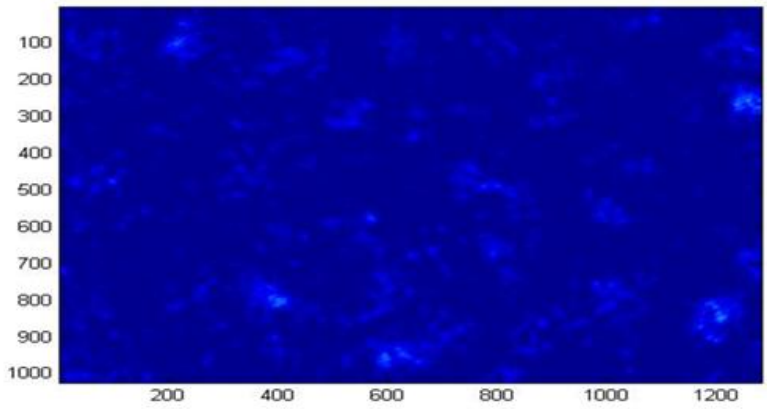

Figure 60 Speckle pattern from the artificial structure

We are still talking about the structure shown in E2, randomly spaced voids in lines. It corresponds with the same geometry that was used in [45], only much smaller. So we moved the imaging system around 5mm away from the sample. Then took a photo of the speckle pattern on white mask and started optimization, figure [60].

We optimized it to various positions. And it was successful every time. We present two optimizations in different positions, this can be viewed in images [61]. We proceeded a step forward and we focused on two different positions.

This concept of multi focusing simultaneously is a procedure to show that our results correspond with all the data in literature. In fine optimized set-ups multi foci share the enhancement that only one foci could have. In the experiment of Mosk for one focus the enhancement was 1000 but for double foci, each had 500. In our example each focus is unequal because the process required further optimization.

With this we conclude the experimental results. The experimental work might appear short, but the samples and the time of generation was much larger. Here is presented only the basic skeleton of this work and the functional results.

For scattering enough structures one should work further than 500μm for soda lime glass. Materials with higher refractive index like LaSF glass should show higher scattering for less thickness.

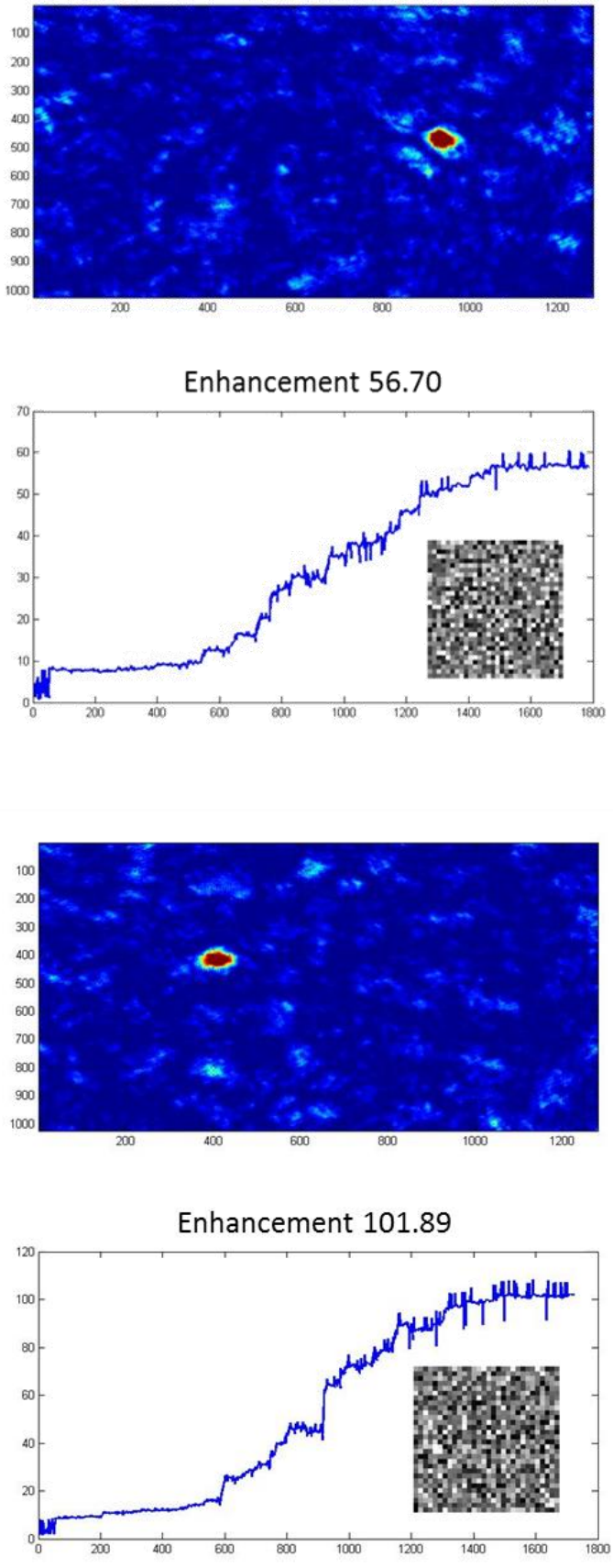

Figure 61 the focus at various locations on the back of the scattering medium

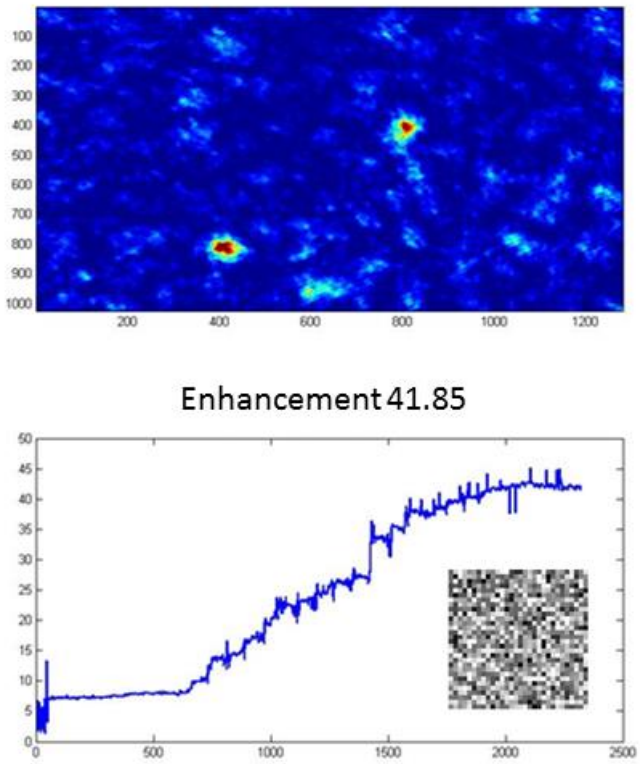

Figure 62 The double focus, on the first graph enhancement for the first focus and the second for the second graph

Conclusions

This work has the misfortune to close quick but at least proved that artificial scattering media can be coupled with the wavefront shaping techniques successfully. There is still work needed to characterize the scattering coefficient of the arterial structures and a more accurate characterization of the voids. Apart from reaching the scattering properties of a biology tissue which is only a matter of time, there is a new operation window opening.

Following the latest works of Mosk, Pinkse and Vos one can see that the need of an artificial, optimized and replicable scattering media is needed. This means, laser micromachining has a number of contributions to offer in the field.

Appendix

The appendix sums up the most important codes I have made for this thesis. It's in two parts, the first one, A1, is to create coordinates for the structures and A2 the codes for focusing and calibration of the SLM.

A1 Structure Codes

```
function [ out ] = xytissue(x,y,z, nfak, layer, d , step)
%xytissue: it's a code to make random layered structures!
% x,y,z: it's the point where the structure begins to build%
% nfak: number of spots for each layer
% layer: number of the layers we put
% d: Dimensions of a structure (it's square) and mm
% step: the step between the layers


%The output file must have five rows,
% (x) (y) (z) (time of shutter) (Pi)

% 1 row it's the angle of the polarizer
% 2 it's the y coordinator of the spot
% 3 it's the z coordinator of the spot
% 4 Time exposure for each spot, it's in miliseconds
% 5 it's the y coordinator of the spot


%************************** INTRO***********************


lim=layer*nfak; % Total number of spots in the structure
A=ones(lim,5)*1000; % Creating an array for all the spots
h=1;

n=1.641276; % The refractive index of the glass
zo=0.05/n; % Adjusting z dimension because of refraction
step=step/n; % Adjusting the step
oops=0; % variable to check if there is overlaping
z=zo+(layer*step); % last layer (we begin from bottom)

% ################## Creating Coordinates ###############

for p=1:1:layer

          for i=1:1:nfak
             A(h,1)=0;
             A(h,2)=(rand*d)+y;
             A(h,5)=(rand*d)+x;
             A(h,3)=z;
             h=h+1;

          end

          %A function to check if there is overlapping between
the spots.
```

```
          %First call of the function, at least once manualy
          [A,oops]=check(A,p,nfak,d,x,y);
          %Now it works until oops get zero again
          while oops==1
          [A,oops]=check(A,p,nfak,d,x,y);

          end
p
         z=(z-step); % Changing layer


end


for m=1:1:(lim)
    s(m)= A(m,2);
    t(m)= A(m,5);
    q(m)=A(m,3);

end
plot3(s,t,q,'o')
out=A;


nm=['tissue.txt'];
dlmwrite(nm,A,'delimiter','\t','precision',
'%6.6f','newline','pc' )

out=A;
end


%@@@@@@@@@@@@@@@@@@@@@@@@ function @@@@@@@@@@@@@@@@@@@@@@@@@@@@


function [A,oops] = check(A,p,nfak,d,x,y)
oops=0;

fc=(p-1)*nfak;

ka=1+fc;
la=1+fc;
kf=p*nfak;
lf=p*nfak;

for k=ka:1:kf
    for l=la:1:lf

        if A(k,2)==A(l,2)&& k~=l
            if A(k,5)==A(l,5) && k~=l % Checking if they have
same coordinates
            A(l,5)=(rand*d)+x;
            A(l,2)=(rand*d)+y;
            oops=1;
            end
```

```
        end

        % Criterion of overlapping by the radius of the spots!
        if k~=l
            X=((A(k,2)-A(l,2)))^2;
            Y=((A(k,5)-A(l,5)))^2;
            cr=(X+Y)^0.5;
        if cr<=0.003;
            A(l,2)=(rand*d)+y;
            A(l,5)=(rand*d)+x;
            oops=1;
        end


       end


    end

end

end
```

```
function [ out ] = monolayer(x,y,z,nfak,d,num)
%this code produces only one layer in random positions

% x,y,z: it's the point where the structure begins to build%
% nfak: number of spots for each layer
% layer: number of the layers we put
% d: Dimensions of a structure (it's square) and mm
% step: the step between the layers


%The output file must have five rows,
% (x) (y) (z) (time of shutter) (Pi)

% 1 row it's the angle of the polarizer
% 2 it's the y coordinator of the spot
% 3 it's the z coordinator of the spot
% 4 Time exposure for each spot, it's in miliseconds
% 5 it's the y coordinator of the spot


%************************** INTRO***********************

zi=z;
n=1.641276;
z=z/n;

A=zeros(nfak,5);%
oops=0;
% ################## Creating Coordinates ###############

          for i=1:1:nfak
             A(i,1)=0;
             A(i,2)=(rand*d) ;
             A(i,3)=z;
             A(i,4)=1000;
             A(i,5)=(rand*d);

          end

     % Checking for overlaping
     [A,oops]=check(A,i,d);
     ,

     while oops==1
             [A,oops]=check(A,i,d);
     end



     A(:,2)=A(:,2)+y;
     A(:,5)=A(:,5)+x;

     s=zeros(nfak);
     t=zeros(nfak);
     for m=1:1:nfak
```

```
        s(m)= A(m,2);
        t(m)= A(m,5);
    end
    plot(s,t, 'o')

 nm=['monolayer',num2str(zi),' ',num2str(num),'.txt'];
   dlmwrite(nm,A,'delimiter','\t','precision',
'%6.6f','newline','pc' )



out=A;
end




function [A,oops] = check(A,i,d)
oops=0;
ka=1;
la=1;
for k=ka:i-1
    for l=la:i-1

        if A(k,2)==A(l,2)&& k~=l
            if A(k,5)==A(l,5)&& k~=l
            A(l,5)=(rand*d)+x;
            A(l,2)=(rand*d)+y;
            oops=1;
            end
        end

         if k~=l
            X=(A(k,2)-A(l,2))^2;
            Y=(A(k,5)-A(l,5))^2;
        cr=(X+Y)^0.5;
            if cr<=0.002;
            A(l,5)=(rand*d);
            A(l,2)=(rand*d);
            oops=1;
            end
        end



        l=l+1;
    end
    k=k+1;
end

end
```

```
function [  out] = qpertissue3d( zi,zf, per, d, na)

%this code produces only one layer in random positions

% zi,zf: Starting and ending coordinates
% per: percent of cover we want to make
% d: Dimensions of a structure (it's square) and mm
% na: numerical aperture of the lens,now works only for NA=0.4


%The output file must have five rows,
% (x) (y) (z) (time of shutter) (Pi)

% 1 row it's the angle of the polarizer
% 2 it's the y coordinator of the spot
% 3 it's the z coordinator of the spot
% 4 Time exposure for each spot, it's in miliseconds
% 5 it's the y coordinator of the spot


%*************************** INTRO************************

oops=0; %
n=1.641276;

zi=zi/n;
zf=zf/n;
min=0.0002;
vxy=round(d/min);
vz=round((zf-zi)/min);

if na==0.40

    r=1/1000;

    b=8/1000;
    v=r*r*b*3.141592*(4/3);
    V=d*d*(zf-zi)*n;
    nf=round(V/v);
    nfak=round(((per)*nf)/100);
    A=zeros(nfak,5);
end
diafora=-nfak+nf;

st=['The final amount of voids is ',num2str(nfak),' and the
total voids removed were ',num2str(diafora),' Total number
could stack in is ',num2str(nf),' Maximum coverage is
',num2str((100*nf*v)/V)]


%#################### Creating Coordinates ###################


          for h=1:1:nfak
             A(h,1)=0;
             A(h,2)=(round(vxy)*rand)*min; %y
```

```
            A(h,3)=zi+(round(rand*vz)*min); %z
            A(h,4)=1000; %z
            A(h,5)=round(vxy*rand)*min; %x


        end

        %sunartisi elegxou taytosimon simeion

        %Proto kalesma, edo exoume idi to proto layer
        [A,oops]=check(A,nfak,d,zi,zf);
        %vrogxos elegxou gia diples suntetagmenes,
        while oops==1
        [A,oops]=check(A,nfak,d,zi,zf);

        end

   miaou=1;
    while miaou==1
            miaou=0;
        for i=1:1:nfak-1
            j=i+1;
                if A(i,3)<A(j,3)
                x=A(j,5);
                y=A(j,2);
                z=A(j,3);
                A(j,5)=A(i,5);
                A(j,2)=A(i,2);
                A(j,3)=A(i,3);
                A(i,5)=x;
                A(i,2)=y;
                A(i,3)=z;
                miaou=1;

            end
        end
    end


    r=date;

B=A;
nm=['qfree3d number of spot',num2str(nfak),'dimensions d',
num2str(nfak), ' Thickness ',num2str(zf-zi),' on the date',r,'
.txt'];
dlmwrite(nm,B,'delimiter','\t','precision',
'%6.6f','newline','pc' )


diafora=-nfak+nf;

 plot3(A(:,5), A(:,2), A(:,3),'o')
   st=['The final amount of voids is ',num2str(nfak),' and the
total voids removed were ',num2str(diafora),' Total number
could stack in is ',num2str(nf),' Maximum coverage is
',num2str((100*nf*v)/V)]
```

```
out=A;

end


%@@@@@@@@@@@@@@@@@ function overlapping check @@@@@@@@@@@@@@@@@


function [A,oops] = check(A,nfak,d,zi,zf)
oops=0;

min=0.0002;
ka=1;
la=1;
kf=nfak;
lf=nfak;
vxy=round(d/min);
vz=(zf-zi)/min;

for k=ka:1:kf
    for l=la:1:lf

        if A(k,2)==A(l,2)&& k~=l
            if A(k,5)==A(l,5) && k~=l
                if A(k,5)==A(l,5) && k~=l
                A(l,5)=round(vxy*rand)*min;
                A(l,2)=round(vxy*rand)*min;
                A(l,3)=zi+(round(rand*vz)*min); %z
            oops=1;
                end
            end
        end

        % Criterion for overlapping
        if k~=l
            X=((A(k,2)-A(l,2)))^2;
            Y=((A(k,5)-A(l,5)))^2;
            Z=((A(k,3))-A(l,3))^2;
            cr=(X+Y+Z)^0.5;
        if cr<=0.001 && (Z^0.5)<0.005
            A(l,2)=round(vxy*rand)*min;
            A(l,5)=round(vxy*rand)*min;
            A(l,3)=zi+(round(rand*vz)*min); %z
            oops=1;
        end

       end
       end


    end

end
```

```
function [ B ] = randspacinglayer(z,d,num)
%This will be a function to create coordinates to make a
scattering
%layer.the difference compared to monolayer, it's that this
can achieve
%more that 50% coverage.
%To do so, i start by a very organised structure, and later on
I'll remove
%randomly voids from the ensemble. So i'll gradualy de
organise it.

%Variables
%per: What percentage I want it to be covered, (%)
%d: The dimension of the quare
%Layer Number


x=0;
y=0;
r=1.7;
aa=3.14*r*r;
%************************ INTRO ******************************
zi=z;1
n=1.641276;
z=z/n;

%The first program is for square structures, but i in the
future i
%might need the rectagular
dx=d*1000;
dy=d*1000;

stepmin=3.5;
stepmax=7.0;
dstep=stepmax-stepmin;
stepv=(stepmin);
% For NA=0.40 the voids are r=1μm so, they must be seperated
2μm! and we
% begin
a=round(dx/stepv);
b=round(dy/stepv);
dim=a*b;

A=zeros(dim,6);
xi=1;
yj=1;
l=1;

while xi<=dx
    while yj<=dy
            A(l,1)=0;% Energy Angle
            A(l,2)=(yj/1000); %y
            A(l,3)=z;
            A(l,4)=1000; %Duration ms of the irradiation
            A(l,5)=(xi/1000); %  x
            A(l,6)=1;
```

```
            stepv=((dstep*rand)+stepmin);
            yj=yj+stepv ;
            l=l+1;
    end
    stepv=((dstep*rand)+stepmin);
    xi=xi+(stepv);
     yj=1;
end

%Here we have a full layer of voids, stacked one after the
other and
%working perfectly :D

%%%%%%%%%%%%%%%%%%%%%%%%%%%%%%%%%%%%%%%%%%%%%%%%%%%%%%%%%%%%%%%%%%%%%%%%
%%%%%%%%%%%%%
%                              Removing Voids
%
%%%%%%%%%%%%%%%%%%%%%%%%%%%%%%%%%%%%%%%%%%%%%%%%%%%%%%%%%%%%%%%%%%%%%%%%
%%%%%%%%%%%%%
%On this part i remove the voids randomly
[dim,u]=size(A);
 [dim,u]=size(A);
e=0;
for i=1:1:dim
   if A(i,6)==1
       e=e+1;
   end
end
e;
diafora=dim-e;
B=zeros(e,5);
j=1;
for i=1:1:dim

   if A(i,6)==1
            B(j,1)= A(i,1);
            B(j,2)=A(i,2) ;
            B(j,3)=A(i,3);
            B(j,4)=A(i,4);
            B(j,5)=A(i,5);
            j=1+j;
   end
end

%
figure(1)
plot(B(:,5),B(:,2), 'o')
r=date;
coverage=(aa*e*100)/(dx*dy);

 nm=['random spacing Number of Voids ',num2str(e),' Dimension
of the sample ',num2str(d),' Depth from the Ref ',num2str(z),'
Number of Layer ',num2str(num),' Made on ',r,'.txt'];
   dlmwrite(nm,B,'delimiter','\t','precision',
'%6.6f','newline','pc' )
```

```
   st=['The final amount of voids is ',num2str(e),' and the
total coverage is ',num2str(coverage),' percent',' estimation
time is ',num2str(4.5*e/3600)]

%}

end
```

```
function [ B ] = hdmonolayer(z,per,d,num)
%This will be a function to create coordinates to make a
scattering
%layer.the difference compared to monolayer, it's that this
can achieve
%more that 50% coverage.
%To do so, i start by a very organised structure, and later on
I'll remove
%randomly voids from the ensemble. So i'll gradualy de
organise it.

%Variables
%per: What percentage I want it to be covered, (%)
%d: The dimension of the quare
%Layer Number


x=0;
y=0;


%************************* INTRO ***************************
zi=z;
n=1.641276;
z=z/n;

%The first program is for square structures, but i in the
future i
%might need the rectagular
dx=d*1000;
dy=d*1000;
stepv=3;%poly konta 2;
% For NA=0.40 the voids are r=1μm so, they must be seperated
2μm! and we
% begin
a=round(dx/stepv);
b=round(dy/stepv);
dim=a*b;

A=zeros(dim,6);
xi=1;
yj=1;
l=1;
for i=1:2:dx

    for j=1:2:dy

            A(l,1)=0;% Energy Angle
            A(l,2)=yj/1000 ; %y
            A(l,3)=z;
            A(l,4)=1000; %Duration ms of the irradiation
            A(l,5)=xi/1000; %  x
            A(l,6)=1;
            yj=yj+2;
            l=l+1;
    end
```

```
    xi=xi+2;
     yj=1;
end

%Here we have a full layer of voids, stacked one after the
other and
%working perfectly :D

%%%%%%%%%%%%%%%%%%%%%%%%%%%%%%%%%%%%%%%%%%%%%%%%%%%%%%%%%%%%%%
%%%%%%%%%%%%%
%                            Removing Voids
%
%%%%%%%%%%%%%%%%%%%%%%%%%%%%%%%%%%%%%%%%%%%%%%%%%%%%%%%%%%%%%%
%%%%%%%%%%%%%
%On this part i remove the voids randomly
[dim,u]=size(A);
nr=((100-per)*dim)/100;
nr=round(nr);
k=0;
while k<nr
   i=rand*dim;
   i=round(i);
   if i==0
       i=1;
   end
   if A(i,6)==1
       A(i,6)=0;
       k=k+1;
   end
end


[dim,u]=size(A);
e=0;
for i=1:1:dim
   if A(i,6)==1
       e=e+1;
   end
end
e;
diafora=dim-e;
B=zeros(e,5);
j=1;
for i=1:1:dim

   if A(i,6)==1
            B(j,1)= A(i,1);
            B(j,2)=A(i,2) ;
            B(j,3)=A(i,3);
            B(j,4)=A(i,4);
            B(j,5)=A(i,5);
            j=1+j;
   end
end

%
```

```
figure(1)
plot(B(:,2),B(:,5), 'o')
r=date;

 nm=['HD-monolayer Number of Voids ',num2str(e),' Dimension of
the sample ',num2str(d),' Depth from the Ref ',num2str(z),'
Number of Layer ',num2str(num),' Made on ',r,'.txt'];
   dlmwrite(nm,B,'delimiter','\t','precision',
'%6.6f','newline','pc' )

   st=['The final amount of voids is ',num2str(e),' and the
total voids removed were ',num2str(diafora)]



end


function [  ] = layergen( )
%UNTITLED2 Summary of this function goes here
%   Detailed explanation goes here
dim=10;
r=date;
l=1;

for i=1:1:dim
    z=0.5-((i-1)*0.01);
    B=hdmonolayer(z,50,0.1,i);
    %B=randspacinglayer(z,0.1,i);
    [dim1,k]=size(B);

        if i==1
            dimx=dim1*(dim+1);
            C=zeros(dimx,6);
        end

    for j=1:1:dim1
            C(l,1)=B(j,1);% Energy Angle
            C(l,2)=B(j,2); %y
            C(l,3)=B(j,3);
            C(l,4)=B(j,4); %Duration ms of the irradiation
            C(l,5)=B(j,5); %  x
            C(l,6)=1;
            l=l+1;
    end
end

l=1;
e=0;
    dim=size(C);

     for y=1:1:dim
        if C(y,6)==1
            e=e+1;
        end
    end
```

```
    D=zeros(e,5);

      for r=1:1:dim
        if C(r,6)==1
            D(l,1)=C(r,1);% Energy Angle
            D(l,2)=C(r,2); %y
            D(l,3)=C(r,3);
            D(l,4)=C(r,4); %Duration ms of the irradiation
            D(l,5)=C(r,5);
            l=l+1;
        end
      end
r=date;
nm=['layergen the Number of spots ',num2str(e),' Made on
',r,'.txt'];
   dlmwrite(nm,D,'delimiter','\t','precision',
'%6.6f','newline','pc' )
figure(3)
x=D(:,5);
y=D(:,2);
z=D(:,3);
plot3(x,y,z,'o')

end
```

A2. Appendix Wavefront shaping codes

```
function [ ] = callibration()
%Here is the core program to initialize callibration of a SLM
%   Detailed explanation goes here

%we clear memory and screen
close all
clear all
%Loading the background noise
load('BackGround')
%initializing the camera
vid = videoinput('winvideo', 1, 'RGB32_1280x1024');
src = getselectedsource(vid);
src.BacklightCompensation = 'off';
src.ExposureMode = 'manual';
src.Exposure = -6;
src.GainMode = 'manual';
src.Gain = 50;
src.ContrastMode = 'manual';
src.Contrast = 0;
src.Gamma = 100;
src.Brightness = 0;
src.Contrast = 0;
src.Sharpness = 0;
src.VerticalFlip = 'off';
src.HorizontalFlip = 'off';



%We initialize a second window, covering the whole of the
second screen/SLM
window=Screen('OpenWindow',2);

%We define the absolut values
white = WhiteIndex(window);
black = BlackIndex(window);

%I begin with a black screen
A=[0,0];
B=kron(A,ones(500));
Screen(window, 'PutImage',B);
Screen(window,'Flip');
image(B);

scale=255;

%%%%%%%%%%%%%%%%%%%%%%%%%%%%%%%%%%%%%%%%%%%%%%%%%%%%%%%%%%%%%%%%%%%%%%%%
%%%%%%%%%%%%

%%%%%%%%%%%%%%%%%%%%%%%%%%%%%%%%%%%%%%%%%%%%%%%%%%%%%%%%%%%%%%%%%%%%%%%%
%%%%%%%%%%%%
```

```
%here we begin to calculate the dl and DL for various
grayscales

for i=1:1:scale+1
    i
    A=[i-1,0];
    B=kron(A,ones(500));
    Screen(window, 'PutImage',B);
    Screen(window,'Flip');

[Isum,img1]=callcam(vid,back_noise);


figure(2)
subplot(2,2,1)
colormap('gray')
image(B);
KM=num2str(i);
string=['Mask graylevel is ' KM];
title(string)

subplot(2,2,2)
image(img1);
grid on;
string=['Image from the Camera'];
title(string)


subplot(2,2,3)
imagesc(img1);
grid on;
string=['Image from the Camera'];
title(string)

str1=['p' KM];
str2=['m' KM];

save(str1, 'img1');
save(str2, 'B');



end


Screen('CloseAll')

end




function [Isum,img1]=callcam(vid,back_noise)
%This is a function to start the camera and take a shot!
% It requires the vid parameter which addres the camera.
```

```
% we also add the background to remove the noise.

%Here we set the attribures of the camera

src.BacklightCompensation = 'off';
src.ExposureMode = 'manual';
src.Exposure = -6;
src.GainMode = 'manual';
src.Gain = 50;
src.ContrastMode = 'manual';
src.Contrast = 0;
src.Gamma = 100;
src.Brightness = 0;
src.Contrast = 0;
src.Sharpness = 0;
src.VerticalFlip = 'off';
src.HorizontalFlip = 'off';

%We initialize the camera
start(vid);
pause(0.2)
%We close the camera
stoppreview(vid);
%The collected data, about 11 frames
img0= getdata(vid);
img0=mean(img0,4);
img0=mean(img0,3);
%After we got our final image, we remove the background noise
img1=img0-back_noise;
%I get a final frame matrix that is the one that I will use
for my experiment
%it is the result of the mean on 10 frames

%On this point we take average value of the final frame
[dx,dy]=size(img1);
Isum=0;
for i=1:1:dx
    for j=1:1:dy
       Isum=Isum+img1(i,j);
    end
end
Isum=Isum/(dx*dy);


end


function [ df1, dl] = dataprocess()
%Here is the core program to initialize callibration of a SLM
%   Detailed explanation goes here

%we clear memory and screen
close all
clear all
scale=256;%i define the available shade of gray
```

```
sti=num2str(1);
str1=['p' sti '.mat' ];%'.mat'];
str2=['img' sti ];


img0 = importdata( str1 );
%img0=load( matlab.lang.makeValidName(str1) ,
matlab.lang.makeValidName(str2)  );
%image(matlab.lang.makeValidName(str2) )
figure(12)
img0=imrotate(img0,-4.5);
image(img0)

%%%%%%%%%%%%%%%%%%%%%%%%%%%%%%%%%%%%%%%%%%%%%%%%%%%%%%%%%%%%%%%%%%%%%%%
[dy,dx]=size(img0);
sumx0=zeros(dx);
for x=1:1:dx
    for y=1:1:dy
    sumx0(x)=img0(y,x)+sumx0(x);
    end
end
sumx0=sumx0/dx;
line0=zeros(dx,1);
linx0=zeros(dx,1);

for i=1:1:dx
    line0(i)=sumx0(i);
    linx0(i)=i;
end


%%%%%%%%%%%%%%%%%%%%%%%%%%%%%%%%%%%%%%%%%%%%%%%%%%%%%%%%%%%%%%%%%%%%%%%
%%%%%%%%%%%%%

%%%%%%%%%%%%%%%%%%%%%%%%%%%%%%%%%%%%%%%%%%%%%%%%%%%%%%%%%%%%%%%%%%%%%%%
%%%%%%%%%%%%%

%here we begin to calculate the dl and DL for various
grayscales
%df=zeros(scale);
%dl=zeros(scale);

for i=2:1:scale
    [o]=fringesdistance(i);
    DL(i)=o;
    [m,w] = fringesmove(i,line0);
    dl(i)=m;
    B=[i-1,0];
    B=kron(B,ones(500));

    figure(2)
    subplot(2,2,1)
    colormap('gray')
    image(B);
    KM=num2str(i);
```

```
    string=['Mask graylevel is' KM];
    title(string)

    subplot(2,2,2)
    image(w);
    grid on;
    string=['Image from the Camera'];
    title(string)

    subplot(2,2,3)
    string=['Here we how much the fringes moved'];
    title(string)
    plot(dl)
    dl0=abs(dl(i)-dl(i-1));

    df(i)=(2*pi)*(DL(i)/dl0);
    subplot(2,2,4)
    plot(df)
    string=['graylevel to df'];
    title(string)

end
    df1=zeros(scale);
    %so we have an array for DL one for each gray scale
    for i=2:1:scale
    df1(i)=(2*pi)*(DL(i)/dl(i));
    end

    f2=figure(1);
    movegui(f2,'center')
    plot(df1)
    string=['Callibration Plot'];
    title(string)
    nm=['dl.txt'];
    dlmwrite(nm,dl,'delimiter','\t','precision',
'%6.6f','newline','pc' )


end

function [DL] = fringesdistance(i)
%On this small function we call the camera, then we found the
distance of
%two first fringes
%Simultaneously we save the graph of the fringes distribution,
so we could
%correlate them in the main Function and found how much have
the translated
sti=num2str(i);
str1=['p' sti '.mat'];
str2=['img' sti ];
w= importdata( str1 );
w=imrotate(w,-4.2);
[dy,dx]=size(w);

sumx=zeros(dx);
```

```
for x=1:1:dx
    for y=1:1:dy
    sumx(x)=w(y,x)+sumx(x);
    end
end
sumx=sumx/dx;
line=zeros(dx,1);
linx=zeros(dx,1);

for i=1:1:dx
    line(i)=sumx(i);
    linx(i)=i;
end

f3=figure(3);
movegui(f3,'northeast')
string=['The fringes plot'];
title(string)
plot(linx,line)

[peaks,locs]=findpeaks(line,'MINPEAKHEIGHT',3,'MINPEAKDISTANCE
',20,'SORTSTR','descend');
 %}

DL=abs(locs(1)-locs(2));



end

function [dl,w] = fringesmove(i,line0)
sti=num2str(i);
str1=['p' sti '.mat'];
w= importdata( str1 );
w=imrotate(w,-4.2);

%%%%%%%%%%%%%%%%%%%%%%%%%%%%%%%%%%%%%%%%%%%%
[dy,dx]=size(w);
sumx=zeros(dx);
for x=1:1:dx
    for y=1:1:dy
    sumx(x)=w(y,x)+sumx(x);
    end
end
sumx=sumx/dx;
line=zeros(dx,1);
linx=zeros(dx,1);

for i=1:1:dx
    line(i)=sumx(i);
    linx(i)=i;
end


[peaks,locs]=findpeaks(line,'MINPEAKHEIGHT',3,'MINPEAKDISTANCE
',20,'SORTSTR','descend');
```

```
[peaks0,locs0]=findpeaks(line0,'MINPEAKHEIGHT',3,'MINPEAKDISTA
NCE',20,'SORTSTR','descend');


dl=(abs(locs(1)-locs0(1))+abs(locs(2)-locs0(2))+abs(locs(3)-
locs0(3)))/3;



end
```

```
clear all
close all
% global var
% global frame


%%%%%%%%%%%%%%%%%%%%%%%%%%%%%%%%



vid = videoinput('winvideo', 1, 'RGB32_1280x1024');
src = getselectedsource(vid);
vid.FramesPerTrigger = 10;

src.BacklightCompensation = 'off';
src.ExposureMode = 'manual';
src.Exposure = -3;
src.GainMode = 'manual';
src.Gain = 0;
src.ContrastMode = 'manual';
src.Contrast = 0;
src.Gamma = 100;
src.Brightness = 0;
src.Contrast = 0;
src.Sharpness = 0;
src.VerticalFlip = 'off';
src.HorizontalFlip = 'off';
start(vid);
pause(0.2)
%We close the camera
stoppreview(vid);
stoppreview(vid);
frame= getdata(vid);
back_noise=mean(frame,4);
back_noise=mean(back_noise,3);
%I get a final frame matrix that is the one that I will use
for my experiment
%it is the result of the mean on 10 frames
figure(1)
imagesc(back_noise)
save('BackGround', 'back_noise');
```

```
function [ ] = fastfocus(  )
%Focusing Alrgorythm
%Detailed explanation goes here

%we clear memory and screen
close all
clear all


%First we define the target on the camere, wehre we would like
to have a
%focusing

%Adjustable Variables:

%Target to optimize
xt=400;
yt=400;
d=3;
dx=xt-d;
dy=yt-d;

pi2=78; %The value of gray level where the phase change for
the specific wavelength is 2pi
ch=round(pi/2);
numpixels=30; %In how many pixels of the SLM we want to have
the same Phase.
numberofrandomematrixes=50; %Number of random matrixes we try
step=round(pi2/2);%The control step each pixel will do

%Premeasure the number of step the code will have
step1=step; %dumb variable
k0=0; %dumb variable
while step1>1
  step1=round(step1/2);
  k0=k0+1;
end

rows=30; %number of rows on the SLM
collum=30; %number of collums on the SLM
%%%%%%%%%%%%%%%%%%%%%%%%%%%%%%%%%%%%%%%%%%%%%%%%%%%%%%%%%%%%%
%%%%%%%%%%%%%
%*************************************************************
*************%
%%%%%%%%%%%%%%%%%%%%%%%%%%%%%%%%%%%%%%%%%%%%%%%%%%%%%%%%%%%%%
%%%%%%%%%%%%%

%This code, works with Psycholtoolbox, so we initialize the
application

%We initialize a second window, covering the whole of the
second screen/SLM
window = Screen('OpenWindow',2);
%We define the absolut values
white = WhiteIndex(window);
```

```
black = BlackIndex(window);

%A blanck image of the background noise should be made and
removed from
%each frame, Please use the function graback
load ('Background');

% Here we define the camera iin use
vid = videoinput('winvideo', 1, 'RGB32_1280x1024');
src = getselectedsource(vid);
vid.FramesPerTrigger = 10;%The namumber of frames per each
call
pause(2)
src.BacklightCompensation = 'off';
src.ExposureMode = 'manual';
src.Exposure = -4;
src.GainMode = 'manual';
src.Gain = 0;
src.ContrastMode = 'manual';
src.Contrast = 0;
src.Gamma = 100;
src.Brightness = 0;
src.Contrast = 0;
src.Sharpness = 0;

%%%%%%%%%%%%%%%%%%%%%%%%%%%%%%%%%%%%%%%%%%%%%%%%%%%%%%%%%%%%%%%%%%%%%%%
%%%%%%%%%%%%
%            Initial conditions, we take a white mask image
%
%%%%%%%%%%%%%%%%%%%%%%%%%%%%%%%%%%%%%%%%%%%%%%%%%%%%%%%%%%%%%%%%%%%%%%%
%%%%%%%%%%%%

d=40; %number of pixels, but d*d
w=255*ones(d,d);%They take the same value
w=kron(w,ones(30));%I fill the SLM
Screen(window, 'PutImage',w);%I sent the white mask on the SLM
Screen(window,'Flip');
[Isum,img1]=callcam(vid,back_noise);
focus=calc(img1,dx,dy,d);%here we get back the intensity at
the targe for dxd pixels around the focus
avgfocus(1)=focus/Isum; %the focus averaged by the total
average intensity of the frame
save('white mask image ','img1')
I0=focus; %initial value
%A window will initialize at this point and show what the
camera
%sees.
ratio(1)=focus/I0;
ploty(w,img1,avgfocus,focus,ratio,1)

save ('white mask speckle','img1');

%%%%%%%%%%%%%%%%%%%%%%%%%%%%%%%%%%%%%%%%%%%%%%%%%%%%%%%%%%%%%%%%%%%%%%%
%%%%%%%%%%%%
%************************************************************
************%
```

```
%%%%%%%%%%%%%%%%%%%%%%%%%%%%%%%%%%%%%%%%%%%%%%%%%%%%%%%%%%%%%%%
%%%%%%%%%%%%%



%%%%%%%%%%%%%%%%%%%%%%%%%%%%%%%%%%%%%%%%%%%%%%%%%%%%%%%%%%%%%%%
%%%%%%%%%%%%%
%              Here we start the Random Masks on the SLM
%
%%%%%%%%%%%%%%%%%%%%%%%%%%%%%%%%%%%%%%%%%%%%%%%%%%%%%%%%%%%%%%%
%%%%%%%%%%%%%

%Here, we check random mask, to choose the optmimum random
mask to begine
%otpmiazation for focusing. The optimum mask should give the
best intensity
%on the point of choice.



A=zeros(numberofrandomematrixes,rows , collum); %i prelocate a
mtrix with all the random masks
A1=zeros(rows,collum);% I create a dumb matrix

%Here we start with Random matrixes, so we could choose an
optimum one

for i=2:1:numberofrandomematrixes+1%plus one, cause i consider
as 1 the white mask
   for j=1:1:rows
       for k=1:1:collum
           A(i,j,k)=round(rand*pi2);% irandomize the mask
       end
   end

   for r=1:1:rows
       for q=1:1:collum
        A1(r,q)=A(i,r,q);%i save the current ransom matrix
       end
   end

   randmask=kron(A1,ones(numpixels)); % we create megapixels
   %Here we sent an image to the SLM
   Screen(window, 'PutImage',randmask);
   Screen(window,'Flip');
   [Isum,img1]=callcam(vid,back_noise);%camera is senting back
image and average intensity
   focus=calc(img1,dx,dy,d); %it evaluates the focus intensity
   avgfocus(i)=focus/Isum; %it normalizes it to the average
intensity
   ratio(i)=focus/I0; %The enhancement

   ploty(randmask,img1,avgfocus,focus,ratio,i) %plots the
results

end
```

```
[o, indexofmask]=max(avgfocus); %Here it finds which mask had
the best intensity



  for r=1:1:rows
       for q=1:1:collum
        B(r,q)=A(indexofmask,r,q); %we picked the best mask
into var B
       end
  end


save('best initial mask','B')
str1=['optimum mask  '];
save(str1,'B')% it save it on the folder.
   randmask=kron(B,ones(numpixels)); % we create megapixels
   %Here we sent an image to the SLM
   Screen(window, 'PutImage',randmask);
   Screen(window,'Flip')
   [Isum,img1]=callcam(vid,back_noise);
str1=['optimum mask photo '];
save(str1,'img1');% Save the image of the camera


%%%%%%%%%%%%%%%%%%%%%%%%%%%%%%%%%%%%%%%%%%%%%%%%%%%%%%%%%%%%%%%%%%%%%%%
%%%%%%%%%%%%
%************************************************************
***********%
%%%%%%%%%%%%%%%%%%%%%%%%%%%%%%%%%%%%%%%%%%%%%%%%%%%%%%%%%%%%%%%%%%%%%%%
%%%%%%%%%%%%


%%%%%%%%%%%%%%%%%%%%%%%%%%%%%%%%%%%%%%%%%%%%%%%%%%%%%%%%%%%%%%%%%%%%%%%
%%%%%%%%%%%%
%              The start of the optimization procedure
%
%%%%%%%%%%%%%%%%%%%%%%%%%%%%%%%%%%%%%%%%%%%%%%%%%%%%%%%%%%%%%%%%%%%%%%%
%%%%%%%%%%%%


%On this part, we start optimization. Since we have figured
out an
%optimzied mask, we change each pixel to deduce the exact
phase it needs
%for perfact focusing

%We load on the SLM the best mask
C=kron(B,ones(numpixels)); % The enlarged mask
Screen(window, 'PutImage',C);
Screen(window,'Flip');
[Isum,img1]=callcam(vid,back_noise);
focus=calc(img1,dx,dy,d);
i=i+1;
avgfocus(i)=focus/Isum;
```

```
ratio(i)=focus/I0;

ploty(randmask,img1,avgfocus,focus,ratio,i)


%%%%%%%%%%%%%%%%%%%%%%%%%%%%%%%%%%%%%%%%%%%%%%%%%%%%%%%%%%%%%
%%%%%%%%%%%%%


 % I plan to run this program until it gets the value 1! for
exact phase.

    %Now we start checking each pixel, by changing the phase
if enhances
    %the focus or not.

    for x=1:1:rows
        for y=1:1:collum
            index=0;
            ret=B(x,y);
            if B(x,y)<=ch
                B(x,y)=B(x,y)+step;
                index=1;
            else
                B(x,y)=B(x,y)-step;
                index=2;
            end

            ok=0;% A check variable.

            %Here we check the change
            C=kron(B,ones(numpixels)); % The enlarged mask
            Screen(window, 'PutImage',C);
            Screen(window,'Flip');
            i=i+1;
            [Isum,img1]=callcam(vid,back_noise);
            focus=calc(img1,dx,dy,d);
            avgfocus(i)=focus/Isum;
            ratio(i)=focus/I0;

            ploty(B,img1,avgfocus,focus,ratio,i)

            if avgfocus(i)>avgfocus(i-1)&&
avgfocus(i)>avgfocus(i-2)
            ok=1;

            elseif index==1&&ok==0;
                B(x,y)=round(B(x,y)-B(x,y)/2);

                C=kron(B,ones(numpixels)); % The enlarged mask
                Screen(window, 'PutImage',C);
                Screen(window,'Flip');
                i=i+1;
                [Isum,img1]=callcam(vid,back_noise);
                focus=calc(img1,dx,dy,d);
                avgfocus(i)=focus/Isum;
```

```
                ratio(i)=focus/I0;

                ploty(B,img1,avgfocus,focus,ratio,i)
                if avgfocus(i)>avgfocus(i-1)&&
avgfocus(i)>avgfocus(i-2)
                ok=1;
                else
                B(x,y)=ret;
                end
            elseif index==2&&ok==0;
                 B(x,y)=round(B(x,y)+(ch-B(x,y)/2));

                C=kron(B,ones(numpixels)); % The enlarged mask
                Screen(window, 'PutImage',C);
                Screen(window,'Flip');
                i=i+1;
                [Isum,img1]=callcam(vid,back_noise);
                focus=calc(img1,dx,dy,d);
                avgfocus(i)=focus/Isum;
                ratio(i)=focus/I0;

                ploty(B,img1,avgfocus,focus,ratio,i)
                if avgfocus(i)>avgfocus(i-1)&&
avgfocus(i)>avgfocus(i-2)
                ok=1;
                else
                B(x,y)=ret;

                Screen(window, 'PutImage',C);
                Screen(window,'Flip');
                i=i+1;
                [Isum,img1]=callcam(vid,back_noise);
                focus=calc(img1,dx,dy,d);
                avgfocus(i)=focus/Isum;
                ratio(i)=focus/I0;
                ploty(B,img1,avgfocus,focus,ratio,i)
                end

            end
        end
    end

      ststep=num2str(step);
      str1=['optimum mask step ' ststep  ];
      save(str1,'B')
      str2=['final image for step ' ststep ];
      save(str2,'img1')
      ratio(i)=focus/I0;

      figure(2);
      subplot(2,2,1)
        image(B);
        subplot(2,2,2)
        image(img1);
        grid on;
        subplot(2,2,3)
```

```
        plot(avgfocus,'LineWidth',2)
        subplot(2,2,4)
        plot(ratio,'LineWidth',2)
        KM=num2str(ratio(i));
        string=['Spot to average inensity ratio ' KM];
        title(string)

      figure(33)
      image(img1)
      figure(34)
      imagesc(img1)
       done


end

function [focus]=calc(img1,dx,dy,d)
focus=0; %it creates var
k=0; %count the pixels in camera
    for l=dx:1:dx+d
        for m=dy:1:dy+d
            focus=focus+img1(l,m); %adds the pixels
            k=k+1; %numbers the pixels
        end
    end
    focus=focus/k; %it averages the intensity
end

function []=ploty(w,img1,enhance,focus,ratio,i)
figure(1);
subplot(2,2,1)
imshow(w,[]);
subplot(2,2,2)
image(img1);
grid on;
subplot(2,2,3)
plot(enhance,'LineWidth',2)
subplot(2,2,4)
plot(ratio,'LineWidth',2)
KM=num2str(ratio(i));
string=['Spot to average inensity ratio ' KM];
title(string)

end
```

```
function [ ] = fastfocus2(  )
%Focusing Alrgorythm
%Detailed explanation goes here

%we clear memory and screen
close all
clear all


%First we define the target on the camere, wehre we would like
to have a
%focusing

%Adjustable Variables:

%Target to optimize
xt=400;
yt=800;
xt2=800;
yt2=400;
d=3;
dx=xt-d;
dy=yt-d;
dx2=xt2-d;
dy2=yt2-d;


pi2=78; %The value of gray level where the phase change for
the specific wavelength is 2pi
ch=round(pi/2);
numpixels=30; %In how many pixels of the SLM we want to have
the same Phase.
numberofrandomematrixes=50; %Number of random matrixes we try
step=round(pi2/2);%The control step each pixel will do

%Premeasure the number of step the code will have
step1=step; %dumb variable
k0=0; %dumb variable
while step1>1
  step1=round(step1/2);
  k0=k0+1;
end

rows=30; %number of rows on the SLM
collum=30; %number of collums on the SLM
%%%%%%%%%%%%%%%%%%%%%%%%%%%%%%%%%%%%%%%%%%%%%%%%%%%%%%%%%%%%%%%
%%%%%%%%%%%%%
%*************************************************************
************%
%%%%%%%%%%%%%%%%%%%%%%%%%%%%%%%%%%%%%%%%%%%%%%%%%%%%%%%%%%%%%%%
%%%%%%%%%%%%%

%This code, works with Psycholtoolbox, so we initialize the
application
```

```
%We initialize a second window, covering the whole of the
second screen/SLM
window = Screen('OpenWindow',2);
%We define the absolut values
white = WhiteIndex(window);
black = BlackIndex(window);

%A blanck image of the background noise should be made and
removed from
%each frame, Please use the function graback
load ('Background');

% Here we define the camera iin use
vid = videoinput('winvideo', 1, 'RGB32_1280x1024');
src = getselectedsource(vid);
vid.FramesPerTrigger = 10;%The namumber of frames per each
call
pause(2)
src.BacklightCompensation = 'off';
src.ExposureMode = 'manual';
src.Exposure = -4;
src.GainMode = 'manual';
src.Gain = 0;
src.ContrastMode = 'manual';
src.Contrast = 0;
src.Gamma = 100;
src.Brightness = 0;
src.Contrast = 0;
src.Sharpness = 0;

%%%%%%%%%%%%%%%%%%%%%%%%%%%%%%%%%%%%%%%%%%%%%%%%%%%%%%%%%%%%%%%%%%%%%%%%
%%%%%%%%%%%%
%           Initial conditions, we take a white mask image
%
%%%%%%%%%%%%%%%%%%%%%%%%%%%%%%%%%%%%%%%%%%%%%%%%%%%%%%%%%%%%%%%%%%%%%%%%
%%%%%%%%%%%%

d=40; %number of pixels, but d*d
w=255*ones(d,d);%They take the same value
w=kron(w,ones(30));%I fill the SLM
Screen(window, 'PutImage',w);%I sent the white mask on the SLM
Screen(window,'Flip');
[Isum,img1]=callcam(vid,back_noise);
[focus,focus2]=calc(img1,dx,dy,dx2,dy2,d);%here we get back
the intensity at the targe for dxd pixels around the focus
avgfocus(1)=focus/Isum; %the focus averaged by the total
average intensity of the frame
avgfocus2(1)=focus2/Isum; %the focus averaged by the total
average intensity of the frame
save('white mask image ','img1')
I0=focus;
I02=focus2;%initial value
%A window will initialize at this point and show what the
camera
%sees.
ratio(1)=focus/I0;
```

```
ratio2(1)=focus2/I02;
ploty(w,img1,avgfocus,focus,ratio,1)
ploty2(w,img1,avgfocus2,focus2,ratio2,1)

save ('white mask speckle','img1');

%%%%%%%%%%%%%%%%%%%%%%%%%%%%%%%%%%%%%%%%%%%%%%%%%%%%%%%%%%%%%%%%%%%%%%%%%%%%%
%%%%%%%%%%%%%
%***********************************************************************
************%
%%%%%%%%%%%%%%%%%%%%%%%%%%%%%%%%%%%%%%%%%%%%%%%%%%%%%%%%%%%%%%%%%%%%%%%%%%%%%
%%%%%%%%%%%%%



%%%%%%%%%%%%%%%%%%%%%%%%%%%%%%%%%%%%%%%%%%%%%%%%%%%%%%%%%%%%%%%%%%%%%%%%%%%%%
%%%%%%%%%%%%%
%             Here we start the Random Masks on the SLM
%
%%%%%%%%%%%%%%%%%%%%%%%%%%%%%%%%%%%%%%%%%%%%%%%%%%%%%%%%%%%%%%%%%%%%%%%%%%%%%
%%%%%%%%%%%%%

%Here, we check random mask, to choose the optmimum random
mask to begine
%otpmiazation for focusing. The optimum mask should give the
best intensity
%on the point of choice.



A=zeros(numberofrandomematrixes,rows , collum); %i prelocate a
mtrix with all the random masks
A1=zeros(rows,collum);% I create a dumb matrix

%Here we start with Random matrixes, so we could choose an
optimum one

for i=2:1:numberofrandomematrixes+1%plus one, cause i consider
as 1 the white mask
   for j=1:1:rows
       for k=1:1:collum
           A(i,j,k)=round(rand*pi2);% irandomize the mask
       end
   end

   for r=1:1:rows
       for q=1:1:collum
        A1(r,q)=A(i,r,q);%i save the current ransom matrix
       end
   end

   randmask=kron(A1,ones(numpixels)); % we create megapixels
   %Here we sent an image to the SLM
   Screen(window, 'PutImage',randmask);
   Screen(window,'Flip');
```

```
   [Isum,img1]=callcam(vid,back_noise);%camera is senting back
image and average intensity
[focus,focus2]=calc(img1,dx,dy,dx2,dy2,d);%here we get back
the intensity at the targe for dxd pixels around the focus
   avgfocus(i)=focus/Isum; %it normalizes it to the average
intensity
   avgfocus2(i)=focus2/Isum; %it normalizes it to the average
intensity
   ratio(i)=focus/I0; %The enhancement
   ratio2(i)=focus2/I02; %The enhancement

   ploty(randmask,img1,avgfocus,focus,ratio,i) %plots the
results
   ploty2(randmask,img1,avgfocus2,focus2,ratio2,i) %plots the
results

end
avgfocus3=avgfocus+avgfocus2;
[o, indexofmask]=max(avgfocus3); %Here it finds which mask had
the best intensity



  for r=1:1:rows
       for q=1:1:collum
        B(r,q)=A(indexofmask,r,q); %we picked the best mask
into var B
       end
  end


save('best initial mask','B')
str1=['optimum mask  '];
save(str1,'B')% it save it on the folder.
   randmask=kron(B,ones(numpixels)); % we create megapixels
   %Here we sent an image to the SLM
   Screen(window, 'PutImage',randmask);
   Screen(window,'Flip')
   [Isum,img1]=callcam(vid,back_noise);
str1=['optimum mask photo '];
save(str1,'img1');% Save the image of the camera


%%%%%%%%%%%%%%%%%%%%%%%%%%%%%%%%%%%%%%%%%%%%%%%%%%%%%%%%%%%%%%%
%%%%%%%%%%%%%
%*************************************************************
************%
%%%%%%%%%%%%%%%%%%%%%%%%%%%%%%%%%%%%%%%%%%%%%%%%%%%%%%%%%%%%%%%
%%%%%%%%%%%%%


%%%%%%%%%%%%%%%%%%%%%%%%%%%%%%%%%%%%%%%%%%%%%%%%%%%%%%%%%%%%%%%
%%%%%%%%%%%%%
%              The start of the optimization procedure
%
```

```
%%%%%%%%%%%%%%%%%%%%%%%%%%%%%%%%%%%%%%%%%%%%%%%%%%%%%%%%%%%%%%%%%%%%%%%%%%%%
%%%%%%%%%%%%


%On this part, we start optimization. Since we have figured
out an
%optimzied mask, we change each pixel to deduce the exact
phase it needs
%for perfact focusing

%We load on the SLM the best mask
C=kron(B,ones(numpixels)); % The enlarged mask
Screen(window, 'PutImage',C);
Screen(window,'Flip');
[Isum,img1]=callcam(vid,back_noise);
[focus,focus2]=calc(img1,dx,dy,dx2,dy2,d);%here we get back
the intensity at the targe for dxd pixels around the focus
i=i+1;
avgfocus(i)=focus/Isum;
ratio(i)=focus/I0;
avgfocus2(i)=focus2/Isum;
ratio2(i)=focus2/I02;

ploty(randmask,img1,avgfocus,focus,ratio,i)
ploty2(randmask,img1,avgfocus2,focus2,ratio2,i)

%%%%%%%%%%%%%%%%%%%%%%%%%%%%%%%%%%%%%%%%%%%%%%%%%%%%%%%%%%%%%%%%%%%%%%%%%%%%
%%%%%%%%%%%%


 % I plan to run this program until it gets the value 1! for
exact phase.

    %Now we start checking each pixel, by changing the phase
if enhances
    %the focus or not.

    for x=1:1:rows
        for y=1:1:collum
            index=0;
            ret=B(x,y);
            if B(x,y)<=ch
                B(x,y)=B(x,y)+step;
                index=1;
            else
                B(x,y)=B(x,y)-step;
                index=2;
            end

            ok=0;% A check variable.

            %Here we check the change
            C=kron(B,ones(numpixels)); % The enlarged mask
            Screen(window, 'PutImage',C);
            Screen(window,'Flip');
            i=i+1;
```

```
            [Isum,img1]=callcam(vid,back_noise);
[focus,focus2]=calc(img1,dx,dy,dx2,dy2,d);%here we get back
the intensity at the targe for dxd pixels around the focus
            avgfocus(i)=focus/Isum;
            ratio(i)=focus/I0;
            avgfocus2(i)=focus2/Isum;
            ratio2(i)=focus2/I02;
            ploty(B,img1,avgfocus,focus,ratio,i)
            ploty2(B,img1,avgfocus2,focus2,ratio2,i)



            if avgfocus(i)>avgfocus(i-1)&&
avgfocus(i)>avgfocus(i-2)&&avgfocus2(i)>avgfocus2(i-1)&&
avgfocus2(i)>avgfocus2(i-2)
            ok=1;

            elseif index==1&&ok==0;
                B(x,y)=round(B(x,y)-B(x,y)/2);

                C=kron(B,ones(numpixels)); % The enlarged mask
                Screen(window, 'PutImage',C);
                Screen(window,'Flip');
                i=i+1;
                [Isum,img1]=callcam(vid,back_noise);
[focus,focus2]=calc(img1,dx,dy,dx2,dy2,d);%here we get back
the intensity at the targe for dxd pixels around the focus
                avgfocus(i)=focus/Isum;
                ratio(i)=focus/I0;

                avgfocus2(i)=focus2/Isum;
                ratio2(i)=focus2/I0;

                ploty(B,img1,avgfocus,focus,ratio,i)
                ploty2(B,img1,avgfocus2,focus2,ratio2,i)
                if avgfocus(i)>avgfocus(i-1)&&
avgfocus(i)>avgfocus(i-2)&&avgfocus2(i)>avgfocus2(i-1)&&
avgfocus2(i)>avgfocus2(i-2)
                ok=1;
                else
                B(x,y)=ret;
                end
            elseif index==2&&ok==0;
                 B(x,y)=round(B(x,y)+(ch-B(x,y)/2));

                C=kron(B,ones(numpixels)); % The enlarged mask
                Screen(window, 'PutImage',C);
                Screen(window,'Flip');
                i=i+1;
                [Isum,img1]=callcam(vid,back_noise);
[focus,focus2]=calc(img1,dx,dy,dx2,dy2,d);%here we get back
the intensity at the targe for dxd pixels around the focus
                avgfocus(i)=focus/Isum;
                ratio(i)=focus/I0;
                avgfocus2(i)=focus2/Isum;
```

```
                ratio2(i)=focus2/I0;

                ploty(B,img1,avgfocus,focus,ratio,i)
                ploty2(B,img1,avgfocus2,focus2,ratio2,i)

                if avgfocus(i)>avgfocus(i-1)&&
avgfocus(i)>avgfocus(i-2)&&avgfocus2(i)>avgfocus2(i-1)&&
avgfocus2(i)>avgfocus2(i-2)
                ok=1;
                else
                B(x,y)=ret;

                Screen(window, 'PutImage',C);
                Screen(window,'Flip');
                i=i+1;
                [Isum,img1]=callcam(vid,back_noise);
[focus,focus2]=calc(img1,dx,dy,dx2,dy2,d);%here we get back
the intensity at the targe for dxd pixels around the focus
                avgfocus(i)=focus/Isum;
                ratio(i)=focus/I0;
                avgfocus2(i)=focus2/Isum;
                ratio2(i)=focus2/I0;
                ploty2(B,img1,avgfocus2,focus2,ratio2,i)
                end

            end
        end
    end

      ststep=num2str(step);
      str1=['optimum mask step ' ststep  ];
      save(str1,'B')
      str2=['final image for step ' ststep ];
      save(str2,'img1')
      ratio(i)=focus/I0;

      figure(2);
      subplot(2,2,1)
        image(B);
        subplot(2,2,2)
        image(img1);
        grid on;
        subplot(2,2,3)
        string=['Average intensity ' ];
        title(string)
        plot(avgfocus,'LineWidth',2)
        subplot(2,2,4)
        plot(ratio,'LineWidth',2)
        KM=num2str(ratio(i));
        string=['Spot to average inensity ratio ' KM];
        title(string)

        figure(22);
      subplot(2,2,1)
        image(B);
        subplot(2,2,2)
```

```
        image(img1);
        grid on;
        subplot(2,2,3)
        string=['Average intensity ' ];
        title(string)
        plot(avgfocus2,'LineWidth',2)
        subplot(2,2,4)
        plot(ratio,'LineWidth',2)
        KM=num2str(ratio2(i));
        string=['Spot to average inensity ratio ' KM];
        title(string)

      figure(33)
      image(img1)
      figure(34)
      imagesc(img1)
       done


end

function [focus,focus2]=calc(img1,dx,dy,dx2,dy2,d)
focus=0; %it creates var
k=0; %count the pixels in camera
    for l=dx:1:dx+d
        for m=dy:1:dy+d
            focus=focus+img1(l,m); %adds the pixels
            k=k+1; %numbers the pixels
        end
    end
    focus=focus/k; %it averages the intensity
    focus2=0; %it creates var
k=0; %count the pixels in camera
    for l=dx2:1:dx2+d
        for m=dy2:1:dy2+d
            focus2=focus2+img1(l,m); %adds the pixels
            k=k+1; %numbers the pixels
        end
    end
    focus2=focus2/k; %it averages the intensity
end

function []=ploty(w,img1,enhance,focus,ratio,i)
figure(1);
subplot(2,2,1)
imshow(w,[]);
subplot(2,2,2)
image(img1);
grid on;
subplot(2,2,3)
string=['normalized intensity on the focus ' ];
title(string)
plot(enhance,'LineWidth',2)
subplot(2,2,4)
plot(ratio,'LineWidth',2)
KM=num2str(ratio(i));
```

```
string=['Spot to average inensity ratio ' KM];
title(string)

end

function []=ploty2(w,img1,enhance,focus,ratio,i)
figure(11);
subplot(2,2,1)
imshow(w,[]);
subplot(2,2,2)
image(img1);
grid on;
subplot(2,2,3)
string=['normalized intensity on the focus ' ];
title(string)
plot(enhance,'LineWidth',2)
subplot(2,2,4)
plot(ratio,'LineWidth',2)
KM=num2str(ratio(i));
string=['Spot to average inensity ratio 2 ' KM];
title(string)

end
```

```
function [ ] = focus(  )
%Focusing Alrgorythm
%Detailed explanation goes here

%we clear memory and screen
close all
clear all


%First we define the target on the camere, wehre we would like
to have a
%focusing

%Adjustable Variables:

%Target to optimize
xt=800;
yt=800;
d=3;
dx=xt-d;
dy=yt-d;

pi2=78; %The value of gray level where the phase change for
the specific wavelength is 2pi
ch=round(pi/2);
numpixels=30; %In how many pixels of the SLM we want to have
the same Phase.
numberofrandomematrixes=10; %Number of random matrixes we try
step=round(pi2/2);%The control step each pixel will do

%Premeasure the number of step the code will have
step1=step; %dumb variable
k0=0; %dumb variable
while step1>1
  step1=round(step1/2);
  k0=k0+1;
end

rows=30; %number of rows on the SLM
collum=30; %number of collums on the SLM
%%%%%%%%%%%%%%%%%%%%%%%%%%%%%%%%%%%%%%%%%%%%%%%%%%%%%%%%%%%%%%
%%%%%%%%%%%%%
%*************************************************************
************%
%%%%%%%%%%%%%%%%%%%%%%%%%%%%%%%%%%%%%%%%%%%%%%%%%%%%%%%%%%%%%%
%%%%%%%%%%%%%

%This code, works with Psycholtoolbox, so we initialize the
application

%We initialize a second window, covering the whole of the
second screen/SLM
window = Screen('OpenWindow',2);
%We define the absolut values
white = WhiteIndex(window);
```

```
black = BlackIndex(window);

%A blanck image of the background noise should be made and
removed from
%each frame, Please use the function graback
load ('Background');

% Here we define the camera iin use
vid = videoinput('winvideo', 1, 'RGB32_1280x1024');
src = getselectedsource(vid);
vid.FramesPerTrigger = 10;%The namumber of frames per each
call
pause(2)

%%%%%%%%%%%%%%%%%%%%%%%%%%%%%%%%%%%%%%%%%%%%%%%%%%%%%%%%%%%%%%%%%%%%%%%
%%%%%%%%%%%%
%            Initial conditions, we take a white mask image
%
%%%%%%%%%%%%%%%%%%%%%%%%%%%%%%%%%%%%%%%%%%%%%%%%%%%%%%%%%%%%%%%%%%%%%%%
%%%%%%%%%%%%

d=40; %number of pixels, but d*d
w=255*ones(d,d);%They take the same value
w=kron(w,ones(30));%I fill the SLM
Screen(window, 'PutImage',w);%I sent the white mask on the SLM
Screen(window,'Flip');
[Isum,img1]=callcam(vid,back_noise);
focus=calc(img1,dx,dy,d);%here we get back the intensity at
the targe for dxd pixels around the focus
avgfocus(1)=focus/Isum; %the focus averaged by the total
average intensity of the frame
save('white mask image ','img1')
I0=focus; %initial value
%A window will initialize at this point and show what the
camera
%sees.
ratio(1)=focus/I0;
ploty(w,img1,avgfocus,focus,ratio,1)

save ('white mask speckle','img1');

%%%%%%%%%%%%%%%%%%%%%%%%%%%%%%%%%%%%%%%%%%%%%%%%%%%%%%%%%%%%%%%%%%%%%%%
%%%%%%%%%%%%
%************************************************************
************%
%%%%%%%%%%%%%%%%%%%%%%%%%%%%%%%%%%%%%%%%%%%%%%%%%%%%%%%%%%%%%%%%%%%%%%%
%%%%%%%%%%%%



%%%%%%%%%%%%%%%%%%%%%%%%%%%%%%%%%%%%%%%%%%%%%%%%%%%%%%%%%%%%%%%%%%%%%%%
%%%%%%%%%%%%
%              Here we start the Random Masks on the SLM
%
%%%%%%%%%%%%%%%%%%%%%%%%%%%%%%%%%%%%%%%%%%%%%%%%%%%%%%%%%%%%%%%%%%%%%%%
%%%%%%%%%%%%
```

```
%Here, we check random mask, to choose the optmimum random
mask to begine
%otpmiazation for focusing. The optimum mask should give the
best intensity
%on the point of choice.



A=zeros(numberofrandomematrixes,rows , collum); %i prelocate a
mtrix with all the random masks
A1=zeros(rows,collum);% I create a dumb matrix

%Here we start with Random matrixes, so we could choose an
optimum one

for i=2:1:numberofrandomematrixes+1%plus one, cause i consider
as 1 the white mask
   for j=1:1:rows
       for k=1:1:collum
           A(i,j,k)=round(rand*pi2);% irandomize the mask
       end
   end

   for r=1:1:rows
       for q=1:1:collum
        A1(r,q)=A(i,r,q);%i save the current ransom matrix
       end
   end

   randmask=kron(A1,ones(numpixels)); % we create megapixels
   %Here we sent an image to the SLM
   Screen(window, 'PutImage',randmask);
   Screen(window,'Flip');
   [Isum,img1]=callcam(vid,back_noise);%camera is senting back
image and average intensity
   focus=calc(img1,dx,dy,d); %it evaluates the focus intensity
   avgfocus(i)=focus/Isum; %it normalizes it to the average
intensity
   ratio(i)=focus/I0; %The enhancement

   ploty(randmask,img1,avgfocus,focus,ratio,i) %plots the
results

end

[o, indexofmask]=max(avgfocus); %Here it finds which mask had
the best intensity



  for r=1:1:rows
       for q=1:1:collum
        B(r,q)=A(indexofmask,r,q); %we picked the best mask
into var B
       end
```

```
  end


save('best initial mask','B')
str1=['optimum mask  '];
save(str1,'B')% it save it on the folder.
   randmask=kron(B,ones(numpixels)); % we create megapixels
   %Here we sent an image to the SLM
   Screen(window, 'PutImage',randmask);
   Screen(window,'Flip')
   [Isum,img1]=callcam(vid,back_noise);
str1=['optimum mask photo '];
save(str1,'img1');% Save the image of the camera


%%%%%%%%%%%%%%%%%%%%%%%%%%%%%%%%%%%%%%%%%%%%%%%%%%%%%%%%%%%%%%%%%%%%%%%%
%%%%%%%%%%%%%
%*************************************************************
***********%
%%%%%%%%%%%%%%%%%%%%%%%%%%%%%%%%%%%%%%%%%%%%%%%%%%%%%%%%%%%%%%%%%%%%%%%%
%%%%%%%%%%%%%


%%%%%%%%%%%%%%%%%%%%%%%%%%%%%%%%%%%%%%%%%%%%%%%%%%%%%%%%%%%%%%%%%%%%%%%%
%%%%%%%%%%%%%
%              The start of the optimization procedure
%
%%%%%%%%%%%%%%%%%%%%%%%%%%%%%%%%%%%%%%%%%%%%%%%%%%%%%%%%%%%%%%%%%%%%%%%%
%%%%%%%%%%%%%


%On this part, we start optimization. Since we have figured
out an
%optimzied mask, we change each pixel to deduce the exact
phase it needs
%for perfact focusing

%We load on the SLM the best mask
C=kron(B,ones(numpixels)); % The enlarged mask
Screen(window, 'PutImage',C);
Screen(window,'Flip');
[Isum,img1]=callcam(vid,back_noise);
focus=calc(img1,dx,dy,d);
i=i+1;
avgfocus(i)=focus/Isum;
ratio(i)=focus/I0;

ploty(randmask,img1,avgfocus,focus,ratio,i)


%%%%%%%%%%%%%%%%%%%%%%%%%%%%%%%%%%%%%%%%%%%%%%%%%%%%%%%%%%%%%%%%%%%%%%%%
%%%%%%%%%%%%%


while step>1 % I plan to run this program until it gets the
value 1! for exact phase.
```

```
    %Now we start checking each pixel, by changing the phase
if enhances
    %the focus or not.

    for x=1:1:rows
        for y=1:1:collum
            index=0;
            ret=B(x,y);
            if B(x,y)<=ch
                B(x,y)=B(x,y)+step;
                index=1;
            else
                B(x,y)=B(x,y)-step;
                index=2;
            end

            ok=0;% A check variable.

            %Here we check the change
            C=kron(B,ones(numpixels)); % The enlarged mask
            Screen(window, 'PutImage',C);
            Screen(window,'Flip');
            i=i+1;
            [Isum,img1]=callcam(vid,back_noise);
            focus=calc(img1,dx,dy,d);
            avgfocus(i)=focus/Isum;
            ratio(i)=focus/I0;

            ploty(B,img1,avgfocus,focus,ratio,i)

            if avgfocus(i)>avgfocus(i-1)&&
avgfocus(i)>avgfocus(i-2)
            ok=1;

            elseif index==1&&ok==0;
                B(x,y)=round(B(x,y)-B(x,y)/2);

                C=kron(B,ones(numpixels)); % The enlarged mask
                Screen(window, 'PutImage',C);
                Screen(window,'Flip');
                i=i+1;
                [Isum,img1]=callcam(vid,back_noise);
                focus=calc(img1,dx,dy,d);
                avgfocus(i)=focus/Isum;
                ratio(i)=focus/I0;

                ploty(B,img1,avgfocus,focus,ratio,i)
                if avgfocus(i)>avgfocus(i-1)&&
avgfocus(i)>avgfocus(i-2)
                ok=1;
                else
                B(x,y)=ret;
                end
            elseif index==2&&ok==0;
                 B(x,y)=round(B(x,y)+(ch-B(x,y)/2));
```

```
                C=kron(B,ones(numpixels)); % The enlarged mask
                Screen(window, 'PutImage',C);
                Screen(window,'Flip');
                i=i+1;
                [Isum,img1]=callcam(vid,back_noise);
                focus=calc(img1,dx,dy,d);
                avgfocus(i)=focus/Isum;
                ratio(i)=focus/I0;

                ploty(B,img1,avgfocus,focus,ratio,i)
                if avgfocus(i)>avgfocus(i-1)&&
avgfocus(i)>avgfocus(i-2)
                ok=1;
                else
                B(x,y)=ret;

                Screen(window, 'PutImage',C);
                Screen(window,'Flip');
                i=i+1;
                [Isum,img1]=callcam(vid,back_noise);
                focus=calc(img1,dx,dy,d);
                avgfocus(i)=focus/Isum;
                ratio(i)=focus/I0;
                ploty(B,img1,avgfocus,focus,ratio,i)
                end

            end
        end
    end

      ststep=num2str(step);
      str1=['optimum mask step ' ststep  ];
      save(str1,'B')
      str2=['final image for step ' ststep ];
      save(str2,'img1')
      ratio(i)=focus/I0;

      figure(2);
      subplot(2,2,1)
        image(B);
        subplot(2,2,2)
        image(img1);
        grid on;
        subplot(2,2,3)
        plot(avgfocus,'LineWidth',2)
        subplot(2,2,4)
        plot(ratio,'LineWidth',2)
        KM=num2str(ratio(i));
        string=['Spot to average inensity ratio ' KM];
        title(string)
 figure(3)
 imagesc(img1)
 figure(4)
 imagesc(img1)
      step=round(step/2);
```

```
end

end

function [focus]=calc(img1,dx,dy,d)
focus=0; %it creates var
k=0; %count the pixels in camera
    for l=dx:1:dx+d
        for m=dy:1:dy+d
            focus=focus+img1(l,m); %adds the pixels
            k=k+1; %numbers the pixels
        end
    end
    focus=focus/k; %it averages the intensity
end

function []=ploty(w,img1,enhance,focus,ratio,i)
figure(1);
subplot(2,2,1)
imshow(w,[]);
subplot(2,2,2)
image(img1);
grid on;
subplot(2,2,3)
plot(enhance,'LineWidth',2)
subplot(2,2,4)
plot(ratio,'LineWidth',2)
KM=num2str(ratio(i));
string=['Spot to average inensity ratio ' KM];
title(string)

end
```

```
% script : Done, it mails me back that it's done
% Modify these two lines to reflect
% your account and password.
myaddress = '******@gmail.com';
mypassword = '********';

setpref('Internet','E_mail',myaddress);
setpref('Internet','SMTP_Server','smtp.gmail.com');
setpref('Internet','SMTP_Username',myaddress);
setpref('Internet','SMTP_Password',mypassword);

props = java.lang.System.getProperties;
props.setProperty('mail.smtp.auth','true');
props.setProperty('mail.smtp.socketFactory.class', ...
                  'javax.net.ssl.SSLSocketFactory');
props.setProperty('mail.smtp.socketFactory.port','465');

sendmail(myaddress, 'optimization done', 'come and check me')
```